

Physiological responses of six temperate tree species to water limitation

Inauguraldissertation

zur

Erlangung der Würde eines Doktors der Philosophie
vorgelegt der
Philosophisch-Naturwissenschaftlichen Fakultät
der Universität Basel

von

Lars Dietrich

aus Meschede, Deutschland

Freiburg im Breisgau, 2018

Originaldokument gespeichert auf dem Dokumentenserver der Universität Basel

edoc.unibas.ch

Genehmigt von der Philosophisch-Naturwissenschaftlichen Fakultät
auf Antrag von

Prof. Dr. Ansgar Kahmen (Universität Basel) und

Prof. Dr. Christiane Werner (Albert-Ludwigs-Universität Freiburg)

Basel, den 17.10.2017

Prof. Dr. Martin Spiess (Dekan)

*In den Wäldern sind Dinge,
über die nachzudenken,
man jahrelang im Moos liegen könnte.*

Franz Kafka

To my parents.

Table of Contents

Introduction.....	7
Chapter 1: <i>Daily stem diameter variations can predict the canopy water status of mature temperate trees</i>	15
Chapter 2: <i>Quantification of uncertainties in conifer sap flow measured with the thermal dissipation method</i>	51
Chapter 3: <i>No role for xylem embolism or carbon decrease in temperate trees during a severe drought</i>	109
Chapter 4: <i>Losing half the conductive area hardly impacts the water status of tall trees</i>	149
Chapter 5: <i>Water relations of drought-stressed temperate trees recover quickly after drought-intermittent short rainfall events</i>	173
Concluding Discussion.....	203
References.....	207
Acknowledgements.....	213
Curriculum Vitae.....	215

Introduction

Forests around the globe are assumed to be threatened by an increasing number of droughts in the near future (Bréda *et al.* 2006; Allen *et al.* 2010; Carnicer *et al.* 2011). Yet, forests are important global elements of the water and carbon cycle and society depends on a variety of forest ecosystem goods and services (Myers 1997). Future droughts triggering a decline in forest cover would, thus, have severe implications for the carbon and water cycles of the earth as well as potentially generate societal and economic problems (Ciais *et al.* 2005; Bonan 2008; Reichstein *et al.* 2013).

Indeed, climate scenarios for the coming decades suggest a strong increase in summer drought frequency and temperatures (Kirtman *et al.* 2103). In Central Europe, decreasing summer precipitation along with increasing summer temperatures is projected to bear heat waves and drought events like those in 2003 and 2015 more frequently (Fischer *et al.* 2014). It is, however, still unclear up to what degree those future drought events will threaten Europe's temperate forests (Hartmann *et al.* 2015).

A number of studies has investigated the effects of dry-spells and summer drought on the physiology of temperate tree species using different measurement techniques one of which is the comparative assessment of tree water deficit (Brinkmann *et al.* 2016). Tree water deficit (TWD) is a promising technical approach to quantify a tree's water stress as it is a measure for the water loss of the stem during periods of progressively drying soil (Zweifel *et al.* 2001; 2005). It is calculated from stem diameter variations (SDV) at the basal part of the trunk, which are measured with sensitive girth tapes or point dendrometers (De Swaef *et al.* 2015). In these terms, TWD is the shrinkage of the tree's trunk over time when water in the soil gets short. Shrinkage mostly occurs in the elastic bark tissues over the day when water demand in the atmosphere is high and is a result of the lag between transpiration and soil water uptake (De Schepper *et al.* 2012). It undergoes daily cycles with refilling and, thus, swelling of the tissues during night-time when water demand in the canopy is low (Zweifel & Hasler 2001). Usually, this night-time refilling of tissues can account for shrinkage, i.e. the water loss, over the day when the soil is rich in water. Therefore, a tree will shrink over the day but not over a longer period of time as it will be able to refill its storage during the night. During dry periods, however, when water in the soil is short, water uptake during the night is strongly

impeded and tissues cannot re-fill to their previous water content leading to an overall shrinkage of the stem throughout the whole dry period (Zweifel *et al.* 2001).

Being a measure for the progressive water depletion of tissues, TWD has been shown to correlate with water potential in saplings and small trees (Drew *et al.* 2011; Ehrenberger *et al.* 2012). Yet, it is not clear whether TWD measured at the base of the stem is also tightly related to the canopy water status, i.e. foliar/branch water potentials, in mature and tall trees. A tight correlation between these two variables would be exciting as it would strongly facilitate the assessment of a tree's canopy water status which can otherwise only be assessed by expensive or destructive methods like tree climbing, branch shooting or measurements from a canopy crane. Furthermore, since it is not clear whether radial increment growth is possible during periods of shrinking diameter (Zweifel *et al.* 2016), there is a need to test whether accounting for or neglecting radial growth in the calculation of TWD from SDV does affect the relationship with canopy water status.

Besides this very recent technique to study changes in the water status of tall trees, the assessment of sap-flow density as a measure for transpiration has extensively been used to describe and compare the water use of trees during drought (Pataki *et al.* 2000; Hölscher *et al.* 2005; Leuzinger *et al.* 2005). The most frequently used variety of this technique is based on the thermal capacity of water that flows around a heating copper-constantan thermocouple radially inserted into the sapwood (Granier 1985; 1987). The faster water is moving upward the stem, the more heat is convectively removed from the thermocouple which thereby gets cooled. By comparing the extent of cooling of this thermocouple to the temperature of an upstream axially aligned thermocouple that is not heating, the velocity of the upward water flow can be determined (Granier 1985). This measured water flux has widely been accepted as a reliable measure for transpiration (Granier 1987; Oren *et al.* 1999; Ewers & Oren 2000).

As it is difficult and very time-consuming to assess a species-specific conversion factor for the calculation of sap-flow densities from the temperature differences between the two sensors, most studies have used the universal factor proposed by Granier (1985) until now. However, depending on the xylem anatomy of the respective species, radial differences in sap-flow speed and potential wounding effects after the insertion of the two sensor needles, the Granier sap-flow system may

considerably under- or overestimate water fluxes both over time and among different tree species (Clearwater *et al.* 1999; Lu *et al.* 2004; Gebauer *et al.* 2008; Wullschlegel *et al.* 2011). Since sap-flow is often used to compare water use strategies among species and to scale up transpiration from the individual tree level to the forest or even the ecosystem level, it is very important to estimate the error introduced by not differentiating between species-specific particularities.

Together with measurements of water potentials and stomatal conductance, the two discussed techniques have been used in order to characterise the physiological response of temperate forest trees to moderately or strongly drying soil (e.g. (Hölscher *et al.* 2005; Köcher *et al.* 2009). Most of these studies found a pronounced effect of drought, i.e. soil water limitation accompanied by a strong atmospheric water demand, on the species' physiology with sap-flow and stomatal conductance decreasing by up to 80% in coniferous trees during dry spells and by 50% in broad-leaved trees during the summer heat drought of 2003 (Leuzinger *et al.* 2005; Brinkmann *et al.* 2016). Coniferous trees were always found to respond more sensitively to drought than broad-leaved trees and were, thus, categorised as more prone to drought-related health decline (Pataki *et al.* 2000; Brinkmann *et al.* 2016). However, up to now, no study has ever shown if and how these observed physiological responses are related to serious impacts on health and survival in temperate trees. Thus, we are currently lacking knowledge on the imminence of a future increase in drought frequency for temperate European forest tree species. It would, therefore, be extremely helpful to relate the observed patterns in drought responses to the mechanisms discussed for drought-induced tree mortality.

Among others, two different major concepts are discussed to explain forest die-offs and health decline due to drought: (i) the hydraulic failure and (ii) the carbon starvation hypothesis.

The concept of hydraulic failure relates to the water transport through capillary conduits in the xylem of the trees. The basic assumption of this concept is that, during drought, water potentials in the xylem progressively decrease and approach a critical value at which, once reached, some water columns in the conduits that experience the strongest tensions cannot stand the respective forces anymore and spontaneously disintegrate (i.e., cavitation; Milburn 1973; Blizzard & J 1980; Tyree &

Dixon 1983). By reducing the hydraulic conductance of the stem, this might lead to a severed water supply of the leaves and eventually would result in a rapidly increasing number of cavitation events if transpirational demands do not decrease since the same pulling force would be exerted on a smaller number of water columns (Sperry 2000). This fatal potentiation of cavitation events was named 'runaway embolism' (Tyree & Sperry 1989) and is assumed to finally end in the complete hydraulic separation of leaves and roots and, therefore, the death of the tree. Until now, the hydraulic failure hypothesis has gained a lot of supporters and xylem embolism is assumed to be the major factor determining tree mortality due to drought by many authors (Brodrribb & Cochard 2009; Urli *et al.* 2013; Barigah *et al.* 2013; Anderegg *et al.* 2016) while hydraulic traits of trees are seen as important determinants of a tree's drought resistance (Delzon & Cochard 2014; Bouche *et al.* 2014).

The carbon starvation hypothesis, by contrast, does not assume a severed water supply of the tree to be the ultimate cause of tree mortality but focuses on the physiological consequences of water limitation for the carbon household (McDowell *et al.* 2008). Theory predicts that stomatal closure during prolonged drought episodes will impede carbon uptake to an extent that photosynthesis cannot meet the respirational demand of the tree eventually leading to tree death due to a complete depletion in exploitable carbon reserves (McDowell & Sevanto 2010). Since it would take some time for the tree to completely exhaust its carbon reserves, carbon starvation is thought to occur more likely during long-lasting drought episodes (McDowell 2011). The carbon starvation hypothesis, however, is difficult to examine since we do not know which concentration of non-structural carbohydrates (NSC) would mark the point of no return for trees (Sala *et al.* 2010). Moreover, NSC observations in trees that recently died from drought have only rarely been observed (Adams *et al.* 2017). In general, most studies find the carbon starvation hypothesis to be inferior to the hydraulic failure theory for drought-induced tree mortality (Sala 2009; Hartmann *et al.* 2013; Adams *et al.* 2017). Yet, there is a growing consensus among authors that both theories need to be integrated and examined for interactions (also with insect outbreaks) in order to make progress in understanding drought-induced tree mortality (McDowell *et al.* 2011; McDowell 2011; Sevanto *et al.* 2014; Hartmann *et al.* 2015; Hartmann 2015).

While criticism and uncertainties are high concerning the carbon starvation hypothesis, the hydraulic failure concept seems to be widely accepted at this point in time (Brodribb & Cochard 2009; Choat *et al.* 2012). In fact, studies have found rigid numbers of stem water potentials associated with different amounts of embolism-induced reduction in the stem to be related to tree death for different functional types of trees. For conifers, it is assumed that a stem water potential leading to 50% reduction of xylem conductance (P_{50}) would be lethal for the tree (Choat 2013). In angiosperm trees, this value is expected to be around an 88% loss of conductance (P_{88}) (Urli *et al.* 2013).

Yet, previous experiments from decades ago challenge this view. Studies have shown that saplings of different tree species only show a strong decrease in water potentials when losing distinctly more than 90% of their cross sectional area and manage the rest with varying stomatal conductance (Sperry *et al.* 1993; Hubbard *et al.* 2001). Another study did not find any effect of up to 91% reduced cross sectional area unless severe overlapping cuts were made closely together (Mackay & Weatherley 1973). These results were obtained under well-watered conditions and it is not sure whether they apply to dry conditions as well. However, theoretical considerations suggest that under very dry conditions the trees completely shut their stomata. Under these conditions, transpiration would only account for about 5 – 10 % (cuticular transpiration) of maximum transpiration or even less since a drying epidermis can additionally decrease the remaining hydraulic conductance by up to 50% (Körner 1995; Larcher 2003). Whether this transpirational suction would be enough to break the water columns in the xylem can only be assumed and is a matter of debate. Also, the distinct localisation of embolism in the stem xylem can be doubted. A recent study in grapevine suggests that, under drought, embolism occurs first in petioles and leaves are shed before a significant amount of embolism could accumulate in the stem (Hochberg *et al.* 2017). This would definitely be a different case for a coniferous species that cannot shed its needles (e.g. *Juniperus spec.*) but if assumed that embolism occurs in the petioles first, then the water column in the stem would be relaxed and drought resistance would simply rest upon desiccation tolerance of the tree body. It is, therefore, unclear whether we are using the right measures to determine a tree's vulnerability to drought.

The impact of drought on trees is not only defined by the strength of the drought (i.e., extent of soil drying and atmospheric water demand) but is also determined by the

duration of the water limitation (Allen *et al.* 2010; McDowell 2011). However, the amount and duration of a drought that would be sufficient to heavily affect a tree's water status is unclear. Since climate projections for Central Europe predict several-day wet-spells to become less frequent (Fischer *et al.* 2014), single precipitation events might become more important for the trees during prolonged drought episodes if they could benefit the water status of the trees. Therefore, it is important to assess whether and to what extent such single-day precipitation events will benefit the trees during severe drought events and how long this beneficial effect would last.

During my doctoral research from April 2014 until October 2017, I tested methods to assess the water relations of temperate trees during drought and comparatively investigated the physiological responses of six different temperate tree species to water limitations. I specifically addressed the following questions:

- 1) Do stem diameter variations, and more specifically tree water deficit, measured at the base of the trunk of tall trees correlate to water potentials in the crown and if yes, by what kind of relationship are these two variables linked to each other?
- 2) To what extent are sap-flow estimates deriving from Granier-type sensors influenced by inter- and intra-species differences in xylem anatomy and wounding effects after needle insertion?
- 3) How close do mature trees in a temperate forest get to hydraulic failure and/or carbon starvation during naturally occurring severe drought events?
- 4) Does the loss of 50% conductive sapwood area in the stem have a fatal impact on the water status of mature individuals of temperate tree species?
- 5) To what extent can single low-amount drought-intermittent precipitation events benefit the water status of mature temperate trees?

The chapters of this thesis specifically address one of these questions and represent independent manuscripts that either are published or are submitted for assessment in internationally acknowledged peer-reviewed journals. Since the specific manuscripts are envisaged for different journals the formatting and citation style differs among the single chapters and each chapter does have its own references section. References from

this introduction can be found at the end of this thesis after the Concluding discussion.
Co-authors of each chapter are explicitly named on the title pages.

Chapter 1

Daily stem diameter variations can predict the canopy water status of mature temperate trees

Lars Dietrich^{†,1}, Roman Zweifel², Ansgar Kahmen¹

¹Department of Environmental Sciences - Botany, University of Basel, Schönbeinstrasse 6, CH-4056 Basel, Switzerland

²Swiss Federal Institute for Forest, Snow and Landscape Research (WSL), Zürcherstrasse 111, CH-8903 Birmensdorf, Switzerland

[†]Corresponding author:

E-mail: larsdietrich.plantphys@gmail.com

Phone: +41612073518

Published in Tree Physiology.

Abstract

Direct evidence for the link between stem diameter variations (SDV) and the daily canopy water status, i.e. daily water potentials (Ψ), is rare, particularly for tall trees. It thus remains unclear up to what degree SDV readings are useful to estimate daily canopy Ψ . We measured SDV with point dendrometers at the stem base of tall, mature individuals of six European forest tree species in a near-natural temperate forest and compared them to daily canopy Ψ during the growing seasons of 2014 (wet) and 2015 (dry). SDV were de-trended for growth with two different approaches leading to the so-called tree water deficit (TWD). We found that midday Ψ can be predicted from TWD, independent of the growth-de-trending procedure to obtain TWD from SDV. Further, daily TWD was a better indicator for daily midday Ψ , particularly under dry conditions, than maximum daily shrinkage (MDS), another common quantity derived from SDV. Based on data from six temperate tree species, we conclude that TWD measured at the stem base is a consistent proxy for daily canopy midday Ψ of tall trees over the entire range of measured conditions.

Keywords: drought, mature trees, maximum daily shrinkage, stem diameter variations, tree water deficit, water potential

Introduction

Daily stem diameter variations (SDV) in trees have become a frequently-used and intensively-discussed research tool in plant eco-physiology (De Swaef et al. 2015). Measured by sensitive girth tapes or point dendrometers (e.g., Linear Variable Differential Transformers or potentiometers), SDV have been shown to be sensitive to both radial growth and the water-related shrinkage and refilling of the stem tissue (Kozłowski and Winget 1964). Radial growth means the irreversible radial expansion of the stem as a consequence of the development of newly formed sapwood and bark tissue cells but does not include secondary growth (cf. Cuny et al. 2015). Reversible radial stem shrinkage and expansion is caused by changing water contents of stem tissues, mainly the bark (De Swaef et al. 2015).

Stem shrinkage and refilling typically follows a diurnal pattern with a minimum stem radius in the afternoon and a maximum stem radius in the early morning. It is proportional to the loss of water from elastic tissues and can cover up to 100% of the transpired water on a cloudy day (Zweifel and Hasler 2001, De Schepper et al. 2012). The shrinkage of tree stems has mostly been attributed to the water depletion of bark cells (i.e. living phloem, fibrous phloem and the living and dead cells of the *phellem*). This can be explained by dynamic flow-and-storage processes (based on Ohm's law) driven by water potential (Ψ) gradients between the different compartments of the soil-tree-atmosphere system (Kozłowski 1972, Zweifel et al. 2001, Steppe et al. 2006, De Swaef et al. 2015). Differences in Ψ induce a progressive water flow from the point of higher to the point of lower Ψ , i.e., a radial transport of water between the stem sapwood and the bark. During daytime, this results in water flow from the bark to the xylem inducing a water content-related shrinkage of the bark cells. During the night, water potentials and flows are reversed resulting in the rehydration and re-expansion of the bark cells. Depending on the species, the shrinkage of the stem can additionally be attributed to the elastic behaviour of the xylem (Sevanto et al. 2002, Zweifel et al. 2014, Pfautsch, Renard, et al. 2015, Pfautsch, Hölttä, et al. 2015). The xylem elasticity itself has been explained to be a function of wood density (Scholz et al. 2008) and/or specific tissue elasticity (Zweifel et al. 2014).

In dry periods when soil water potential (Ψ_{soil}) progressively decreases, Ψ in trees does not fully recover during night-time, which in turn slows down the rehydration of the bark tissue. In such cases, the elastic stem tissues are not completely refilled

during the night and the stem remains in a partly shrank state (Kozłowski and Winget 1964, Zweifel et al. 2001). Over time, this can lead to a marked gross shrinkage of the stem. Several authors have thus proposed a link between SDV and the overall water status of the tree that is typically described by Ψ_{leaf} or Ψ_{branch} (Klepper et al. 1971, Hellkvist et al. 1980, Irvine and Grace 1997, Ueda and Shibata 2001, Zweifel et al. 2005). SDV reflecting canopy Ψ is of high interest because it could strongly simplify the assessment of the water status of tall trees, which otherwise can only be determined by accessing the canopy via tree climbers, branch-shooting or a canopy crane to measure Ψ in the crown. Most importantly, SDV could provide continuous information on tree water status when automated dendrometers are used, thereby providing high-resolution information on tree and forest health in experimental and monitoring studies (Zweifel 2016).

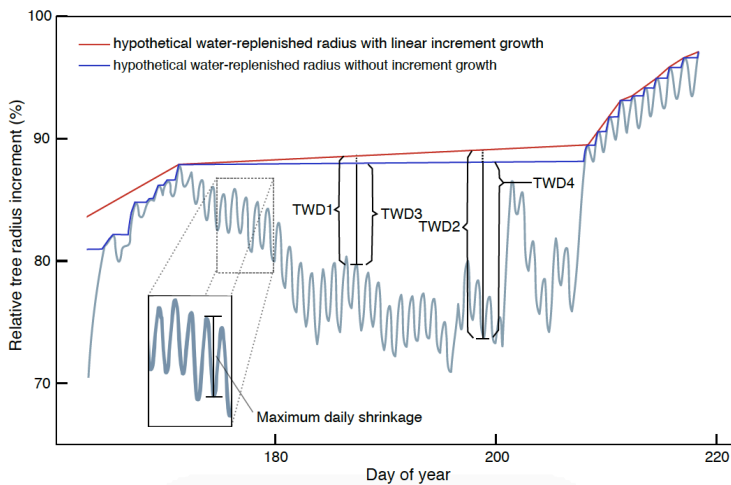


Figure 1 Exemplary stem radial growth curve during 60 days of the 2015 growing season and visualization of the different approaches for calculating tree water deficit (TWD) we used for our investigations. TWD1 and 3 are relating to the daily maximum, TWD2 and 4 are referring to the daily minimum in stem diameter. Maximum daily shrinkage (MDS) is considered to be the difference between the daily maximum occurring in the first half and the daily minimum occurring in the second half of the day.

Different approaches have been proposed for the calculation of SDV-derived variables reflecting the water status of a tree (Fig. 1). A frequently employed approach

to assess the daily water status of a tree via SDV uses the maximum daily shrinkage (MDS) of the tree stem (Conejero et al. 2007, Velez et al. 2007, Ortuño et al. 2010, Fernández and Cuevas 2010, Conejero et al. 2010, Puerto et al. 2013). Good linear relationships between MDS, Ψ_{stem} (measured with a psychrometer) and Ψ_{leaf} have been reported for grapevine, citrus, peach, and plum trees when assessed over relatively short time periods (a couple of weeks to a few months) under mostly well-watered conditions (DeSwaef et al. 2009, Ortuño et al. 2010, Fernández and Cuevas 2010). Significant relationships between MDS and Ψ_{stem} or Ψ_{leaf} have also been found in timber plantations and forests (Lassoie 1973, Braekke and Kozłowski 1975, Zweifel and Hasler 2001, Cermák et al. 2007, Deslauriers et al. 2007, Turcotte et al. 2011, King et al. 2013, Biondi and Rossi 2014). As an alternative to MDS, the progressive shrinkage of the stem over longer time periods called tree water deficit (TWD) (Hölttä et al. 2005, Zweifel et al. 2005, Drew et al. 2011, Brinkmann et al. 2016), has been shown to also correlate with Ψ_{stem} and Ψ_{leaf} in tree species (McBurney and Costigan 1984, Milne 1989, Irvine and Grace 1997, Offenthaler et al. 2001, Daudet et al. 2005, Ehrenberger et al. 2012). In essence, TWD is the difference between the theoretical radius of a tree at full hydration and its current actual radius (Fig. 1). TWD is thus an indicator for the absolute water deficit of the stem. It equals zero when the tree's tissues are fully hydrated. Therefore, and in contrast to MDS, TWD allows accounting for accumulated water deficits also over extended periods (few days to months) of drought. Despite the potential of SDV measurements, important uncertainties remain for the application of TWD and MDS as a proxy for canopy Ψ of tall and mature trees and a comparative empirical assessment of the relationship between different SDV-derived variables and canopy Ψ of mature trees is still missing. In particular, it remains unclear whether TWD could potentially be underestimated by a growth-induced stem radius increase during times of water deficit (Kozłowski 1972, Zweifel 2006, Chan et al. 2015, Mencuccini et al. 2017) and whether MDS is reliably applicable as a proxy for the water status of the canopy during longer dry periods (Intrigliolo and Castel 2007, Puerto et al. 2013).

In addition to the above uncertainties, a mechanistic explanatory concept for the qualitative and quantitative assessment of daily tree canopy Ψ using TWD from automated stem diameter measurements does not exist yet. We propose here that the relationship between TWD and canopy Ψ follows a logistic pattern (Fig. 2): When canopy Ψ is close to zero and the tension in the stem is low, the living cells in the

corresponding tissues should be close to full turgescence and TWD, thus, close to zero (Fig. 2). The more negative canopy Ψ becomes, the more negative Ψ_{stem} at the base of the tree gets. However, this does not necessarily lead to an instantaneous and linear shrinkage of the bark tissue along the stem. This is, because the relationship between cell turgor and cell volume depends on the volumetric elastic modulus of the cell wall, which itself is a function of turgor pressure, and varies in its steepness with a steeper slope at low turgor pressures (Steudle and Zimmermann 1977, Franks et al. 2001). Therefore, we expect the trunk to start shrinking only slowly with the initial decrease of Ψ_{stem} . Only beyond this slow decrease in cell volume a linear phase of shrinkage will occur, where declining Ψ_{stem} reduces the turgor of the bark tissue cells. This linear part of the relationship lasts until the bark cells have mostly lost turgor and the protoplasts start to detach from the cell walls. From this point on, we expect TWD to asymptotically approach a maximum that cannot be further exceeded by water withdrawal from the bark cells. Since the volumetric elastic modulus of the bark cells can be expected to be species-specific, we assume inter-species differences in the logistic relationship between TWD and Ψ .

In the work presented here, we set out to test the general relationship between daily stem shrinkage and canopy Ψ over two growing seasons in mature individuals of six different central European forest tree species. We tested (i) how strongly MDS and daily TWD correlate with daily pre-dawn and midday canopy Ψ ($\Psi_{\text{pre-dawn}}$ and Ψ_{midday}), (ii) whether the explanatory power of the relationship between daily TWD and daily canopy Ψ changes with different approaches to de-trend SDV for growth, and (iii) whether the general relationship between daily TWD and daily canopy Ψ is of a logistic nature with saturating TWD at very negative canopy Ψ .

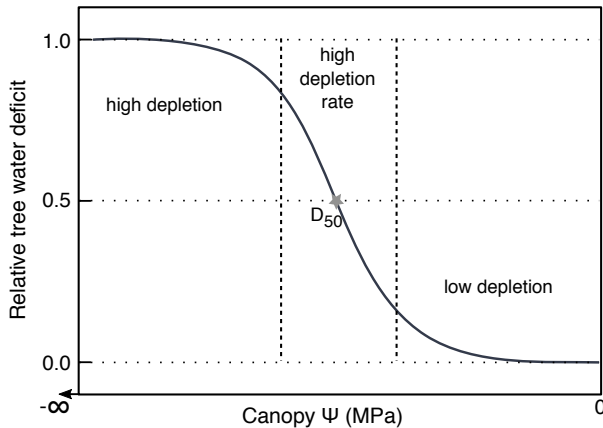


Figure 2 Scheme of the hypothesized logistic pattern of the relationship between canopy water potential (Ψ) and TWD. At high and low Ψ , TWD only slightly increases with declining Ψ . However, close to the point of 50% depletion of internal storage tissues (D_{50}), there is a strong linear dependency of TWD on Ψ , suggesting high depletion rates and strong water flows from storage tissues to the sapwood.

Materials and Methods

Study site and study species

The study was conducted in a mixed temperate forest 15 km south of Basel, Switzerland, at an elevation of 550 m a.s.l. (47°28'N, 7°30'E) during the growing seasons of 2014 and 2015. We chose those two years because of their contrasting soil water availability (Supporting Fig. 1) to assess a range in TWD and Ψ as broad as possible. The soil of the site belongs to the Rendzina type and the shallow bedrock (starting at ~1 m depth) is calcareous. The site has a temperate humid climate with mild winters and moderately warm summers. Mean January and July temperatures are 2.1 and 19.2°C, respectively. Total annual precipitation of the region sums to ca. 900 mm. We measured air temperature, relative humidity, precipitation and solar radiation during both years with a weather station (Davis Vantage Pro 2, Scientific Sales Inc., Lawrenceville, NJ, USA) and recorded soil water potential (Ψ_{soil}) at -20 cm depth and 20 cm distance from the stems of the investigated trees with a dielectric sensor (MPS-2, Decagon Devices, Pullman, WA, USA) on ten-minutes intervals. In 2014, we employed 20 Ψ_{soil} -sensors

and 12 in 2015. The trees of the forest are between 100 – 130 years old and have been studied very intensively as part of the Swiss Canopy Crane Project (Pepin and Körner 2002). The forest consists of deciduous and coniferous tree species dominated by *Fagus sylvatica* and *Quercus petraea*. Other species are *Abies alba*, *Larix decidua*, *Picea abies*, *Pinus sylvestris* and *Carpinus betulus*. Average tree height is between 35 and 40 m. For this study, we performed measurements on four mature individuals of the species *C. betulus*, *F. sylvatica*, *L. decidua*, *P. abies*, *P. sylvestris* and *Q. petraea* resulting in a total of 24 investigated trees (Tab. 1). *L. decidua* was only investigated in 2015.

Table 1 Mean diameter at breast height (DBH) for the investigated tree species.

Tree species	DBH (mean \pm SE, n = 4)
<i>Carpinus betulus</i>	34.4 \pm 7.4 cm
<i>Fagus sylvatica</i>	60.0 \pm 5.0 cm
<i>Larix decidua</i>	50.1 \pm 1.8 cm
<i>Picea abies</i>	59.6 \pm 3.1 cm
<i>Pinus sylvestris</i>	51.4 \pm 4.6 cm
<i>Quercus petraea</i>	47.9 \pm 3.5 cm

Dendrometer measurements

Each investigated tree was equipped with a point dendrometer (ZN11-T-WP, Natkon, Oetwil am See, Switzerland) installed at 2 m height at the north-east facing site of the stem. The electronic part of the dendrometer was placed on a carbon frame, which itself was anchored in the stem with three stainless steel rods, holding the pin of the dendrometer to point towards the center of the stem. In species with rough bark the surface of the dead bark beneath the pin of the dendrometer was carefully flattened to provide an undisturbed point of contact for the pin. Data were recorded every ten minutes with a logging node (Channel Node, Decentlab GmbH, Dübendorf, Switzerland) wirelessly transmitting onto a data logger (Base Station, Decentlab GmbH) and broadcasting the data to a server via cellular network. For visualization of the trees' growth and radius variation on a species level (species means), we first calculated relative radius values for each individual tree to reduce noise in the species-specific mean radius curves resulting from small but significant differences in DBH. This was

done by dividing the radius values by the overall maximum radius measured over both growing seasons (values given in %).

Water potential measurements

Pre-dawn water potential ($\Psi_{\text{pre-dawn}}$) and midday water potential (Ψ_{midday}) were measured with a Scholander pressure bomb (Model 1000, PMS Instruments, Albany, OR, USA) on terminal shoots from the upper part of the sunlit crown of each investigated tree. A gondola operated by a canopy crane provided canopy access. We measured three, max. 10 cm long shoots with three to four leaves (broad-leaved) or brachyblasts (*L. decidua*) in the deciduous species and current year shoots in the evergreen species (*P. abies* and *P. sylvestris*). The cut surface of the shoots was smoothed with a razor blade before measuring. We did not cover the leaves in tin foil before measuring. Ψ_{midday} was assessed around noon on 28 days at an irregular interval throughout the two growing seasons. $\Psi_{\text{pre-dawn}}$ was measured shortly before sunrise on nine days throughout the progressing drought in 2015.

Calculation of MDS and TWD

We determined maximum daily shrinkage (MDS) of absolute stem diameter variations (SDV) by calculating the differences between the daily pre-dawn maximum and the daily afternoon minimum in stem radius (Fig. 1). Tree water deficit (TWD) was calculated according to the two approaches of Zweifel *et al.* (2005 & 2016): In the first approach, an envelope curve is computed as a line connecting the running maxima in the absolute stem radius (red line, Fig. 1). This was obtained by calculating linear regression lines that interpolate between all the running maxima (the current and the next higher maximum) in stem radius over time. The difference between the respective value of the resulting line and either the daily maximum (early morning) or minimum (afternoon) in stem radius is then called TWD (TWD1 and TWD2 in Fig.1, respectively). This approach assumes that there is a constant, unimpeded radial growth rate (cell division and expansion) in the cambium of the stem over time no matter how much water-depleted the stem tissues become and how different environmental conditions are. In the second approach, a horizontal line from the current maximum stem radius is drawn to the next higher maximum stem radius in time. From there, this procedure is continuously repeated until the next respective maximum is reached

eventually terminating at the final maximum stem radius of the season. The obtained horizontal lines therefore always represent the value of the last maximum stem radius in time (blue line, Fig.1). The difference between the values of this line (i.e. the current potential stem radius maximum) and the current daily stem radius maximum or minimum is then calculated as TWD3 or TWD4, respectively. In this approach, it is assumed that growth only occurs during days when the radius exceeds the maximum radius of the previous period. In all four approaches to calculate TWD, TWD is an indicator for the absolute water deficit of the stem. It equals zero when the tree's tissues are fully hydrated. TWD and MDS were obtained in the unit μm .

In our analysis of the relationship between TWD and Ψ , we separately related $\Psi_{\text{pre-dawn}}$ and Ψ_{midday} with all SDV variables. When testing the specific shape of the relationship between TWD and Ψ we focussed on the relationship between TWD4 and Ψ_{midday} because these showed the strongest relationship in the above analysis. In all regressions, we always plotted values of TWD against values of Ψ that were obtained on the same measurement day.

Normalization of TWD and Ψ_{midday}

To fit a sigmoidal function into the relationships between Ψ and TWD, we normalized TWD for each species. This was done to facilitate the calculation of logistic parameters by the non-linear least squares function in R (*nls()*). We normalized TWD by dividing daily TWD values by the highest species-specific TWD value measured over both seasons. We call normalized TWD values from here on *relative TWD*. We also normalized Ψ_{midday} in order to compare the sigmoidal relationships between Ψ and TWD across species. Since we did not have continuous data of Ψ_{midday} over the two growing seasons we might have missed the most negative values for Ψ . It was therefore not possible to normalize the obtained values on the most negative measured values. To overcome this limitation, we calculated a reference minimum Ψ value for each species from the species-specific logistic relationship we found between relative TWD and absolute canopy Ψ_{midday} . Given the asymptotic nature of the relationship between TWD and Ψ at very low values, we defined minimum Ψ_{midday} to occur at a relative TWD value of 0.95.

Statistical analyses

Statistical analyses and data visualization were done using *R*, version 3.3.2 (R Foundation for Statistical Computing, Vienna, Austria 2013), with its packages *caTools* (Tuszynski 2014), *data.table* (Dowle et al. 2015), *ggplot2* (Wickham 2009), *gridExtra* (Auguie 2015), *MPV* (Braun 2015), *scales* (Wickham 2015), *xts* (Ryan and Ulrich, 2014) and *zoo* (Zeileis and Grothendieck 2005). We tested if linear or logistic functions can better explain the relationships between daily TWD and daily Ψ_{midday} . Linear fits between daily TWD/MDS and daily Ψ_{midday} were obtained from linear models using the *lm()* function ($y = mx + n$), logistic fits were done using the *nls()* function with the equation

$$(1) \quad y = \frac{1}{1 + e^{-a \cdot (x+b)}} \cdot$$

The parameters *a* and *b* thereby determine the steepness of the curve (rate of bark depletion per MPa Ψ , *a*) and the inflection point of the function (Ψ at which 50 % of the bark is depleted, *b*). We assumed $p < 0.05$ to represent the level of significance for all statistical tests. To quantitatively evaluate if linear or logistic regressions best explain the observed relationships, we compared the R^2 of the two functions. For this purpose, we transformed the logistic regression into a linear relationship by calculating the fitted values for Ψ and then relating them to the respective measured values of Ψ . Then we compared the R^2 values of the resulting linear relationship with those of the linear regressions. For the evaluation of the best predictive power of either linear or logistic regressions, we calculated the predicted residual error sum of squares (PRESS) (Montgomery et al. 2015).

Results

The two investigated growing seasons differed in terms of their average meteorological conditions. The year 2014 was moist, and the year 2015 was one of the driest years on the central European weather record (Tab. 2, Supporting Fig. S1, Orth et al. 2016).

Table 2 Environmental conditions during the two growing seasons (May 1st to October 31st) of the study period. Precipitation is the sum of all events during the season. Ψ_{soil} is the mean of 20 (2014) and 12 (2015) sensors at depth of -20 cm (\pm SD). Mean daily temperature and mean relative humidity are averages of daily means (\pm SD).

Environmental variable	2014	2015
Precipitation	551 mm	348 mm
Ψ_{soil}	-0.043 ± 0.048 MPa	-0.421 ± 0.330 MPa
Mean daily temperature	16.8 ± 4.1 °C	16.5 ± 6.0 °C
Maximum daily temperature	29°C	30.9°C
Minimum daily temperature	5.5°C	2.5°C
Mean daily rel. humidity	73.0 ± 12.5 %	67.9 ± 14.7 %

Stem radius measurements showed a net growth in all species in both years and substantially more stem shrinkage during the dry periods in 2015 than in 2014 (Fig. 3). *C. betulus*, *L. decidua* and *P. sylvestris* showed relatively large stem shrinkage compared to their growth, whereas *F. sylvatica*, *Q. petraea*, and *P. abies* shrank much less in relation to their growth.

Maximum daily shrinkage (MDS) generally covered the same range in both seasons for most species except for *C. betulus* and *Q. petraea*, which showed higher MDS in 2015 compared to 2014 (Fig. 4). In contrast, we observed strong differences in daily tree water deficit (TWD) between 2014 and 2015 for all species (Fig. 4). While daily TWD was moderate in 2014 it reached substantially larger values in 2015. Further, *L. decidua* and *P. sylvestris* showed higher TWD earlier in the dry year 2015 while TWD of the other species increased more gradually during the whole season. The absolute values of MDS and TWD were highly different among species: *F. sylvatica* and *C. betulus* had the smallest absolute shrinkage while the conifers (*P. sylvestris*, *P. abies* and *L. decidua*) showed the highest values (Fig. 4).

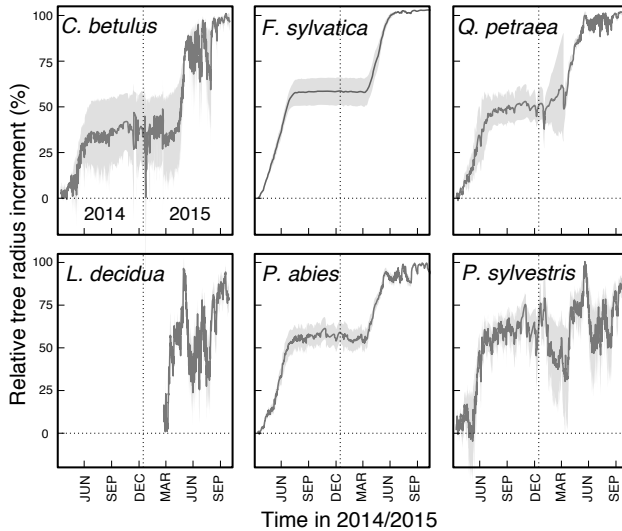


Figure 3 Relative radius increment of the six species during the years 2014 and 2015. Note that periods of stem shrinkage are more or less visible depending on the relative strength of the shrinkage as compared to the overall growth increment which was especially strong in *F. sylvatica* and *P. abies*. Radius was measured with point dendrometers on the NE side of the trunks of 4 individuals of each species (n=4) at around 2 m height. Data are given \pm SD.

Values of Ψ_{midday} found in the two growing seasons across species ranged from -0.66 ± 0.04 MPa (mean \pm SD) in *F. sylvatica* to -2.7 ± 0.08 MPa (mean \pm SD) in *Q. petraea* (Supporting Fig. S2). Ψ_{midday} was less variable in the growing season of 2014 than in 2015. In 2015, there was a decrease of $\Psi_{\text{pre-dawn}}$ and Ψ_{midday} throughout the summer (July – September) in most of the species.

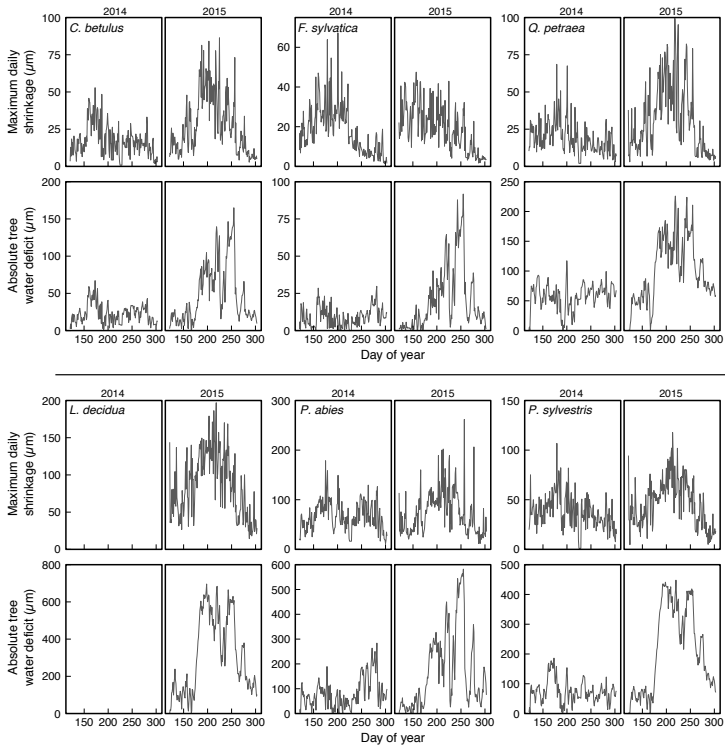


Figure 4 Absolute maximum daily shrinkage (MDS) and daily tree water deficit (TWD4) of the six species during the growing seasons of 2014 and 2015 (n = 4 individuals per species).

Linear regressions were used to test the relationship between different SDV variables and $\Psi_{\text{pre-dawn}}$ and Ψ_{midday} for each species. MDS strongly correlated with Ψ_{midday} of *Q. petraea*, *L. decidua* and *C. betulus* but weakly with Ψ_{midday} of *P. abies*. No correlations between MDS and Ψ_{midday} were found for *F. sylvatica* and *P. sylvestris*. (Fig. 5). When moist and dry periods were considered separately, the two relationships between MDS and Ψ_{midday} were equal for the two species *Q. petraea* and *L. decidua*, similar for *C. betulus*, and inverse for *P. sylvestris*, *F. sylvatica*, and *P. abies* (Supporting Fig. S3). $\Psi_{\text{pre-dawn}}$ did not correlate with MDS for none of the species (Fig. 5).

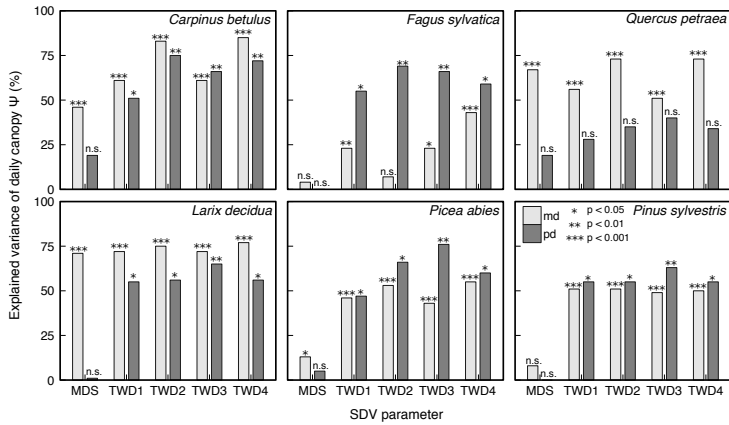


Figure 5 Explained variance (R^2 values) and levels of significance (p) for the linear correlations between the different calculated absolute parameters of SDV and Ψ_{midday} (md) and $\Psi_{\text{pre-dawn}}$ (pd). Ψ was measured throughout the growing seasons of 2014 and 2015 at around 30-40 m height with a canopy crane, each time at nearly the same positions in the sunlit crown of the individuals.

In contrast to MDS, we found strong correlations between daily TWD and $\Psi_{\text{pre-dawn}}$ and Ψ_{midday} for all species (Fig. 5). In general, TWD of *F. sylvatica* and *P. abies* showed better correlations with $\Psi_{\text{pre-dawn}}$, whereas TWD of *C. betulus*, *Q. petraea* and *L. decidua* exhibited stronger correlations with Ψ_{midday} . For *P. sylvestris* there was no distinct difference between the correlations of TWD and the two canopy Ψ measures. In general, we found that TWD1 and 3 explained $\Psi_{\text{pre-dawn}}$ almost equally well. The same was found for TWD2 and 4 concerning Ψ_{midday} . Yet, TWD3 correlated slightly better with $\Psi_{\text{pre-dawn}}$ than TWD1 and TWD4 showed a better correlation with Ψ_{midday} than TWD2. Overall, the approach assuming no growth during stem shrinkage (TWD3 and TWD4) showed slightly better correlations to canopy Ψ .

To test the shape of the relationship between TWD and Ψ_{midday} we used TWD4, since it revealed the strongest correlation to Ψ_{midday} . Logistic regressions between TWD4 and Ψ_{midday} had a slightly higher explanatory power for most species than linear functions (Fig. 6, Tab. 3). Only for *Q. petraea*, the linear regression showed a slightly better R^2 than the logistic regression. Interestingly, the slope of the logistic relationship between Ψ_{midday} and TWD4 showed substantial variability across species,

with *P. sylvestris* exhibiting the steepest slope and *Q. petraea* showing the flattest slope at the point of inflection (Fig. 7A). We calculated the predicted residual error sum of squares (PRESS) for all relationships to compare the fit of the logistic and linear functions to the measured data. PRESS values suggested a better fit of the logistic regression than the linear regression for *C. betulus* and the three conifers. Only for *F. sylvatica* and *Q. petraea*, PRESS suggested a better fit for the linear regression. When tested across all species, the logistic regression between TWD4 and Ψ_{midday} explained 2% more of the variation than the linear regression (Fig. 7B, Tab. 3) indicating that both models are almost equally good predictors of TWD. Importantly, however, the PRESS value of the logistic regression was considerably smaller than the PRESS value of the linear regression, which suggests a generally better fit and higher predictive power of the logistic function compared to the linear one (Tab. 3).

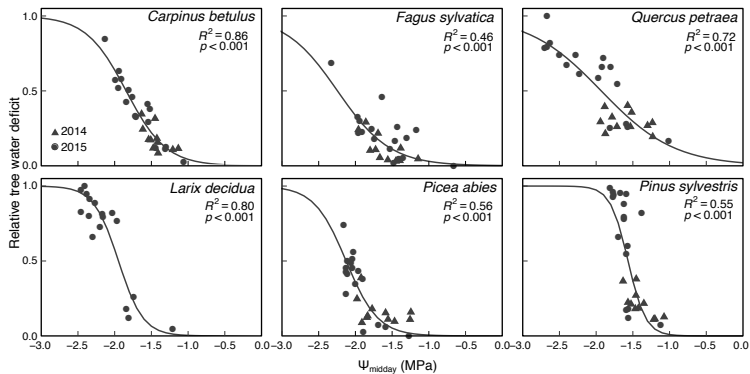


Figure 6 Logistic relationships between relative values of TWD4 and Ψ_{midday} for the six species during the growing seasons of 2014 and 2015. Each point represents the mean of three measurements of Ψ_{midday} in the crown of four individuals ($n=4$) and the mean relative TWD of four individuals ($n=4$). Relative TWD was calculated by dividing the respective absolute TWD value by the highest absolute TWD measured during the period of investigation.

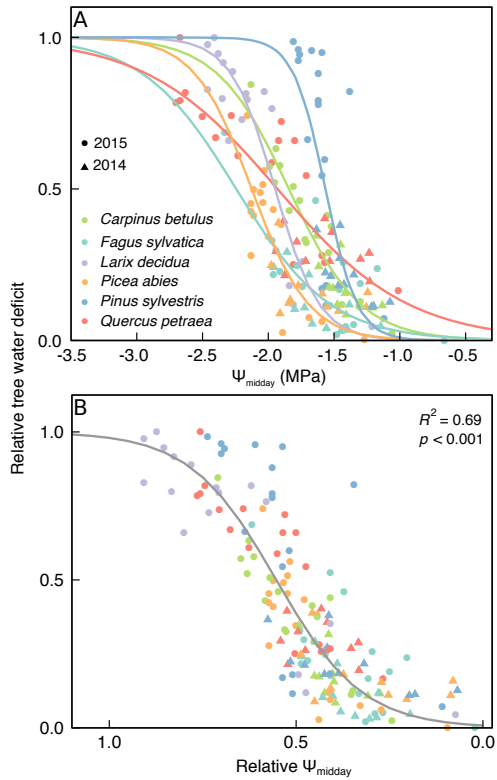


Figure 7 A Comparison of the logistic relationships between Ψ_{midday} and relative TWD4 among the different species (c.f. Fig. 6). B Logistic relationship between relative Ψ_{midday} and relative TWD4 across all species during the growing seasons of 2014 and 2015. Relative Ψ_{midday} was calculated by standardizing the absolute value on the value where the species-specific regression curves in Fig. 6 reach a relative TWD of 0.95.

Discussion

Relationship between SDV-derived measures and canopy Ψ

We found that maximum daily shrinkage (MDS) was only correlated to Ψ_{midday} for *C. betulus*, *L. decidua* and *Q. petraea*, but not (or only marginally significantly) for *F. sylvatica*, *P. abies* and *P. sylvestris* (Fig. 5). Furthermore, we did not find a consistent relationship between MDS and $\Psi_{\text{pre-dawn}}$ for either species, suggesting MDS to be unable to take up the long-term changes in daily canopy Ψ induced by changes in soil water conditions. In contrast to the data we show here, several previous studies have shown a close relationship between MDS and Ψ for orchard trees with increasing MDS at decreasing Ψ (Feres et al. 1999, Ortuño et al. 2006, Intrigliolo and Castel 2007) and MDS has been proposed to be a useful and reliable tool to assess tree water status for irrigation scheduling in orchard science (Ortuño et al. 2010, Fernández and Cuevas 2010). Several of these studies have, however, also indicated variations in the quality of the correlations between MDS and Ψ depending on different phenological stages over the season, temperature, fruit load and tree size (Molz and Klepper 1973, Fernández and Cuevas 2010). Further, MDS has been shown to gradually decline when trees are experiencing poor water supply for extended periods of time (Klepper et al. 1973, Hinckley and Bruckerhoff 1975, DeSwaef et al. 2009, King et al. 2013). The reason for declining MDS with declining soil water supply is an insufficient tissue rehydration during night time, so that the stem undergoes a constant shrinkage (on a daily cadence) during dry periods. Since MDS is proportional to the volume of daily used storage water (Zweifel et al. 2000), poor night-time rehydration, and therefore declining storage water, will have a decreasing effect on MDS during dry periods. We therefore conclude that while MDS is a reasonable proxy for tree water status as long as the trees are well watered, it seems not to be a reliable predictor of daily canopy Ψ over longer time scales, in particular if these include dry periods.

In contrast to MDS, we found consistently strong relationships between tree water deficit (TWD) and Ψ_{midday} and $\Psi_{\text{pre-dawn}}$ across the two growing seasons for all species (Fig. 5). TWD is calculated as the difference between the hypothetical maximum stem size under fully hydrated conditions (with the two variations of including or not including a linear growth fraction during periods of stem shrinkage) and the current actual stem size (Fig. 1). As such, TWD had been proposed to be a good measure for the absolute water loss from storage tissues of a tree stem previously (Zweifel et al.

2000) and our data show that this absolute water loss is indeed tightly linked to the overall water status, i.e. $\Psi_{\text{pre-dawn}}$ and Ψ_{midday} , of a tree. In a desiccation experiment. Cochard et al. (2001) demonstrated that the difference in Ψ between xylem and bark is closely related to the absolute shrinkage of branches of 18-year-old individuals of *Juglans regia*. Also, Drew et al. (2011) were able to show a relationship between TWD and Ψ_{leaf} in 10 m tall individuals of *Callitris intratropica*. Our study corroborates these findings and shows that the previously implied relationship between SDV and canopy Ψ according to Cochard et al. (2001) and Drew et al. (2011) is not only valid for small and medium sized trees but also for 30-40 m tall individuals of six different temperate tree species and that stem and canopy water relations are tightly coupled on a daily basis.

It is interesting to note that during periods of continuous tree growth over several days, values for TWD4 equal those of MDS while differences between these two variables only become apparent during longer periods of stem shrinkage. Thus, the fact that TWD4 describes daily canopy Ψ better than MDS clearly points out the advantage of the TWD over the MDS concept during longer periods of stem shrinkage. TWD thus offers a simple approach to assess the daily water status of mature trees in experiments and monitoring studies and has the potential to substitute labour-intensive manual measurements of daily canopy Ψ , a particular challenge in tall trees.

Growth-de-trending to extract TWD from SDV with little effect on findings

It has been intensively discussed whether trees are able to grow during periods of stem shrinkage (Zweifel et al. 2016, Mencuccini et al. 2017). This indirectly raises the question whether growth during stem shrinkage might confound possible relationships between TWD and the tree's water status. We employed different approaches to calculate TWD in order to assess the robustness of the relationship between daily TWD and canopy Ψ with and without considering growth to occur during periods of stem shrinkage (Fig. 1). Two of the approaches assumed no growth during stem shrinkage (TWD3, 4) and two accounted for a linear and progressive growth during periods of stem shrinkage (TWD1, 2). We found that all of the applied approaches led to a strong relationship between daily TWD and canopy Ψ and that potential growth processes during times of stem shrinkage were either not existent or were small enough to not confound the relationship.

It is important to mention that the definition of growth used in our study is only accounting for primary growth leading to an increment in stem size. Not included are secondary growth processes which increase wood density without an impact on stem size (Cuny et al. 2015). Primary growth consists of cell division and cell elongation leading to an increase in stem radius. This expansion is proposed to be strictly limited by a water potential threshold below which cells are not able to expand and elongate due to low turgor pressure in the cambium (Génard et al. 2001, Larcher 2003, Steppe et al. 2006). Our results might indeed support the theory that growth is only possible above a certain threshold Ψ (Hinckley and Bruckerhoff 1975, Zweifel 2006, Intrigliolo and Castel 2007) and that this threshold is associated with the onset of stem shrinkage. We would like to caution, however, that there is some evidence that plant cells are able to adapt their growth processes to low Ψ (Cosgrove 2005) and that cell division (but not elongation) might occur during periods of lowered Ψ and thus periods of stem shrinkage (Ruts et al. 2012, Zweifel et al 2016). Growth due to newly formed but not expanding cells is, however, relatively small and would be negligible when using SDV for estimating tree water status.

Table 3 Statistical coefficients of the linear and logistic regression analyses on the relationship of (relative) TWD4 and Ψ_{midday} for the six investigated species and the across-species (i.e. all species) relationship of relative TWD4 and relative Ψ_{midday} during the growing seasons of 2014 and 2015.

Species	Linear regression			Logistic regression		
	<i>p</i>	<i>R</i> ²	<i>PRESS</i>	<i>p</i>	<i>R</i> ²	<i>PRESS</i>
<i>C. betulus</i>	< 0.001	0.85	0.70	< 0.001	0.86	0.13
<i>F. sylvatica</i>	< 0.001	0.43	0.50	< 0.001	0.46	0.77
<i>Q. petraea</i>	< 0.001	0.73	0.66	< 0.001	0.72	0.74
<i>L. decidua</i>	< 0.001	0.77	0.91	< 0.001	0.81	0.08
<i>P. abies</i>	< 0.001	0.55	0.80	< 0.001	0.56	0.30
<i>P. sylvestris</i>	< 0.001	0.50	2.65	< 0.001	0.55	0.16
All species	< 0.001	0.67	8.90	< 0.001	0.69	2.27

General pattern of the TWD – canopy Ψ relationship

We found that across all species, the logistic function explained more of Ψ_{midday} as predicted from TWD than the linear function (Fig. 6, Tab. 3). This is true for both the explained variance (R^2) but even more for the predictive power of the function (PRESS statistic). The difference in explanatory power between the two functions was also found at the species level for *C. betulus*, *L. decidua*, *P. abies* and *P. sylvestris*. No differences between the two functions were, however, found for *F. sylvatica* and *Q. petraea* (Tab. 3). Our data are therefore in support of our hypothesis of a general logistic relationship between TWD and canopy Ψ , where TWD and canopy Ψ are decoupled at low and high canopy Ψ (Fig. 2). The decoupling of TWD and canopy Ψ has already been reported for Norway spruce trees by Zweifel et al. (2000). In addition to a non-linear relationship between cell size and cell turgor, the decoupling of TWD and canopy Ψ at very negative canopy Ψ could be the result of the cavitation of tracheids or vessels in the xylem and the associated loss in axial and radial conductance resulting in disproportionately lower Ψ in the canopy than at the stem base (Hölttä et al. 2002, Steppe et al. 2015) thereby possibly preventing a too strong depletion of bark water storage (Vergeynst et al. 2015).

Although our data are generally in support of the logistic function, it is important to note that our data for canopy Ψ of several species, in particular those of *F. sylvatica* and *Q. petraea*, fall mainly into the linear range of the logistic relationship between daily TWD and canopy Ψ . This is, although the summer 2015 was exceptionally dry (Orth et al. 2016) with canopy Ψ reaching low values for these species (Dietrich et al. unpublished data). This suggests that linear functions should be appropriate to predict Ψ from TWD as long as values for Ψ are not approaching zero or exceptionally negative values. Our data do caution, however, that for Ψ in the saturation regions of the curve especially during severe or extreme drought the use of linear instead of logistic functions for the continuous quantitative modelling of canopy Ψ from TWD will likely over- or underestimate Ψ . This is supported by the better PRESS (predictive power) statistic of the logistic function.

Our data also show that the shape of the logistic relationship between daily canopy Ψ and daily TWD (steepness of the function) varies depending on the respective species (Fig. 6). This is explicable with different wood anatomies, i.e. different hydraulic resistances to water flow in the xylem of the species and different elastic properties of the tissues involved in shrinkage (Heine 1971, Steppe and Lemeur 2007). Plants with a

higher hydraulic resistance more readily exhibit more negative Ψ at the base of the stem leading to a faster depletion of the bark tissues and, thus, a steeper relationship between TWD and canopy Ψ . This can particularly explain the steeper curves in the three conifers which have a significantly higher vertical resistance to water flow than the other three species (Evert 2006). Hooke's law further predicts differences in the shrinkage of the bark tissues to be dependent on the elastic modulus of the cell walls of the cells involved into shrinkage (Irvine and Grace 1997, Peramaki et al. 2001). Based on macroscopic considerations of the bark (e.g. bark rigidity) of the different tree species, we can expect clearly different elastic moduli.

Given the different shapes of the relationship between daily TWD and canopy Ψ , we recommend species- and site-specific calibration curves. If possible, we also suggest to establish separate relationships for daily TWD with $\Psi_{\text{pre-dawn}}$ and Ψ_{midday} , since they might correlate better with different variants of daily TWD (c.f. Fig. 5) and to check the consistency of this relationship across DBH and age classes since tree hydraulics have been shown to change with time (Yoder et al. 1994, Hubbard et al. 1999). Moreover, we recommend to work with absolute instead of normalized TWD values when continuously measuring SDV in a forest since reference values should preferably be the extreme values measured under very dry conditions to properly represent the range of Ψ that can be expected in a species. While additional assessments will further improve the predictive power of TWD values for canopy Ψ , our data show that TWD can yet be readily applied for the qualitative assessment of a tree's daily water status without further calibrations. This is especially important if no quantitative relationships could be established because of a usually limited canopy access in large trees.

Acknowledgements

We acknowledge the help of crane operator Lucio Rizzelli and student assistant Florian Cueni, statistical hints from Dr. Peter Stoll and technical support by Decentlab GmbH and Georges Grun. We thank eight anonymous reviewers for helpful comments on an earlier version of the manuscript. Funding for this project came from the University of Basel. The canopy crane was sponsored by the Swiss Federal Office for the Environment (FOEN). The authors assert that the reported study bears no conflict of interest.

References

- Augie B (2015) gridExtra: Miscellaneous Functions for “Grid” Graphics. R package version 2.0.0. <http://CRAN.R-project.org/package=gridExtra>.
- Biondi F, Rossi S (2014) Plant-water relationships in the Great Basin Desert of North America derived from *Pinus monophylla* hourly dendrometer records. *Int J Biometeorol* 59:939–953.
- Braekke FH, Kozlowski TT (1975) Shrinkage and swelling of stems of *Pinus resinosa* and *Betula papyrifera* in northern Wisconsin. *Plant and Soil* 43:387–410.
- Braun WJ (2015) MPV: Data Sets from Montgomery, Peck and Vining’s Book. R package version 1.38. <https://CRAN.R-project.org/package=MPV>
- Brinkmann N, Eugster W, Zweifel R, Buchmann N, Kahmen A (2016) Temperate tree species show identical response in tree water deficit but different sensitivities in sap flow to summer soil drying. *Tree Physiology* 36:1508–1519.
- Cermák J, Kucera J, Bauerle WL, Phillips N, Hinckley TM (2007) Tree water storage and its diurnal dynamics related to sap flow and changes in stem volume in old-growth Douglas-fir trees. *Tree Physiology* 27:181–198.
- Chan T, Hölttä T, Berninger F, Mäkinen H, Nöjd P, Mencuccini M, Nikinmaa E (2015) Separating water-potential induced swelling and shrinking from measured radial

- stem variations reveals a cambial growth and osmotic concentration signal. *Plant Cell & Environment* 39:233–244.
- Cochard H, Forestier S, Améglio T (2001) A new validation of the Scholander pressure chamber technique based on stem diameter variations. *Journal of Experimental Botany* 52:1361–1365.
- Conejero W, Alarcón JJ, García-Orellana Y, Abrisqueta JM, Torrecillas A (2007) Daily sap flow and maximum daily trunk shrinkage measurements for diagnosing water stress in early maturing peach trees during the post-harvest period. *Tree Physiology* 27:81–88.
- Conejero W, Mellisho CD, Ortuño MF, Galindo A, Pérez-Sarmiento F, Torrecillas A (2010) Establishing maximum daily trunk shrinkage and midday stem water potential reference equations for irrigation scheduling of early maturing peach trees. *Irrigation Science* 29:299–309.
- Cosgrove DJ (2005) Growth of the plant cell wall. *Nat Rev Mol Cell Biol* 6:850–861.
- Cuny HE, Rathgeber CBK, Frank D, Fonti P, Mäkinen H, Prislan P, Rossi S, del Castillo EM, Campelo F, Vavrčik H, Camarero JJ, Bryukhanova MV, Jyske T, Gričar J, Gryc V, De Luis M, Vieira J, Čufar K, Kiryanov AV, Oberhuber W, Trembl V, Huang J-G, Li X, Swidrak I, Deslauriers A, Liang E, Nöjd P, Gruber A, Nabais C, Morin H, Krause C, King G, Fournier M (2015) Woody biomass production lags stem-girth increase by over one month in coniferous forests. *Nature Plants* 1:1–6.
- Daudet F-A, Améglio T, Cochard H, Archilla O, Lacoite A (2005) Experimental analysis of the role of water and carbon in tree stem diameter variations. *Journal of Experimental Botany* 56:135–144.
- De Schepper V, van Dusschoten D, Copini P, Jahnke S, Steppe K (2012) MRI links stem water content to stem diameter variations in transpiring trees. *Journal of Experimental Botany* 63:2645–2653.

- De Swaef T, Steppe K, Lemeur R (2009) Determining reference values for stem water potential and maximum daily trunk shrinkage in young apple trees based on plant responses to water deficit. *Agricultural Water Management* 96:541-550.
- De Swaef T, De Schepper V, Vandegehuchte MW, Steppe K (2015) Stem diameter variations as a versatile research tool in ecophysiology. *Tree Physiology* 35:1047–1061.
- Deslauriers A, Anfodillo T, Rossi S, Carraro V (2007) Using simple causal modeling to understand how water and temperature affect daily stem radial variation in trees. *Tree Physiology* 27:1125–1136.
- Dowle M, Srinivasan A, Short T, Lianoglou S (2015) data.table: Extension of Data.frame. R package version 1.9.6. <http://CRAN.R-project.org/package=data.table>.
- Drew DM, Richards AE, Downes GM, Cook GD, Baker P (2011) The development of seasonal tree water deficit in *Callitris intratropica*. *Tree Physiology* 31:953–964.
- Ehrenberger W, Rüger S, Fitzke R, Vollenweider P, Günthardt-Georg M, Kuster T, Zimmermann U, Arend M (2012) Concomitant dendrometer and leaf patch pressure probe measurements reveal the effect of microclimate and soil moisture on diurnal stem water and leaf turgor variations in young oak trees. *Functional Plant Biology* 39:297–305.
- Evert RF (2006) *Esau's plant anatomy: meristems, cells, and tissues of the plant body: their structure, function, and development*, 3rd edn. John Wiley and sons Inc., Hoboken.
- Fereres E, Orgaz F, Castro J, Humanes MD (1999) The relations between trunk diameter fluctuations and tree water status in olive trees (*Olea europea* L.). *Acta Horticulturae* 537:293–297.
- Fernández JE, Cuevas MV (2010) Irrigation scheduling from stem diameter variations:

- A review. *Agricultural and Forest Meteorology* 150:135–151.
- Franks PJ, Buckley TN, Shope JC, Mott KA (2001) Guard cell volume and pressure measured concurrently by confocal microscopy and the cell pressure probe. *Plant Physiology* 125:1577–1584.
- Génard M, Fishman S, Vercambre G, Hugué JG, Bussi C, Besset J, Habib R (2001) A biophysical analysis of stem and root diameter variations in woody plants. *Plant Physiology* 126:188 – 202.
- Heine RW (1971) Hydraulic conductivity in trees. *Journal of Experimental Botany* 22:503–511.
- Hellkvist J, Hillerdal-Hagströmer K, Mattson-Djos E (1980) Field studies of water relations and photosynthesis in Scots pine using manual techniques. *Ecological Bulletins* 32:183–204.
- Hinckley TM, Bruckerhoff DN (1975) The effects of drought on water relations and stem shrinkage of *Quercus alba*. *Canadian Journal of Botany* 53:62-72.
- Hölttä T, Vesala T, Nikinmaa E, Peramaki M, Siivola E, Mencuccini M (2005) Field measurements of ultrasonic acoustic emissions and stem diameter variations. New insight into the relationship between xylem tensions and embolism. *Tree Physiology* 25:237–243.
- Hölttä T, Vesala T, Peramaki M, Nikinmaa E (2002) Relationships between Embolism, Stem Water Tension, and Diameter Changes. *Journal of Theoretical Biology* 215:23–38.
- Hubbard RM, Bond BJ, Ryan MG (1999) Evidence that hydraulic conductance limits photosynthesis in old *Pinus ponderosa* trees. *Tree Physiology* 19:165–172
- Intrigliolo DS, Castel JR (2007) Evaluation of grapevine water status from trunk diameter variations. *Irrigation Science* 26:49–59.

- Irvine J, Grace J (1997) Continuous measurements of water tensions in the xylem of trees based on the elastic properties of wood. *Planta* 202:455–461.
- King G, Fonti P, Nievergelt D, Büntgen U, Frank D (2013) Climatic drivers of hourly to yearly tree radius variations along a 6°C natural warming gradient. *Agricultural and Forest Meteorology* 168:36–46.
- Klepper B, Browning VD, Taylor HM (1971) Stem diameter in relation to plant water status. *Plant Physiology* 48:683–685.
- Klepper B, Taylor HM, Huck MG, Fiscus EL (1973) Water Relations and Growth of Cotton in Drying Soil. *Agronomy Journal* 65:307–310.
- Kozlowski TT (1972) Shrinking and swelling of plant tissues. In: Kozlowski TT (ed) *Water deficits and plant growth*, Academic Press. *Water deficits and plant growth*, New York
- Kozlowski TT, Winget CH (1964) Diurnal and seasonal variation in radii of tree stems. *Ecology* 45:149–155.
- Larcher W (2003) *Physiological Plant Ecology*. Springer Berlin Heidelberg, Berlin, Heidelberg.
- Lassoie JP (1973) Diurnal dimensional fluctuations in a Douglas-fir stem in response to tree water status. *Forest Science* 19:251–255.
- McBurney T, Costigan PA (1984) The relationship between stem diameter and water potentials in stems of young cabbage plants. *Journal of Experimental Botany* 35:1787–1793.
- Mencuccini M, Salmon Y, Mitchell P, Hölttä T, Choat B, Meir P, O'Grady A, Tissue D, Zweifel R, Sevanto S, Pfautsch S (2017) An empirical method that separates irreversible stem radial growth from bark water content changes in trees: theory and case studies. *Plant Cell & Environment* 40:290–303.

- Milne R (1989) Diurnal water storage in the stems of *Picea sitchensis* (Bong.) Carr. *Plant, Cell & Environment* 12:63–72.
- Molz FJ, Klepper B (1973) On the Mechanism of Water-Stress-Induced Stem Deformation. *Agronomy Journal* 65:304–306.
- Montgomery DC, Peck EA, Vining GG (2015) Introduction to linear regression analysis. John Wiley and sons.
- Offenthaler I, Hietz P, Richter H (2001) Wood diameter indicates diurnal and long-term patterns of xylem water potential in Norway spruce. *Trees* 15:215–221.
- Orth R, Zscheischler J, Seneviratne SI (2016) Record dry summer in 2015 challenges precipitation projections in Central Europe. *Scientific Reports* 6:1–8.
- Ortuño MF, Conejero W, Moreno F, Moriana A, Intrigliolo DS, Biel C, Mellisho CD, Pérez-Pastor A, Domingo R, Ruiz-Sánchez MC, Casadesus J, Bonany J, Torrecillas A (2010) Could trunk diameter sensors be used in woody crops for irrigation scheduling? A review of current knowledge and future perspectives. *Agricultural Water Management* 97:1–11.
- Ortuño MF, García-Orellana Y, Conejero W (2006) Stem and leaf water potentials, gas exchange, sap flow, and trunk diameter fluctuations for detecting water stress in lemon trees. *Trees* 20:1–8.
- Pepin S, Körner C (2002) Web-FACE: a new canopy free-air CO₂ enrichment system for tall trees in mature forests. *Oecologia* 133:1–9.
- Peramaki M, Nikinmaa E, Sevanto S, Ilvesniemi H, Siivola E, Hari P, Vesala T (2001) Tree stem diameter variations and transpiration in Scots pine: an analysis using a dynamic sap flow model. *Tree Physiology* 21:889–897.
- Pfautsch S, Hölltä T, Mencuccini M (2015) Hydraulic functioning of tree stems—fusing ray anatomy, radial transfer and capacitance Way D (ed). *Tree Physiology*

35:706–722.

- Pfautsch S, Renard J, Tjoelker MG, Salih A (2015) Phloem as Capacitor: Radial Transfer of Water into Xylem of Tree Stems Occurs via Symplastic Transport in Ray Parenchyma. *Plant Physiology* 167:963–971.
- Puerto P, Domingo R, Torres R, Pérez-Pastor A, García-Riquelme M (2013) Remote management of deficit irrigation in almond trees based on maximum daily trunk shrinkage. *Water relations and yield. Agricultural Water Management* 126:33–45.
- R Core Team (2015) R: A language and environment for statistical computing. R Foundation for Statistical Computing, Vienna, Austria.
- Ruts T, Matsubara S, Wiese-Klinkenberg A, Walter A (2012) Diel patterns of leaf and root growth: endogenous rhythmicity or environmental response? *Journal of Experimental Botany* 63:3339–3351.
- Ryan JA, Ulrich JM (2014) xts: eXtensible Time Series. R package version 0.9-7. <http://CRAN.R-project.org/package=xts>.
- Scholz FC, Bucci SJ, Goldstein G, Meinzer FC, Franco AC, Miralles-Wilhelm F (2008) Temporal dynamics of stem expansion and contraction in savanna trees: withdrawal and recharge of stored water. *Tree Physiology* 28:469–480.
- Sevanto S, Vesala T, Peramaki M, Nikinmaa E (2002) Time lags for xylem and stem diameter variations in a Scots pine tree. *Plant Cell & Environment* 25:1071–1077.
- Steppe K, Lemeur R (2007) Effects of ring-porous and diffuse-porous stem wood anatomy on the hydraulic parameters used in a water flow and storage model. *Tree Physiology* 27:43–52.
- Steppe K, De Pauw DJW, Lemeur R, Vanrolleghem PA (2006) A mathematical model linking tree sap flow dynamics to daily stem diameter fluctuations and radial stem growth. *Tree Physiology* 26:257–273.

- Steppe K, Sterck F, Deslauriers A (2015) Diel growth dynamics in tree stems: linking anatomy and ecophysiology. *Trends in Plant Science* 20:335–343.
- Stedle E, Zimmermann U (1977) Effect of turgor pressure and cell size on the wall elasticity of plant cells. *Plant Physiology* 59:285–289.
- Turcotte A, Rossi S, Deslauriers A, Krause C, Morin H (2011) Dynamics of depletion and replenishment of water storage in stem and roots of black spruce measured by dendrometers. *Frontiers in Plant Science* 2:1-8.
- Tuszynski J (2014) caTools: moving window statistics, GIF, Base64, ROC, AUC, etc.. R package version 1.17.1. <http://CRAN.R-project.org/package=caTools>.
- Ueda M, Shibata E (2001) Diurnal changes in branch diameter as indicator of water status of Hinoki cypress *Chamaecyparis obtusa*. *Trees* 15:315–318.
- Velez JE, Intrigliolo DS, Castel JR (2007) Scheduling deficit irrigation of citrus trees with maximum daily trunk shrinkage. *Agricultural Water Management* 90:197–204.
- Vergeynst LL, Dierick M, Bogaerts JAN, Cnudde V, Steppe K (2015) Cavitation: a blessing in disguise? New method to establish vulnerability curves and assess hydraulic capacitance of woody tissues. *Tree Physiology* 35:400–409.
- Wickham H (2009) *ggplot2: elegant graphics for data analysis*. Springer New York.
- Wickham H (2015) scales: Scale Functions for Visualization. R package 0.3.0. <http://CRAN.R-project.org/package=scales>.
- Yoder BJ, Ryan MG, Waring RH, Schoettle AW, Kaufmann MR (1994) Evidence of reduced photosynthetic rates in old trees. *Forest Science* 40:513–527.
- Zeileis A, Grothendieck G (2005) zoo: S3 Infrastructure for Regular and Irregular Time Series. *Journal of Statistical Software* 14:1-27.

- Zweifel R (2006) Intra-annual radial growth and water relations of trees: implications towards a growth mechanism. *Journal of Experimental Botany* 57:1445–1459.
- Zweifel R (2016) Radial stem variations - a source of tree physiological information not fully exploited yet. *Plant, Cell & Environment* 39:231–232.
- Zweifel R, Hasler R (2001) Dynamics of water storage in mature subalpine *Picea abies*: temporal and spatial patterns of change in stem radius. *Tree Physiology* 21:561–569.
- Zweifel R, Drew DM, Schweingruber F, Downes GM (2014) Xylem as the main origin of stem radius changes in *Eucalyptus*. *Functional Plant Biology* 41:520–15.
- Zweifel R, Haeni M, Buchmann N, Eugster W (2016) Are trees able to grow in periods of stem shrinkage? *The New Phytologist* 211:839–849.
- Zweifel R, Häsler R, Item H (2001) Link between diurnal stem radius changes and tree water relations. *Tree Physiology* 21:869–877.
- Zweifel R, Item H, Hasler R (2000) Stem radius changes and their relation to stored water in stems of young Norway spruce trees. *Trees* 15:50–57.
- Zweifel R, Zimmermann L, Newbery DM (2005) Modeling tree water deficit from microclimate: an approach to quantifying drought stress. *Tree Physiology* 25:147–156.

Tree Physiology

Supporting Information

Article title: Daily stem diameter variations can predict the canopy water status of mature temperate trees

Authors: Lars Dietrich, Roman Zweifel, Ansgar Kahmen

Article acceptance date: 18 March 2018

The following Supporting Information is available for this article:

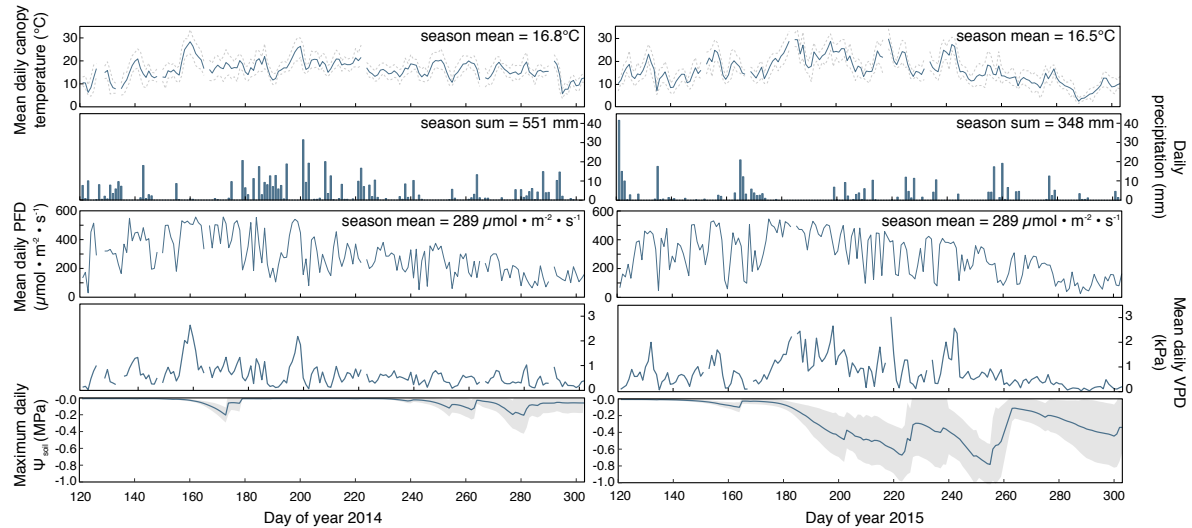


Fig. S1 Environmental data for the growing seasons 2014 and 2015. Dashed lines around mean daily temperature are minimum and maximum temperatures of the respective day. All variables except Ψ_{soil} were measured with a weather station at the top of the canopy crane at 40m above ground. Ψ_{soil} was calculated as the mean of the daily maxima of 20 (2014) and 12 (2015) sensors at a depth of $-20 \text{ cm} \pm \text{SD}$.

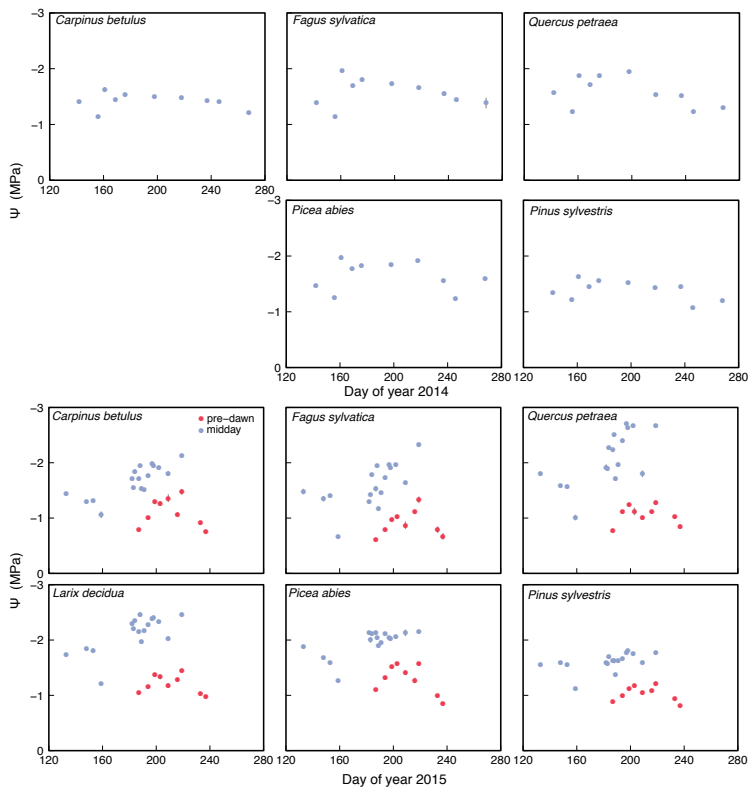


Fig. S2 Measured midday (blue circles) and pre-dawn (red circles) Ψ of the six species during the growing seasons of 2014 and 2015 (mean \pm SD). Ψ was measured as the mean of three terminal shoots always nearly at the same positions in the sunlit crown of 4 individuals per species ($n=4$) around noon (midday) or shortly before sunrise (pre-dawn) with a scholander pressure bomb. Crown access was provided by a canopy crane. Note that the y-axis is twisted.

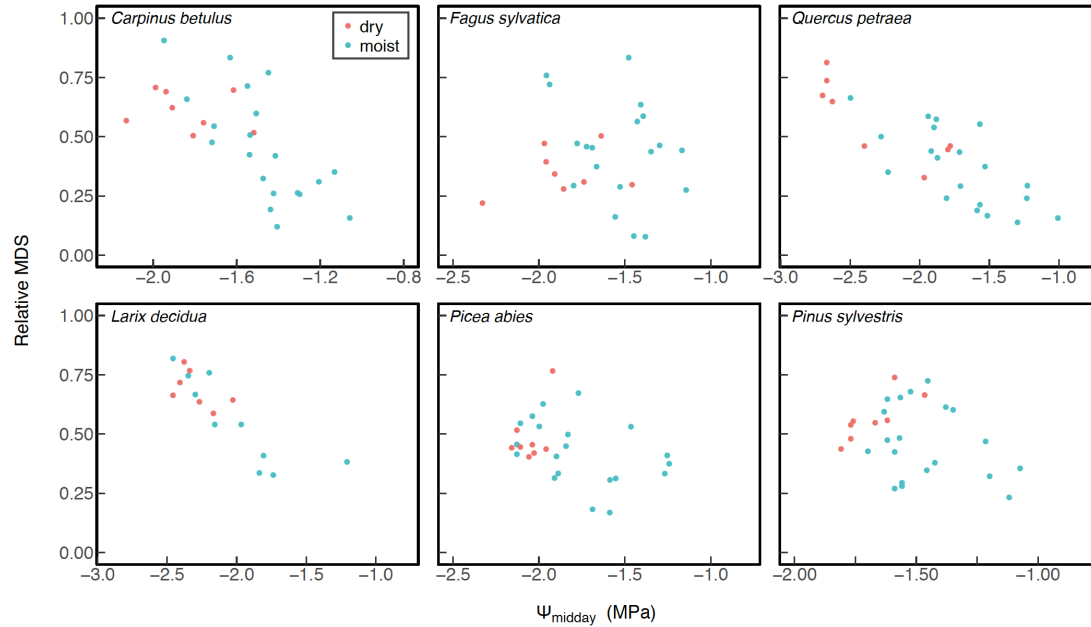


Fig. S3 Relative maximum daily shrinkage (MDS) as related to Ψ_{midday} in the six different species during the growing seasons of 2014 and 2015. Red circles represent values obtained while Ψ_{soil} was below -0.25 MPa, blue circles are values measured at $\Psi_{\text{soil}} > -0.25$ MPa. Statistical parameters can be obtained from Fig. 5. Relative MDS was calculated by dividing each absolute value by the highest measured value throughout the two growing seasons.

Chapter 2

Quantification of uncertainties in conifer sap flow measured with the thermal dissipation method

Richard L. Peters^{1,2,a}, Patrick Fonti¹, David C Frank^{1,3,4}, Rafael Poyatos^{5,6}, Christoforos Pappas⁷, Ansgar Kahmen², Vinicio Carraro⁸, Angela L Prendin⁸, Loïc Schneider¹, Jennifer Baltzer⁹, Greg Barron-Gafford¹⁰, Lars Dietrich², Ingo Heinrich¹¹, Rebecca L. Minor¹⁰, Oliver Sonnentag⁷, Ashley M. Matheny¹², Maxwell G. Wightman¹³, Kathy Steppe¹⁴

¹Landscape Dynamics, Swiss Federal Research Institute for Forest, Snow and Landscape Research (WSL), Zürcherstrasse 111, CH-8903 Birmensdorf, Switzerland

²Department of Environmental Sciences - Botany, Basel University, Schönbeinstrasse 6, CH-4056 Basel, Switzerland

³Laboratory of Tree-Ring Research, 1215 E. Lowell Street, AZ 8572 Tucson, USA

⁴Oeschger Centre for Climate Change Research, Falkenplatz 16, CH-3012 Bern, Switzerland

⁵CREAF, Cerdanyola del Vallès, Barcelona, Catalonia, Spain

⁶Department of Applied Ecology and Environmental Biology, Laboratory of Plant Ecology, Ghent University, Coupure links 653, B-9000 Ghent, Belgium

⁷Département de géographie and Centre d'études nordiques, Université de Montréal, Montréal, QC, Canada

⁸Dept. Territorio e Sistemi Agro-Forestali, Università degli Studi di Padova, Viale dell'Università 16, I-35020 Legnaro (PD), Italy

⁹Department of Biology, Wilfrid Laurier University, Waterloo, ON, Canada

¹⁰School of Geography and Development, University of Arizona, 1064 E Lowell St, AZ 85719 Tucson, USA

¹¹Helmholtz Centre Potsdam, GFZ German Research Centre for Geosciences, Climate Dynamics and Landscape Evolution, Telegrafenberg, 14473 Potsdam, Germany

¹²Department of Geological Sciences, Jackson School of Geosciences, 2305 Speedway Stop,
C1160 Austin, USA

¹³College of Forestry, Oregon State University, 1500 SW Jefferson St., OR 97331 Corvallis,
USA

¹⁴Laboratory of Plant Ecology, Department of Applied Ecology and Environmental Biology,
Faculty of Bioscience Engineering, Ghent University, Coupure links 653, B-9000 Ghent,
Belgium

^aCorresponding author: Tel: +41 44 7392 816

e-mail: richard.peters@wsl.ch

Published in New Phytologist.

Summary

Trees play a key role in the global hydrological cycle and measurements performed with the thermal dissipation method (TDM) have been crucial in providing whole-tree water use estimates. Yet, different data processing to calculate whole-tree water use encapsulate uncertainties that have not been systematically assessed.

We quantified uncertainties in conifer sap flux density (F_d) and stand water use caused by commonly applied methods for deriving zero-flow conditions, dampening and sensor calibration. Their contribution has been assessed using a stem segment calibration experiment and four years of TDM measurements in *Picea abies* (L.) Karst. and *Larix decidua* Mill., growing in contrasting environments. Uncertainties were then projected on TDM data from different conifers across the northern hemisphere.

Commonly applied methods mostly underestimated absolute F_d . Lacking a site- and species-specific calibrations reduced our stand water use measurements by 37% and induced uncertainty in northern hemisphere F_d . Additionally, although the inter-daily variability was maintained, disregarding dampening and/or applying zero-flow conditions that ignored nighttime water use reduced the correlation between environment and F_d .

The presented ensemble of calibration curves and proposed dampening correction, together with the systematic quantification of data-processing uncertainties, provide crucial steps in improving whole-tree water use estimates across spatial and temporal scales.

Introduction

Accurate measurements of whole-tree water use are important as terrestrial plant transpiration plays a key role in the global hydrological cycle (Holbrook & Zwieniecki, 2003; Schlesinger & Jasechko, 2014; Good *et al.*, 2015; Fatichi & Pappas, 2017). Furthermore, measurements of whole-tree transpiration show great value in validating regional water-balance simulations (Wilson *et al.*, 2001; Ford *et al.*, 2007; Reyes-Acosta & Lubczynski, 2013), inter-specific comparison of stomatal conductance behaviour (Damour *et al.*, 2010), modelling stable isotope enrichment (Song *et al.*, 2013; Sutanto *et al.*, 2014) and mechanistically explaining wood formation (De Schepper & Steppe, 2010; Fatichi *et al.*, 2014; Steppe *et al.*, 2015). Whole-tree transpiration can be estimated by upscaling measurements of leaf-level transpiration or by partitioning eddy covariance flux tower data, which both require assumptions on crown and canopy architecture (Ansley *et al.*, 1994; Hatton & Wu, 1995; Lawrence *et al.*, 2007; Matheny *et al.*, 2014; Fatichi *et al.*, 2016). The development of heat-based sap flow methods applied at the tree-stem level avoids these issues, and has provided whole-tree water use estimates across a wide range of spatiotemporal scales (Swanson 1994; Smith & Allen, 1996; Kallarackal *et al.*, 2013, Van de Wal *et al.*, 2015).

Since 1985 over 1200 studies have collected heat-based sap flow measurements, to assess the effect of environment on transpiration and quantify forest stand water use (Fig. 1a). Due to their low cost, ease of use, low energy requirement, and long-term measurement potential (Oliveras & Llorens, 2001; Lu *et al.*, 2004), sap flow data generated with the thermal dissipation method (TDM; Granier *et al.*, 1985, 1987) far exceed any other method (Poyatos *et al.*, 2016), including heat pulse velocity (Green *et al.*, 2003), stem heat balance (Langensiepen *et al.*, 2014), heat field deformation (Čermák *et al.*, 2004), heat ratio method (Burgess *et al.*, 2001) and trunk segment heat balance (Smith & Allen, 1996).

TDM measures sap flux density (F_d) by inserting two axially aligned probes into the sapwood and determining the temperature difference between a continuously heated probe and the non-heated reference (expressed as ΔT [°C]). F_d is typically estimated by first calculating the proportional difference between measured ΔT (denoted as the unitless K [-]) and zero sap flow conditions (denoted as ΔT_{\max} ; cf. Lu *et al.*, 2004). Next, F_d is calculated from K , using a calibration curve (Ganier *et al.*, 1985). Ignoring radial or circumferential profiles F_d can then be multiplied by the sapwood area to obtain

whole-tree sap flow and potentially upscaled to stand water use (Granier *et al.*, 1987; Čermák *et al.*, 1995; Matheny *et al.*, 2014). Despite its simplicity, alternatives to process raw TDM measurements (cf. Fig. 1b) generate a range of potential F_d values, and subsequently cause uncertainty in the quantification of whole-tree and stand water use. Typically, one set of TDM probes is installed per tree, assuming this local measurement represents sap flow in the entire stem. Yet, in some cases, strong radial and circumferential variations in sap flow require the installation of additional probes at different sapwood depths or circumferential positions (Lu *et al.*, 2000; Nadezhdina *et al.*, 2002; Fiora & Cescatti, 2006; Saveyn *et al.*, 2008), which is not always considered (54% of studies do not account for this variability; cf. rad./circ. variation in Fig. 1b). Next, it is frequently assumed that the probes are inserted into the sapwood, although measured ΔT can be altered when partially inserted into non-conducting heartwood (Lu *et al.*, 2004). In spite of available correction methods (cf. Clearwater *et al.*, 1999), heartwood-sapwood boundaries can often not be precisely defined and may vary considerably within the stem (17% of studies apply a correction; cf. heartwood presence in Fig. 1b; Longuetaud *et al.*, 2006; Paudel *et al.*, 2013). Finally, natural variations in thermal conditions may alter ΔT (Köstner *et al.*, 1998; Do & Rocheteau, 2002; Vergeynst *et al.*, 2014), which can be resolved, although this often requires more specialized, expensive and often energy demanding sap flow methods (e.g. Nourtier *et al.*, 2011; Lubczynski *et al.*, 2012; Vandegehuchte & Steppe, 2012).

In addition to anatomical and morphological issues related to ΔT measurements, data-processing procedures to calculate F_d from ΔT present sources of uncertainty. First, zero-flow conditions (ΔT_{\max}) have to be defined as a reference. The common practise is to assume that zero-flow conditions occur pre-dawn, neglecting nighttime activity (42% of the studies do not report the used zero-flow procedure; cf. ΔT_{\max} in Fig. 1b). Yet, previous findings demonstrate nighttime transpiration (Caird *et al.*, 2007; Novick *et al.*, 2009; Berkelhammer *et al.*, 2013). Due to the way in which K and F_d are calculated, a small change in nighttime activity could result in large offsets in daily F_d (Rabbel *et al.*, 2016). This argues for the application of environmentally or tree physiologically based criteria to define when zero flow occurs (Regalado & Ritter, 2007; Oishi *et al.*, 2008). Second, it is often assumed that installation of the probes into living xylem tissue causes only slight dampening of the signal due to probes burrowing deeper into the wood and wounding response that could alter K (Moore *et al.*, 2010;

Wullschleger *et al.*, 2011; Wiedemann *et al.*, 2016). Yet, most studies with a duration equal to or longer than one growing season (58% of studies; cf. duration in Fig. 1b) do not account for these effects (Lu *et al.*, 2004). Finally, most studies use the empirical calibration curve established by Granier (1985) to calculate F_d (90% of studies; cf. calibration in Fig. 1b). Nonetheless, multiple studies contest its validity and propose species-specific calibrations (Bush *et al.*, 2010; Steppe *et al.*, 2010; Sun *et al.*, 2012; Ma *et al.*, 2017). Many different combinations of these data-processing procedures are applied in the literature (Fig. 1b), which might jeopardize climate-response analyses (Poyatos *et al.*, 2005), inter-species comparisons (Kunert *et al.*, 2010; Brinkmann *et al.*, 2016) or large-scale data collection initiatives (Poyatos *et al.*, 2016). Although general reviews exist and individual data-processing procedures have been analysed, a systematic quantification on the impact of different combinations of data-processing on TDM sap flow data is lacking.

In a systematic analysis, this study aims to quantify the impact of commonly applied data-processing procedures on sap flow estimates derived from single-point TDM measurements. In particular, in conifers, we (i) assess the effect of four commonly used methods to define zero-flow conditions on K , (ii) quantify the magnitude of K dampening and propose a correction, (iii) compare species-specific calibration curves to calculate F_d with previous studies, and (iv) quantify the uncertainty generated by combinations of these procedures on F_d , stand water use and inter-daily F_d variability compared to common practises. Four years of TDM sap flow measurements from *Picea abies* and *Larix decidua*, collected under contrasting field conditions in the Lötschental (Switzerland), were used for the uncertainty analysis. Additionally, a laboratory controlled stem calibration experiment was performed to analyse the heat dissipation properties of the wood and the results were compared with existing calibration curves. Observed uncertainties were propagated to TDM datasets collected from conifers across the northern hemisphere to illustrate the importance of carefully selecting TDM data-processing methods when estimating F_d .

Materials and methods

Study design and site description

To analyse the uncertainty caused by (i) data-processing procedures to calculate zero-flow conditions, (ii) signal dampening and (iii) applied calibration curves on K , F_d and stand water use, we continuously monitored sap flow in 27 conifer trees in the Lötschental for four years. This inner Alpine valley in Switzerland (46°23'40"N, 7°45'35"E) is covered by a mixed forest of deciduous *Larix decidua* Mill. and evergreen *Picea abies* (L.) Karst. We collected measurements from contrasting thermal and soil moisture conditions, as consistent differences in environmental conditions might promote nighttime activity and the magnitude of the dampening response. A total of five sites were selected along an elevational gradient, with colder conditions at higher elevations and contrasting dry and wet conditions in the valley bottom (Tab. 1; King *et al.*, 2013).

Table 1. Overview of sites and monitored trees. Mean ring width was calculated for the last 2 cm of wood, covering the extent of the inserted thermal dissipation probes. The three *Larix decidua* and *Picea abies* trees at each Lötschental site were continuously monitored from 2012-2015. Four trees from San Vito di Cadore were used for the cut stem segment calibration. See Table 2 for site coordinates and climatic conditions, indicated with LOT and the site code for the Lötschental and SVD for San Vito di Cadore. The - symbols indicates no data was available.

Site	Site code	Elevation [m a.s.l.]	Species	Age				DBH			Height			Sapwood thickness			Ring width	
																		[cm yr ⁻¹]
Switzerland, Lötschental	N13W	1300 (Wet)	<i>L. decidua</i>	148	164	134	78	89	52	28	33	26	2.2	2.4	2.4	0.06		
			<i>P. abies</i>	85	81	109	81	63	81	30	34	34	9.1	6.9	9.0	0.26		
	N13	1300 (Dry)	<i>L. decidua</i>	131	128	131	30	32	31	20	19	19	1.5	1.8	1.6	0.06		
			<i>P. abies</i>	90	93	87	31	37	48	15	20	19	2.5	5.3	5.1	0.13		
	S16	1600	<i>L. decidua</i>	371	69	69	75	39	42	32	25	24	3.5	2.6	3.7	0.16		
			<i>P. abies</i>	-	62	461	45	38	56	22	25	24	2.0	4.2	2.0	0.14		
	S19	1900	<i>L. decidua</i>	200	326	170	48	49	36	24	22	26	3.2	1.8	2.6	0.08		
			<i>P. abies</i>	137	229	245	34	48	37	25	25	21	1.7	5.5	3.6	0.06		
	S22	2200	<i>L. decidua</i>	269	280	295	47	56	46	18	17	17	2.4	3.1	1.8	0.09		
	Italy, San Vito di Cadore	1000	<i>L. decidua</i>	28	91	30	62	15	17	16	18	17	15	20	2.9	1.7	1.6	1.1
<i>P. abies</i>			50	35	73	28	16	16	20	12	18	16	14	9	3.1	5.0	3.3	2.8

A calibration curve was established for each tree species to calculate F_d using a laboratory calibration experiment on fresh cut-stem segments. The segments, collected from four trees per species, were harvested at the Centre for Studies on Alpine Environment of the University of Padova located in the Dolomite mountain region (Italy, San Vito di Cadore; Tab. 1), as harvesting stems in the Löttschental was logistically difficult. Although smaller in diameter, *P. abies* and *L. decidua* trees were selected with similar recent ring widths as observed in the Löttschental monitoring trees (Tab. 1).

The uncertainty introduced through data-processing methods for zero-flow conditions and sensor calibration was calculated for TDM datasets collected across the northern hemisphere for three conifer genera (Tab. 2). This analysis included datasets from Europe and North America. In total, 131 individual trees from 18 sites were included with climatic conditions ranging from 1.4-19.8 °C mean annual temperature and 428-1452 mm mean annual precipitation (Tab. 2).

Field measurements

At each Löttschental site, three mature dominant trees per species were selected for continuous sap flow monitoring from May 2012 until October 2015 (Tab. 1). New TDM probes were additionally installed with a horizontal distance of 10-15 cm away from the initial probes on four trees to assess dampening effects (one per species at S19 and N13 in June 2015). Environmental conditions were monitored at each site with a 15 to 60 minute interval (King *et al.*, 2013). A radiation-shield covered sensor was installed on a central tower (≈ 2.5 m above the ground) within the canopy to measure both air temperature (T [°C]) and relative humidity (RH [%]; Onset, USA, U23-002 Pro), used to calculate vapour pressure deficit (D [kPa]; cf. WMO, 2008). Soil volumetric water content was measured hourly with five sensors at 10 and 70 cm depth in the centre of each site (θ [%]; Decagon, USA, EC-5). Solar irradiance (R_g [$W\ m^{-2}$]) was measured hourly in an open field at N13 using a micro-station (Onset, USA, H21-002 Micro Station) and pyranometer (Onset, USA, S-LIB-M003). Daily precipitation data was obtained from the nearest weather stations, where the distance to the site was used to calculate a weighted mean from the nine included stations (ranging from 6 to 43 km; Federal Office of Meteorology and Climatology MeteoSwiss).

For upscaling to whole-tree water use, sapwood thickness [cm] and ring width [mm] were measured from two increment wood cores taken perpendicular to the slope at breast height from the monitored trees (avoiding the slope-facing side with installed probes) and trees surrounding the site (cf. Peters *et al.*, 2017). Sapwood area was used for upscaling F_d to whole-tree water use, while ignoring radial and circumferential variability. For upscaling to stand water use, diameter at breast height (DBH) measurements were taken from all trees within 20 m (at S22), 15 m (at S19 and S16) and 10 m (at N13 and N13W) radius fixed plots, and used in combination with sapwood allometric relationships (Fig. S1; cf. Čermák *et al.*, 1995).

Thermal dissipation method

Sap flux density (F_d [$\text{cm}^3 \text{cm}^{-2} \text{h}^{-1}$]) was measured using commercially available TDM probes (cf. Granier 1985; Tesaf, University of Padova, Italy). Two 20 mm long stainless steel probes, with a 2 mm diameter, were radially inserted into the xylem, with a vertical distance of 10 cm on the slope-facing side of the stem at ≈ 1.6 m height. The temperature difference between the continuously heated upper and unheated lower probe was measured (ΔT [$^{\circ}\text{C}$]) and stored with a 15-minute resolution on a data logger (Campbell Scientific, USA, CR1000). The maximum ΔT (ΔT_{\max} [$^{\circ}\text{C}$]) was used to obtain K [-] according to Equation 1. K can be calibrated to obtain F_d using a power-type relationship with α [$\text{cm}^3 \text{cm}^{-2} \text{h}^{-1}$] = 42.84 (0.0119 [$\text{cm}^3 \text{cm}^{-2} \text{s}^{-1}$] \times 3600) and β [-] = 1.231 (Granier *et al.*, 1985), according to Equation 2.

$$K = \frac{\Delta T_{\max} - \Delta T}{\Delta T} \quad (1)$$

$$F_d = \alpha \cdot K^{\beta} \quad (2)$$

ΔT was corrected (denoted as ΔT_{sw} [$^{\circ}\text{C}$]) for the proportion of the probe that was inserted in the sapwood (γ [cm cm^{-1}]) versus the proportion in the inactive heartwood and used instead of ΔT in Equation 1 (Clearwater *et al.*, 1999):

$$\Delta T_{\text{sw}} = \frac{(\Delta T - (1 - \gamma) \cdot \Delta T_{\max})}{\gamma} \quad (3)$$

Because our sensors were measuring over four years and the probes could progressively burrow deeper into the heartwood, γ was annually corrected for the ring width occurring

after the installation year. For this correction we assumed sapwood thickness remained constant.

Zero-flow conditions

Four methods to calculate zero-flow conditions (ΔT_{\max}) were used, including the daily pre-dawn (PD; Lu *et al.*, 2004), maximum moving window (MW; Rabbel *et al.*, 2016), double regression (DR; Lu *et al.*, 2004) and environmental dependent method (ED; Oishi *et al.*, 2016). The PD method was applied by selecting daily maximum ΔT values occurring between 00:00 and 08:00 hours (GMT) when R_g was below 100 W m^{-2} . For the MW method, maximum ΔT_{\max} was calculated during an 11-day window from the pre-dawn ΔT_{\max} values. The DR method was applied by calculating the mean over pre-dawn ΔT_{\max} with a moving-window of 11-days, removing all values below the mean, and calculating a second 11-day moving window which was used as ΔT_{\max} . The ED method was applied according to Oishi *et al.* (2016), where pre-dawn ΔT_{\max} values were selected when $T < 1 \text{ }^\circ\text{C}$ or D was $< 0.1\text{-}0.05 \text{ kPa}$ for a period of two hours (D threshold depending on elevation). In addition, the coefficient of variation of pre-dawn ΔT within this period should be below 0.5% to ensure selection of nights with stable zero-flow conditions. All ΔT_{\max} values were visually checked for drifts or outliers caused by low θ or low T .

Signal dampening detection and correction

First, data from long-term and newly installed probes were compared with linear regressions to demonstrate absolute offsets and daily maximum K variability. Second, the long-term data collected since 2012 was used to assess dampening for each monitored tree. Daily maximum K was used as the dependent variable within a Generalized Least Squares model (GLS in the “nlme” package for R software version 3.2.00, R development core team 2013; Pinheiro *et al.*, 2017), to account for high first-order temporal auto-correlation (cf. Zuur *et al.*, 2010). As independent variables, we selected daily maximum D , T , daily mean θ and day of year (DOY; to account for changes in leaf-phenological stages). Days with a daily maximum $K < 0.05$ and precipitation $> 1 \text{ mm d}^{-1}$ were excluded from the analysis, as these obstructed detection of the environmental relationships. The polynomial structure of the model was established using the Akaike Information Criterion (AIC), while accounting for

interactions between variables (e.g., high D coincides with low θ). Equation 4 was used to fit a function and calculate the residual K (K_{res} [-]; observed minus fitted values; cf. Tab. S1).

$$K_{\text{res}} = \text{resid} (\text{Intercept} + \varepsilon_1 \cdot D^{-1} + \varepsilon_2 \cdot T + \varepsilon_3 \cdot T^2 + \varepsilon_4 \cdot \theta^{-1} + \varepsilon_5 \cdot \text{DOY} + \varepsilon_6 \cdot \text{DOY}^2) \quad (4)$$

Monthly averages of K_{res} were calculated (to reduce first-order auto-correlation) and fitted to the mean time since installation (t [days]) with a third-order polynomial model to determine significant reductions in response to t .

For the study trees with a significant reduction in K ($p < 0.05$), a tree-specific function was fitted to generate a correction curve. To avoid overfitting with environmental variables, used in subsequent analyses, we only included seasonality (DOY) and the time since installation (t) as independent variables for the correction curve. A nonlinear model was fitted to the daily maximum K , excluding rainy days and low values to generate the correction curve (K_{cor} ; cf. Tab. S2):

$$K_{\text{cor}} = \frac{(a + b \cdot t)}{(1 + c \cdot t + d \cdot t^2)} + e \cdot \text{DOY} + f \cdot \text{DOY}^2 \quad (5)$$

The fitted parameters for t (with a , b , c and d) were used to correct K and scale it to the maximum value within the first year of installation (cf. Fig. S2 and S3).

Stem segment calibration

Calibration curves to calculate F_d were established by comparing gravimetrically induced flows through a stem segment against K measured with TDM probes. The stem segments, harvested in San Vito di Cadore, with a length of ~ 1 m (~ 50 cm above and below DBH), were transported to the laboratory in wet black plastic bags to prevent dehydration. Directly after harvesting, the stems were recut under water to ~ 25 cm in length and trimmed with razor blades to reopen closed tracheids. The stem segments were used for calibration within a Mariotte-based verification system (Steppe *et al.*, 2010). In short, a water-filled flask was connected to a plastic cylinder via flexible tubing, functioning as a siphon. The horizontal height of the flask was adjusted to deliver

a specific water flow to a cylinder attached to the top of the stem segment with installed TDM probes, producing a constant pressure head.

Within a temperature-controlled environment, no water flow was applied during a 10 hour period to generate zero-flow conditions. Next, the stem segment was flushed with water for 2 hours until the readings stabilized. The water level was increased and then decreased in 2, 5, 10, 15, 25 and 30 cm (± 0.5 cm) increments and kept constant at every level for 45 min (resulting in sap flux densities ranging from ~ 2 - 45 $\text{cm}^3 \text{cm}^{-2} \text{h}^{-1}$). Finally, no flow was generated for 4 hours, after which post- and pre-zero flow conditions were used to determine ΔT_{\max} with the TDM probes.

A calibration curve was established by fitting a quadratic function between K and the gravimetric F_d (providing a better relationship compared to a power function; cf. Tab. S3 and S4). Mixed-effect modelling was applied to test for species-specific differences in the calibration parameters using the “lme4” R package (Bates *et al.*, 2015), with the individual as a random factor. A literature review was performed on existing species-specific calibration curves in order to compare sampling locations, species, wood types, size of stem segments, sapwood properties, goodness-of-fit for the calibration curve and the calibration parameters.

Uncertainty analysis and upscaling

Uncertainty induced by different data-processing procedures on daily F_d and stand water use estimates was analysed by applying all available data-processing combinations on the Löttschental trees, including: (i) ΔT_{\max} calculation with PD, MW, DR or ED method, (ii) dampening or no dampening correction, and (iii) Granier’s original calibration or tree species-specific calibration. Absolute effects of all possible combinations on mean daily F_d (mean annual F_d in $\text{cm}^3 \text{cm}^{-2} \text{d}^{-1}$, averaged over all years of observation) and stand water use were calculated and compared to the commonly applied procedure (measuring for one growing season, using PD, no dampening correction and Granier’s calibration; Fig. 1b). Mean annual stand water use was calculated by averaging the 15-minute F_d measurements per site and species and multiplying them by the species-specific total sapwood area per site. For addressing inter-daily variability and the environmental response of F_d , daily F_d averaged per species and elevation was correlated against mean daily D (cf. Oren *et al.*, 1999; Moore *et al.*, 2010) with a third-order polynomial to obtain the changes in goodness-of-fit (expressed in R^2).

Northern hemisphere TDM measurements (Tab. 2) were used to illustrate the relevance of selected data-processing procedures. As most datasets had a short monitoring period, no dampening correction was applied and measurements from first year after sensor installation were used (except for VAL and TIL due to data gaps; cf. Tab. 2). The 99th quantile was determined for the maximum daily F_d calculated for all individuals from K within a site (generated with the reported ΔT_{\max} method; cf. Table 2), when using the different calibration curves available for softwood species, to avoid the effect of spurious outliers (excluding the steepest curves proposed by Lundblad *et al.*, 2001). Additionally, for sites where ΔT values were provided, various daily F_d time-series were calculated by using PD, MW or DR ΔT_{\max} and the softwood calibration curves (Tab. 2). The ED ΔT_{\max} method could not be applied due to the lack of high-quality environmental data. Uncertainty was quantified by calculating the mean daily F_d , after which the difference from the most commonly applied data-processing procedure was determined.

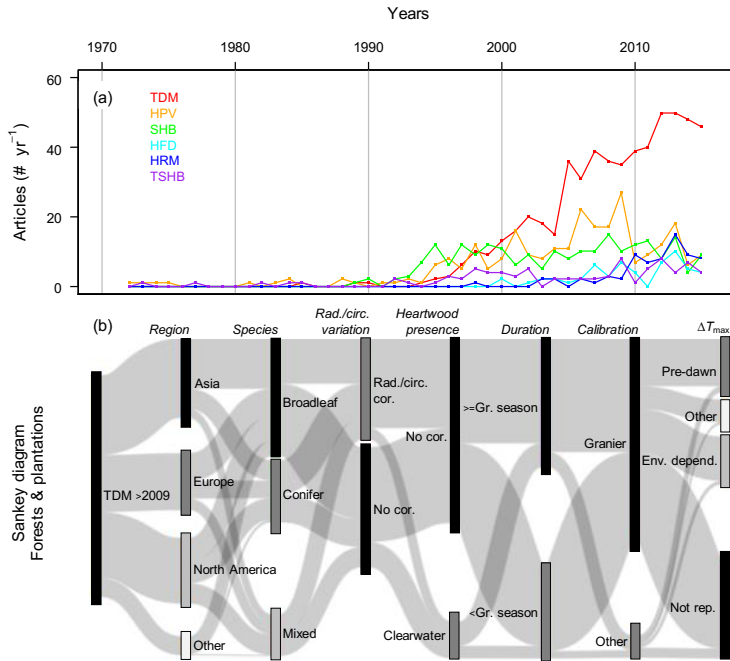


Figure 1. Literature review of heat-based sap flow methods. The search terms; “Stem”, “Tree” and “Sap flow”, were used in Scopus and Web of Science (www.webofknowledge.com and www.scopus.com; accessed on 01-12-2016). (a) Temporal development of the (major) applied methods from 1985-2015, including: Thermal Dissipation Method (TDM), Heat Pulse Velocity (HPV), Stem Heat Balance (SHB), Heat Field Deformation (HFD), Heat Ratio Method (HRM), and Trunk Segment Heat Balance (TSHB). (b) Sankey diagram revealing the proportion of studies from 2010-2016 within forests and plantations using TDM measurements, grouped according to region, species and different assumptions (175 studies). We noted; 1) the study location, 2) the study tree species, 3) whether corrections were made for radial or circumferential variation (Rad./circ. cor.), 4) whether corrections were applied for probes inserted into heartwood (cf. Clearwater *et al.*, 1999), 5) the temporal extent of the measurements (equal and longer or shorter than one growing season; Gr. Season), 6) whether the original (Granier *et al.*, 1985) or a species-specific calibration was used to calculate sap flux density, and 7) the assumptions for estimating zero-flow conditions (ΔT_{max}). Black bars indicate the most widely applied options.

Table 2. Overview of northern hemisphere sap flow measurements for the genera *Picea*, *Larix* and *Pinus* used for the uncertainty analysis. Latitude and longitude are provided in decimal degrees. Only dominant and co-dominant individuals are included within the analysis. Methods include: MW = moving window, DR = double regression and ED = environmental depended. The selected years, average DBH and number of individual trees are provided. Site conditions are described with elevation, mean annual temperature and total annual precipitation. No raw ΔT values were obtained for sites indicated with a * symbol.

Site	Country	Lat.	Long.	Species	Method	Year	DBH [cm]	Trees [#]	Elev. [m a.s.l.]	Temp. [°C]	Prec. [mm]	Source
Picea												
SOBS	Canada	53.987	-105.118	<i>Picea mariana</i>	ED	2016	12	9	598	1.4	428	Pappas <i>et al.</i> , (in press) King <i>et al.</i> , (2013)
LOTS19	Switzerland	46.400	7.746	<i>Picea abies</i>	ED	2012	40	3	1900	3.9	872	
LOTS16		46.397	7.755				47	3	1600	5	872	
LOTN13W		46.400	7.764				75	3	1300	5.5	872	
LOTN13		46.392	7.761				39	3	1300	5.7	872	
SVD*	Italy	46.450	12.214	<i>Picea abies</i>	MW	2008	-	2	1050	7	866	V. Carraro <i>et al.</i> , unpublished
VISP	Switzerland	46.303	7.741	<i>Picea abies</i>	DR	2014	37	3	800	9.2	581	King <i>et al.</i> , (2013)
HOF	Switzerland	47.467	7.500	<i>Picea abies</i>	MW	2014	60	4	550	10.5	990	Pepin and Kömer (2002)
Larix												
SOBS	Canada	53.987	-105.118	<i>Larix laricina</i>	ED	2016	18	9	598	1.4	428	Pappas <i>et al.</i> , (in press) King <i>et al.</i> , (2013)
LOTS22	Switzerland	46.400	7.743	<i>Larix decidua</i>	ED	2012	49	3	2200	3.2	872	
LOTS19		46.397	7.746				44	3	1900	3.9	872	
LOTS16		46.397	7.755				52	3	1600	5	872	

Site	Country	Lat.	Long.	Species	Method	Year	DBH [cm]	Trees [#]	Elev. [m a.s.l.]	Temp. [°C]	Prec. [mm]	Source
LOTN13W		46.394	7.764				73	3	1300	5.5	872	
LOTN13		46.392	7.761				31	3	1300	5.7	872	
SVD*	Italy	46.450	12.214	<i>Larix decidua</i>	MW	2008	-	2	1050	7	866	V. Carraro <i>et al.</i> , unpublished
VISP	Switzerland	46.303	7.741	<i>Larix decidua</i>	DR	2014	47	3	800	9.2	581	King <i>et al.</i> , (2013)
HOF	Switzerland	47.467	7.500	<i>Larix decidua</i>	MW	2015	50	4	550	10.5	990	Pepin and Kömer (2002)
Pinus												
SVD	Italy	46.450	12.214	<i>Pinus sylvestris</i>	MW	2008	-	2	1050	7	866	V. Carraro <i>et al.</i> , unpublished
VAL	Spain	42.196	1.814	<i>Pinus sylvestris</i>	MW	2004	19	10	1257	7.3	924	Poyatos <i>et al.</i> , (2005)
HIN	Germany	53.332	13.192	<i>Pinus sylvestris</i>	ED	2012	58	8	95	8	572	Ford <i>et al.</i> , (2004)
HOF	Switzerland	47.467	7.500	<i>Pinus sylvestris</i>	MW	2014	39	4	550	10.5	990	Pepin and Kömer (2002)
MTL	USA	32.417	-110.725	<i>Pinus strobiformis</i>	DR	2014	-	3	2573	11	800	Brown-Mitic <i>et al.</i> , (2007)
MTL	USA	32.417	-110.725	<i>Pinus ponderosa</i>	DR	2014	29	3	2573	11	800	
TIM	Spain	41.333	1.014	<i>Pinus sylvestris</i>	ED	2010	42	10	1018	11.3	664	Poyatos <i>et al.</i> , (2013)
TIL	Spain	41.328	1.007	<i>Pinus sylvestris</i>	ED	2010	38	9	1065	11.3	664	Aguadé <i>et al.</i> , (2015)
CAN	Spain	41.431	2.074	<i>Pinus halepensis</i>	ED	2011	34	3	270	15.2	608	Sánchez-Costa <i>et al.</i> , (2015)
UMBS*	USA	45.600	-84.700	<i>Pinus strobus</i>	MW	2015	22	4	236	5.9	796	Matheny <i>et al.</i> , (2014)
PER*	USA	30.200	-89.300	<i>Pinus taeda</i>	MW	2013	15	12	14	19.8	1452	Wightman <i>et al.</i> , (2016)

Results

Zero-flow conditions and the effect on K

Offsets in ΔT_{\max} were observed between pre-dawn and other methods (PD in Fig. 2a), with the largest differences found in *L. decidua*. The criteria needed for the environmental dependent method to determine zero-flow conditions (including low nighttime D or T ; ED in Fig. 2a) were in some cases not met for a period longer than 10 days. In these cases, the pre-dawn method resulted in a strong reduction in daily maximum K (squares in Fig. 2b), as it does not allow for nighttime water use (circles in Fig. 2b). The moving-window method showed the highest daily maximum K (MW in Fig. 2b).

Dampening effect on absolute value and inter-daily variability of K

Comparison of new and long-term installed TDM probes at S19 and N13 (Fig. 3a), revealed that all *L. decidua* trees showed steeper slopes than the 1:1 line, indicating dampening of mean daily K although the slope was tree-specific (N13 = 1.42 in Fig. 3b and S19 = 3.41). For *P. abies*, one tree showed dampening (N13 = 3.13, cf. Fig. 3b), while another individual presented a shallower slope (S19 = 0.61), showing little reduction in mean daily K . However, similar variability of mean daily K was observed even after four years (average $R^2 \approx 0.8$, $p < 0.05$).

Dampening of mean daily K was found in trees from both species monitored since 2012, after removing the influence of environmental factors (including D , T , θ , and DOY; Fig. S2 and S3). The residual standard error (RSE) revealed that appropriate fits with environmental factors were achieved for all trees (mean RSE of 0.074; cf. Tab. S1). Only 6 out of 27 trees did not show a significant reduction in monthly mean K_{res} (Table 3). Although the goodness of fit varied among trees showing dampening (R^2 ranges from 0.17 to 0.95), on average a 31% reduction was found when comparing maximum daily K from 2013 with 2012 ($K_{\%2013-12}$ in Table 3). Within the first year of installation both *L. decidua* and *P. abies* showed a significant reduction ranging from approximately -0.0003 to -0.0015 mean monthly K_{res} per days since installation (t ; Tab. 3). By applying a non-linear function including t and DOY (seasonal term), the 15-minute K -values could be corrected for trees showing a significant reduction (cf. Table S2).

Table 3. Descriptive statistics of linear regressions ($K_{res} = \text{Int.} + \eta_1 t + \eta_2 t^2 + \eta_3 t^3$), where monthly mean K_{res} (cf. Equation 4) for individual trees were fitted against time since installation (t [days]), when applying pre-dawn ΔT_{max} . The slope indicates the reduction in mean monthly K_{res} for 2012 when fitting a linear function against t . Change in mean monthly K [%] from the first (2012) to the second (2013) year after installation, in addition to the second last (2014) and last year (2015) of monitoring. The - symbols indicates no data was available.

Site	Species	Tree	Int.	η_1	η_2	η_3	df	R ²	p	K_{res} Slope ₂₀₁₂	K % ₂₀₁₃₋₁₂	K % ₂₀₁₅₋₁₄
N13	<i>P. abies</i>	1	0.0633*	-0.0003*	4.0E-07*	-1.7E-10	29	0.41	0.000	-0.00043	-31	0
		2	0.0867*	-0.0007*	1.2E-06*	-6.7E-10*	25	0.40	0.001	-0.00046	-23	-26
		3	0.0481*	-0.0002	2.0E-07	-8.7E-11	29	0.17	0.039	-0.00034	-17	-12
	<i>L. decidua</i>	1	0.2729*	-0.0012*	1.3E-06*	-4.3E-10	22	0.69	0.000	-0.00150	-38	10
		2	0.0797*	-0.0004*	6.9E-07	-3.3E-10	20	0.24	0.035	-0.00068	-12	-10
		3	0.0809	-0.0009*	1.5E-06	-6.7E-10	28	0.06	0.186	-0.00029	-17	-23
N13W	<i>P. abies</i>	1	0.0596*	0.0002	-7.3E-07*	3.7E-10*	30	0.73	0.000	-0.00007	-7	-33
		2	-0.0208	0.0001	-2.1E-07	9.0E-11	30	0.07	0.843	0.00009	15	-1
		3	0.0512*	0.0001	-3.8E-07*	2.2E-10*	30	0.70	0.000	-0.00017	-26	-26
	<i>L. decidua</i>	1	0.1134*	-0.0004	3.0E-07	-9.2E-11	20	0.47	0.001	0.00003	-22	-6
		2	0.1980*	-0.0003	-4.8E-08	1.0E-10	21	0.72	0.000	0.00026	-32	-14
		3	0.1697*	-0.0005	4.2E-07	-1.2E-10	20	0.66	0.000	-0.00027	-34	-10
S16	<i>P. abies</i>	1	0.0795*	-0.0002	4.9E-08	-4.7E-12	18	0.74	0.000	-0.00023	-	0
		2	0.0343	-0.0002	2.2E-07	-9.5E-11	29	0.03	0.276	-0.00005	-5	1
		3	0.1491*	-0.0008*	1.3E-06*	-6.9E-10*	23	0.75	0.000	-0.00089	-50	-42
	<i>L. decidua</i>	1	0.1232*	-0.0008*	1.2E-06*	-4.8E-10	15	0.68	0.000	-0.00052	-	-2
		2	0.1687*	-0.0008*	1.1E-06	-4.5E-10*	23	0.78	0.000	-0.00051	-49	-11
		3	0.2455*	-0.0007*	1.2E-06*	-7.1E-10	12	0.95	0.000	-0.00051	-	-65
S19	<i>P. abies</i>	1	0.0143	-0.0001	9.2E-08	-7.4E-11	19	0.00	0.422	-0.00090	-19	-15
		2	-0.0054	0.0001	-2.7E-07	1.6E-10	28	0.07	0.838	-0.00025	-10	3
		3	0.0347*	-0.0001	1.2E-07	-3.9E-11	27	0.42	0.000	-0.00028	-33	3
	<i>L. decidua</i>	1	0.1202*	-0.0006*	5.9E-07	-1.7E-10	14	0.79	0.000	-0.00110	-55	-20
		2	0.0191	-0.0001	-6.9E-08	8.8E-11	21	0.02	0.333	0.00028	-9	1
		3	0.1317*	-0.0007*	1.1E-06*	-5.0E-10	14	0.76	0.000	-0.00090	-52	-21
S22	<i>L. decidua</i>	1	0.0239	0.0001	-2.4E-07	1.2E-10	17	0.39	0.010	0.00007	-8	-9
		2	0.1698*	-0.0008*	7.9E-07*	-2.4E-10	18	0.77	0.000	-0.00057	-48	6
		3	0.0916*	-0.0005*	6.5E-07	-2.5E-10	17	0.45	0.004	-0.00028	-27	9

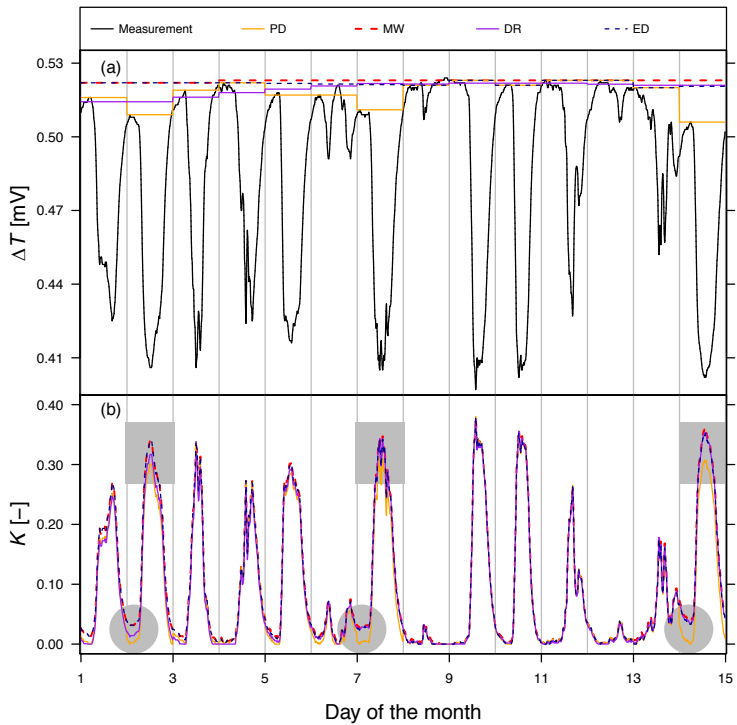


Figure 2. Widely applied zero-flow condition procedures and their implications on K for a *Larix decidua* tree at the S19 in the first week of June 2012. (a) Raw ΔT measurements (expressed in mV instead of $^{\circ}\text{C}$; cf. Lu *et al.*, 2004) and ΔT_{\max} determined by using the pre-dawn maximum (PD), an 11-day moving window (MW), the double regression method (DR) and the environmental dependent method (ED). (b) Implications of the different ΔT_{\max} methods on the resulting K (using Equation 1). Grey circles reveal times when nighttime sap flow activity could be expected and the implication on daily maximum K (grey squares).

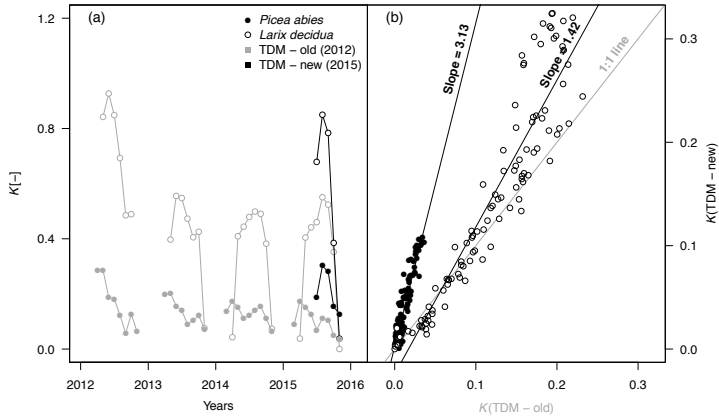


Figure 3. Example of K (Equation 1) in function of time since installation (t [days]) for two trees at the site N13. (a) Mean monthly K for thermal dissipation method (TDM) probes installed at different times on the same tree. Open or closed circles indicate *Larix decidua* and *Picea abies*, while black and grey indicates the new and old sensor, respectively. (b) Linear correlation between daily mean K for the overlapping period between old and new TDM probes (installed in May 2012 and June 2015, respectively). Open and closed circles indicate the species as provided in (a).

Species-specific calibration and literature review

The cut-segment experiment revealed a steeper calibration curve than proposed by Granier *et al.* (1985; Fig. 4). A quadratic polynomial function showed the best fit where $\alpha = 26.236$ and $\beta = 56.495$ ($R^2 = 0.96$, $p < 0.001$). Despite *P. abies* showing a steeper relationship than *L. decidua*, no significant species-specific effect was found (cf. Table S4). Large variability in published calibration curves was apparent (Fig. 4) and on average a maximum K of 1.1 was generated (cf. Table S5). Ring-porous calibration curves were the steepest, followed by diffuse-porous and softwood species (Fig. 4).

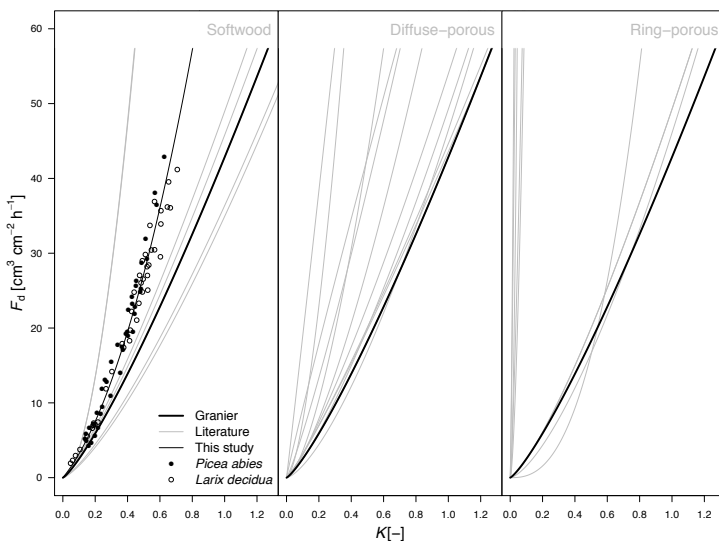


Figure 4. Calibration curves obtained from a cut-stem segment experiment and literature separated by wood type, including; softwood, diffuse-porous and ring-porous (cf. Table S5). A quadratic polynomial function best explained the calibration curve constructed in this study for both *Picea abies* and *Larix decidua*, where $F_d = 26.236K + 56.495K^2$ ($R^2 = 0.96$, $p < 0.001$). The Granier *et al.* (1985) calibration curve is highlighted as it is the most commonly applied calibration (cf. Fig. 1).

Uncertainty analysis for Löttschental F_d and stand water use

Large offsets in mean daily F_d throughout the year (growing season) were attributed to the used calibration method. During the four years of monitoring, Granier's calibration on average reduced mean daily F_d by $39 \text{ cm}^3 \text{ cm}^{-2} \text{ d}^{-1}$ for *L. decidua* and $14 \text{ cm}^3 \text{ cm}^{-2} \text{ d}^{-1}$

¹ for *P. abies* in comparison to our species-specific calibration (Fig. 5a). Lower mean daily F_d was found when using the PD zero-flow condition, while MW produced the highest values (Fig. 5a; change of $39 \text{ cm}^3 \text{ cm}^{-2} \text{ d}^{-1}$ for *L. decidua* and $13 \text{ cm}^3 \text{ cm}^{-2} \text{ d}^{-1}$ for *P. abies*), when using a species-specific calibration. Applying a dampening correction increased F_d by $61 \text{ cm}^3 \text{ cm}^{-2} \text{ d}^{-1}$ for *L. decidua* and $14 \text{ cm}^3 \text{ cm}^{-2} \text{ d}^{-1}$ for *P. abies* (when using a species-specific calibration). When considering the species-specific calibration, the ED method and dampening correction, on average 50, 53, 26, 34% and 14% of the total annual precipitation is transpired at N13, N13W, S16, S19 and S22, respectively. From all commonly applied TDM procedures (Fig. 1b) using a species-specific calibration generated the largest offset in mean annual stand water use, when considering only the first year of measurement (Fig. 6a; reduction from 286 mm to 207 mm). Additionally, PD ΔT_{\max} showed consistently lower mean annual stand water use, which is mainly caused by the in- or exclusion of nighttime water use (Fig. 6b; reduction of 54 mm when considering MW). The effect of dampening is however not pronounced when considering the absolute values in the first year (Fig. 6a; reduction of 10 mm).

Species-specific responses were observed in the relationship between mean D [kPa] and daily F_d (Fig. 5b). A third-order polynomial could explain up to 74% ($p < 0.001$) of the variance for *P. abies* at N13W, when using PD, no dampening correction and Granier's calibration, while for *L. decidua* this was only 36% ($p < 0.001$). No distinct change in goodness of fit with D was observed when using Granier's or species-specific calibration. Slight improvements in correlation strength were found when correcting for dampening (Fig. 5b; from 0.39 to 0.42 across species). The applied zero-flow conditions had little effect on *P. abies*, in contrast to *L. decidua*. Site-specific effects were found for *P. abies* where correlations with D were highest at N13W, followed by S19, S16 and N13. For *L. decidua* pre-dawn ΔT_{\max} showed the weakest correlation to D compared to the other methods (Fig. 5b). Additionally, when correlating nighttime D with nighttime F_d , only strong correlations were found for ED when considering *L. decidua* ($R^2 = 0.30$), DR (0.21) and MW (0.22).

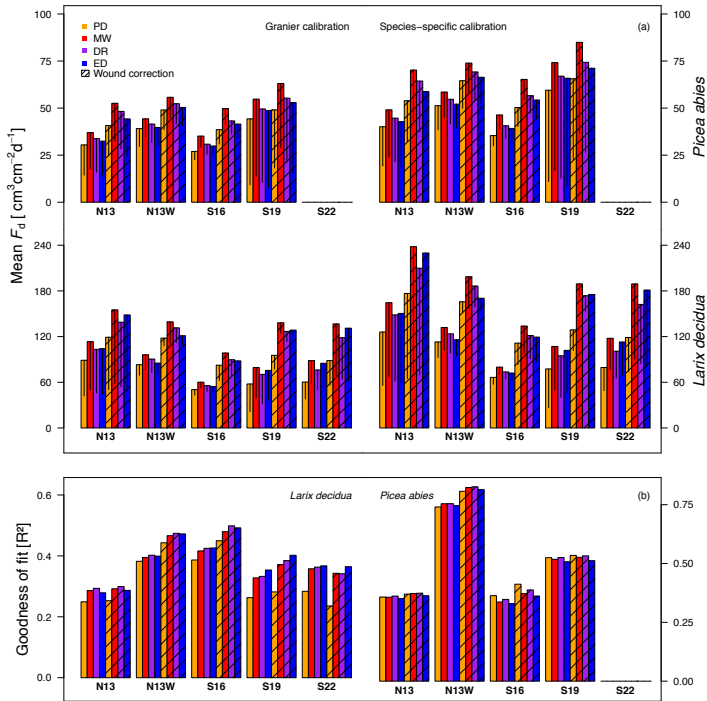


Figure 5. Uncertainty analysis of data-processing procedures on mean daily F_d [$\text{cm}^3 \text{cm}^{-2} \text{d}^{-1}$] and inter-daily sap flux density variability (R^2) arranged per species and Lötschental monitoring site. (a) The effect of zero-flow condition (ΔT_{\max}), dampening correction and calibration curve selection on mean daily F_d . Zero-flow condition methods include: PD = pre-dawn, MW = moving window, DR = double regression and ED = environmental dependent. Standard deviation induced by the individual trees is provided with the vertical lines in the boxes. (b) Goodness of fit (R^2) for a third-order polynomial describing the relationship between D (daily mean [kPa]) and daily F_d when considering the Granier *et al.* (1985) calibration.

Uncertainty in sap flux density on northern hemisphere conifers

Including uncertainty due to calibration (Fig. 4 softwood; excluding the steepest curve from Lundblad *et al.*, 2001) had a strong effect on absolute F_d on the northern hemisphere dataset (Fig. 7a and b). The genus *Pinus* showed the lowest maximum F_d , ranging from 11 to 239 $\text{cm}^3 \text{cm}^{-2} \text{d}^{-1}$ (Fig. 7b), with highest uncertainty ranges at the PER and UMBS sites (Table 2). For the genus *Picea*, maximum F_d ranged from 35 to 294 $\text{cm}^3 \text{cm}^{-2} \text{d}^{-1}$, with the greatest range at the SOBS and LOTS19 sites (Tab. 2). The genus *Larix*, the only deciduous conifer species in our study, showed the highest maximum F_d ranging from 56 to 967 $\text{cm}^3 \text{cm}^{-2} \text{d}^{-1}$.

When comparing mean daily F_d to the most commonly applied data-processing, the different softwood calibration curves introduced an average uncertainty of 31 $\text{cm}^3 \text{cm}^{-2} \text{d}^{-1}$, across species (Fig. 7c). *L. decidua* showed the strongest offset of 51 $\text{cm}^3 \text{cm}^{-2} \text{d}^{-1}$, which increased to 75 $\text{cm}^3 \text{cm}^{-2} \text{d}^{-1}$ when including the uncertainty induced by ΔT_{\max} methods (including PD, MW and DR). The ΔT_{\max} method alone (using a Granier calibration) induced an average uncertainty of 10 $\text{cm}^3 \text{cm}^{-2} \text{d}^{-1}$ across species. When considering the uncertainty generated by both the calibration curves and the ΔT_{\max} methods (with a mean uncertainty of $\Delta 45 \text{cm}^3 \text{cm}^{-2} \text{d}^{-1}$), it becomes apparent that sites with generally higher K values also have larger difference between individuals (Fig. 7c).

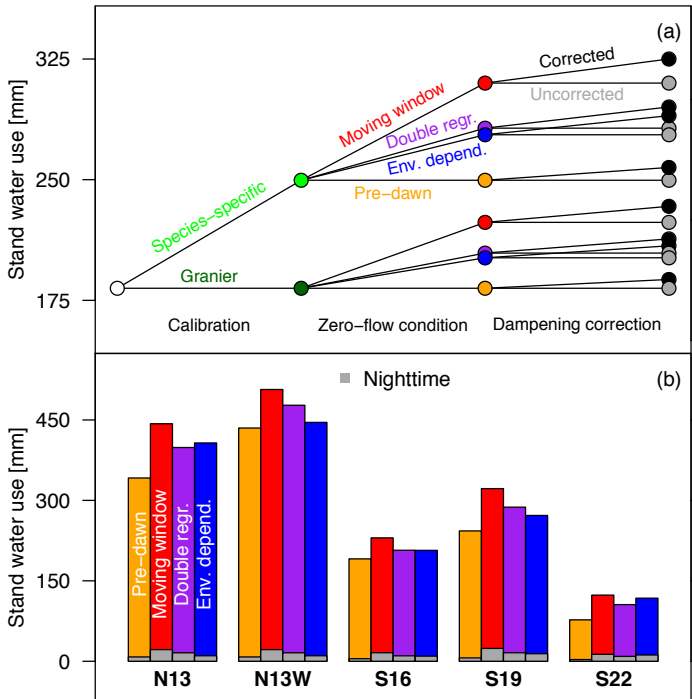


Figure 6. Effects of method combinations on average Lötschental stand water use [mm] for the first year of monitoring (2012). (a) Impact of data-processing assumptions compared to the most commonly applied method: pre-dawn zero-flow conditions (ΔT_{max}), no dampening correction and applying the Granier calibration. Data-processing procedures include; the application of a Species-specific or the Granier calibration, zero-flow conditions defined with the Moving window, Double regression (Double regr.), Environmental dependent (Env. depend.) or Pre-dawn method, and the absence (Uncorrected) or application (Corrected) of a dampening correction. (b) Contribution of nighttime sap flow for the different zero-flow condition methods to stand water use, when considering a species-specific calibration and dampening correction. The values correspond to the filled dots for the species-specific calibration when applying the dampening correction presented in (a), separated by site.

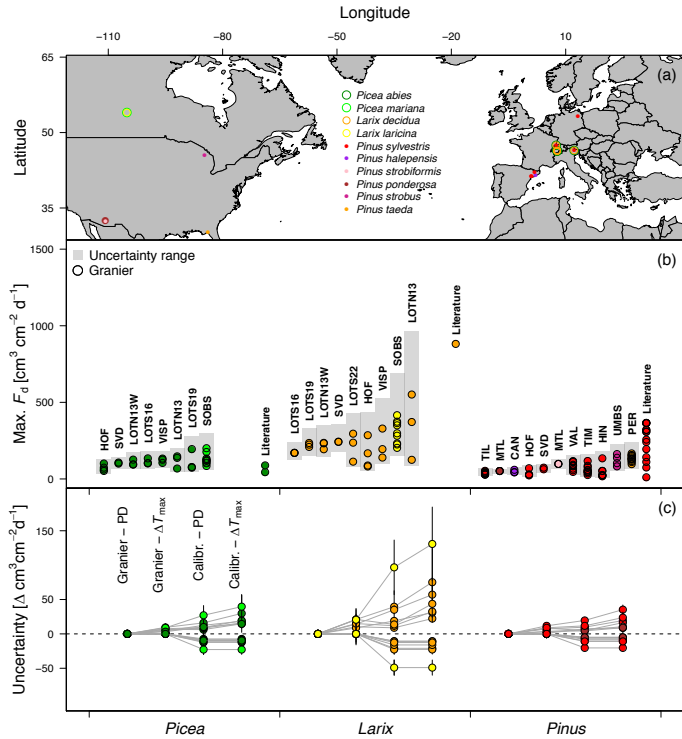


Figure 7. Uncertainty analysis on the northern hemisphere sap flow data. (a) Map indicating the included research sites and species. (b) Maximum of daily sap flux density (99th quantile of F_d [$\text{cm}^3 \text{cm}^{-2} \text{d}^{-1}$]) and the uncertainty generated by calibration curves (cf. softwood in Fig. 4) for three conifer genera; *Picea*, *Larix* and *Pinus*. The dots indicate Granier’s calibration for every individual tree, while the grey area is the maximum range generated by the different softwood calibration curves for all trees within the site (used zero-flow conditions are presented in Table 2). Additionally, reported literature values are described in Wullschlegel *et al.*, (1998) and Kallarackal *et al.*, (2013). (c) Uncertainty of the mean daily F_d , when comparing commonly applied data-processing (Granier calibration and pre-dawn ΔT_{max}) against other softwood calibrations (cf. Fig. 4) and ΔT_{max} methods (PD, MW or DR; cf. Fig. 2). Positive uncertainty is determined when using the Granier calibration and different ΔT_{max} methods (Granier - ΔT_{max}), using different softwood calibrations with PD (Calibr. - PD) and when both are variable (Calibr. - ΔT_{max}). Negative uncertainty is determined for Calibr. - PD, as the data was standardized to PD which provides the lowest values. Each dot connected by grey lines represents a site, in which the standard deviation induced by the individual trees is presented with horizontal black lines. A detailed descriptions of the sites is presented in Tab. 2.

Discussion

We quantified uncertainties introduced by different data-processing procedures when calculating sap flux density (F_d) with the thermal dissipation method (TDM; Fig. 1a). Our results show that commonly applied data processing (using pre-dawn zero-flow conditions, absence of dampening correction and Granier's calibration; Fig. 1b) likely underestimates F_d . Additionally, incorrect handling of zero-flow conditions and dampening of the signal may introduce inaccuracies in inter-daily variability of whole-tree transpiration rates, although the temporal dynamics and relative inter-specific variability of F_d is well captured.

Differences in F_d caused by zero-flow condition assumptions

Determination of ΔT_{\max} requires informed assumptions on when zero-flow conditions occur (cf. Fig. 2). The effect of applying different methods for estimating ΔT_{\max} on mean daily F_d is most pronounced when comparing pre-dawn (PD) ΔT_{\max} , which produced the lowest values, to other zero-flow condition procedures (Fig. 5a). The moving-window (MW) method provides the highest absolute values in mean daily F_d . However, the MW method can be significantly affected by thermal drifts and changes in stem water content (Vergeynst *et al.*, 2014), increasing ΔT_{\max} for an extensive temporal period and thus adding uncertainty (Rabbel *et al.*, 2016). Also, for *L. decidua* the correlation with vapour pressure deficit (D) consistently decreased when using the PD method (e.g., from 0.40 to 0.28 R^2 for S19 when applying a dampening correction; Fig. 5b) in contrast to *P. abies*. Although the mechanism behind this species-specific difference is unclear, one explanation could be the larger water storage capacity of *L. decidua* which requires longer refilling during the night (Zweifel & Häsler 2001; Meinzer *et al.*, 2009; Zheng *et al.*, 2014). These results are in agreement with findings of Kavanagh *et al.* (2007) for *L. occidentalis*, showing the occurrence of nighttime transpiration which impacted ΔT_{\max} .

Although it is difficult to differentiate between refilling of the storage tissue and actual nighttime transpiration (De Schepper and Steppe 2010), the improvement in correlation between daily F_d and D when not using the PD method suggests nighttime activity (Fig. 5b). Evidence for nighttime activity provided by flux tower data supports our findings (cf. Novick *et al.*, 2009). Although in conifers the nighttime to daytime transpiration fraction is relatively small ($\approx 5\%$ of total stand water use), its inclusion has a profound effect on the annual stand water use ($\Delta 67$ mm when comparing PD to MW

in Fig. 6b). When environmental measurements are available, it is advised to apply the environmental dependent (ED) method (Oishi *et al.*, 2016), as it provides independent evidence for selecting periods with zero-flow conditions. If not available, the double regression (DR) method appears to perform well, as both daily F_a values and its intra-daily variability lies closest to the ED method (Fig. 5), although being dependent upon the subjective selection of a window size.

On the causes of apparent signal dampening

We found a significant dampening in TDM-measured K , which reduces climate- F_a relationships (Fig. 5b), although inter-daily K variation appeared to be preserved (Fig. 3b; Oliveras & Llorens, 2001). K decreased up to 55% after the first year of measurement (Table 3) and stabilized afterwards (e.g., Fig. 3a). Also, ΔT consistently increased, indicating a reduced heat dissipation from the upper probe to the surrounding sapwood. The signal dampening and increase in ΔT can be explained by either the sensor being burrowed deeper into wood with lower water conductance (Phillips *et al.*, 1996; Beauchamp *et al.*, 2013; Berdanier *et al.*, 2016), or due to a wound reaction (Wiedemann *et al.*, 2016). Although our probes are progressively grown deeper into the xylem, we find this alone unlikely to explain the strong dampening patterns observed only in the first year after installation. Additionally, the slow growth rates of the monitored trees (~ 1 mm year⁻¹ while the probes are 20 mm in length; cf. Table 1) are not expected to cause burrowing rates which can explain a K reduction of >50%. Although visual confirmation of wound tissue formation or resin build-up is needed (cf. Marañón-Jiménez *et al.*, 2017), we hypothesize that wound reaction occurring in these coniferous species play a major role in altering the thermal properties and reduces the overall water conductance (Moore *et al.*, 2010; Wullschlegel *et al.*, 2011).

It is difficult to establish generally applicable corrections, as wound reactions are likely tree-specific and influenced by abiotic factors and phenology, among others (Wiedemann *et al.*, 2016; Marañón-Jiménez *et al.*, 2017). To avoid the effect of wound reaction a common practise is to reinstall the probes every year (Köstner *et al.*, 1998; Moore *et al.*, 2010). This however may cause issues due to circumferential variability (Oliveras & Llorens, 2001). We thus propose using our statistical correction procedure (Equation 5) which helped to isolate the dampening signal, when longer-term measurements are conducted, and only reinstalling sensors if circumferential variability

is low. However, caution is required for long-term installation with fast-growing species, as the probes will likely grow deeper into the heartwood, and for diffuse- or ring-porous species, as these may exert stronger radial variation in F_d (Beauchamp *et al.*, 2013; Berdanier *et al.*, 2016). Further studies should experimentally test the validity of our proposed correction to corroborate that it can be appropriately applied in monitoring studies, better revealing long-term effects (i.e., climatic) on plant water transport.

Calibration curve comparison

Our species-specific calibration curve demonstrates that Granier's calibration (Granier *et al.*, 1985) produces lower F_d for a given K (Fig. 4). This causes a change in the exponent of the TDM calibration curve (Equation 2; we used $F_d = 26.236K + 56.495K^2$) with implications for the magnitude of fluxes. In some cases, an underestimation of 50% was reported (Paudel *et al.*, 2013), while we found a 37% underestimation (Fig. 5a; difference in stand water use of 71 mm yr^{-1}). In softwood species, the steepest calibration curve was found by Lundblad *et al.*, (2001), but caution should be taken as this calibration curve was established by comparing TDM and the trunk segment heat balance (TSHB), assuming that the latter has no methodological issues (Poyatos *et al.*, 2005; González-Altozano *et al.*, 2008; Renninger & Schäfer, 2012). Cut-stem segment experiments also do not fully portrait natural conditions occurring in the stem, as there might be differences between applying suction or gravimetric pressure to generate flow (Fuchs *et al.*, 2017), which should be investigated.

No species-specific difference between *P. abies* and *L. decidua* was found in the calibration curves (Fig. 4). However, our literature review reveals steeper calibration curves for denser wood types, with the steepest curves found for ring-porous species (Fig. 4). The efficiency by which heat is conducted at different F_d is likely affected by wood anatomical properties (Wullschleger *et al.*, 2011; Fan *et al.*, 2018). Despite *P. abies* showing a smaller earlywood lumen area than *L. decidua* (Cuny *et al.*, 2014; Carrer *et al.*, 2017), thus a smaller proportion of water-filled tracheid to carry heat through conductive woody tissue, we did not find a significantly steeper curve. Also, when including species-specific wood density, no clear patterns were found for the steepness of the reviewed curves (results not shown). We hypothesise that the anticipated relationship between wood density and steepness of the calibration curve is

distorted by variability in local wood properties (e.g., smaller or wider rings that have specific anatomical features), which are affected by site conditions (Anfodillo *et al.*, 2013; Greenwood *et al.*, 2017). Nevertheless, the most accurate estimation of absolute F_d is likely obtained when applying a site- and species-specific calibration curve.

Implications of uncertainty for sap flow measurements

When interested in the response of canopy conductance derived from sap flow measurements to environmental change (cf. Poyatos *et al.*, 2013), the choice of zero-flow conditions to determine ΔT_{\max} is important as it affects the inter-daily variability in F_d . As PD ΔT_{\max} showed consistently weaker correlations with D when considering diurnal F_d variability in the Löttschental (Fig. 5b), studies that apply methods which allow for nighttime sap flow activity are presumed to obtain more appropriate climate-transpiration response patterns, although species dependent. Additionally, dampening occurring within the first year after installation could affect F_d -climate correlations, as they induced a consistent reduction in F_d which could be co-linear with other environmental variables.

Whole-tree water use measured with TDM is commonly collected during one growing season and estimated by using PD ΔT_{\max} , no dampening correction and Granier's calibration (Fig. 1b). When comparing this standard to other data-processing procedures for the Löttschental measurements, employing species-specific calibration curves caused the largest deviation in mean daily F_d and annual stand water use ($\Delta 27 \text{ cm}^3 \text{ cm}^{-2} \text{ d}^{-1}$ in Fig. 5a and $\Delta 79 \text{ mm}$ in Fig. 6a). This uncertainty will most likely increase further when considering circumferential variation in F_d (Lu *et al.*, 2000) and when upscaling from tree to stand water use (Čermák *et al.*, 2004). Dampening appeared less relevant for stand water use when considering one growing season (Fig. 7a). Current studies applying PD ΔT_{\max} most likely underestimate annual stand water use compared to other methods, while causing only minute differences in nighttime transpiration (Fig. 6b; cf. Rabbel *et al.*, 2016).

The uncertainty generated by the calibration curve depends upon the range of K values measured within the individual, as the deviation between the curves increases with K (Fig. 4). Additionally, the uncertainty generated by ΔT_{\max} depends upon species-specific responses and site-specific environmental conditions which allow zero-flow conditions. However, when considering the 131 northern hemisphere conifers, the

uncertainty in maximum F_d caused by the selected calibration curve remains substantial (Fig. 7b; using the reported ΔT_{\max} and ignoring dampening). Due to the power function shape of most softwood calibration curves (Fig. 4), large uncertainties are generated for species with high K such as the genus *Larix* which can be explained by many factors, including a deeper rooting system, greater access to soil resources, or its deciduous strategy (Anfodillo *et al.*, 1998). Additionally, a link has been proposed between xylem structure in conifers and F_d , as wood with larger tracheids and lower density will be able to facilitate higher flow rates (Roderick & Berry 2001; Barbour & Whitehead, 2003).

When comparing the combined uncertainty generated by calibration and ΔT_{\max} methods against commonly applied data-processing (one growing season, Granier calibration and pre-dawn ΔT_{\max}), again the calibration curve appears to generate the largest uncertainty (on average $31 \text{ cm}^3 \text{ cm}^{-2} \text{ d}^{-1}$; Calibr.-PD in Fig. 7c). Yet, ΔT_{\max} methods contribute to an even larger uncertainty of $75 \text{ cm}^3 \text{ cm}^{-2} \text{ d}^{-1}$ (Calibr.- ΔT_{\max} in Fig. 7c). Besides large variations among trees, site conditions likely affected the F_d range, although this requires site-specific environmental measurements. When interested in absolute conifer-stand water use or inter-specific stomatal conductance response, TDM users should thus be critical about decisions regarding the calibration curve and detection of nighttime sap flow activity for conifers. Yet, as the calibration curve might be dependent on wood density, F_d estimates from trees with greater wood density and higher flow rates, like ring- and diffuse-porous species (Wullschlegel *et al.*, 1998), will likely show greater uncertainty.

Conclusion and outlook

TDM will likely remain widely applied and thus a blueprint on data processing and reporting should be established to avoid irreconcilable biases in F_d measurements. Here, we show that Granier's generalized calibration, compared to site- and species-specific calibrations, might cause an underestimation of F_d . This in turn affects stand-level water use estimates and comparisons of site- and species-specific transpiration behaviour. Development of calibration curves is thus important for obtaining more accurate absolute F_d estimates. Also, allowing nighttime sap flow activity (avoiding the use of pre-dawn ΔT_{\max}) improved F_d -climate responses, although being species-specific and less severe compared to absolute effects on F_d . Finally, applying a dampening correction

is important for conserving F_d inter-daily variability, although the timeframe for the application of dampening corrections is still uncertain (Wiedemann *et al.*, 2016).

Indeed, independent whole-tree water use measurements are needed to further quantify all sources of uncertainty in TDM measurements (cf. Oishi *et al.*, 2008). Besides data processing, variable sapwood thickness, radial and circumferential variability, changes in stem water content, and natural temperature gradients most likely increase uncertainty and should be systematically assessed in the future. However, recent progress on the development of free software tools for TDM data processing (Oishi *et al.*, 2016; Ward *et al.*, 2017) and upscaling (Berdanier *et al.*, 2016) will lead to more harmonized, transparent, and reproducible sap flow data, better quantifying the associated uncertainties. This generalisation would then allow for the incorporation of uncertainty quantifications in the global pattern analyses of whole-tree water use.

Acknowledgments

R.L.P. acknowledges funding from the Swiss National Science Foundation project (SNSF), LOTFOR (no. 150205). R.P. acknowledges funding from the grant CGL-2014-5583-JIN awarded by the Spanish MINECO. C.P. acknowledges support from the Stavros Niarchos Foundation, the ETH Zurich Foundation, and the SNSF (Grants P2EZP2_162293, P300P2 174477). I.H. acknowledges support from the Deutsche Forschungsgemeinschaft (DFG project number He7220/1-1) and the Terrestrial Environmental Observatory (TERENO) of the Helmholtz Association. G.A.B.G. acknowledges funding from the United States National Science Foundation (EAR 1417101, EAR 1331906). O.S. acknowledges funding from the Canada Research Chairs, Canada Foundation for Innovation Leaders Opportunity Fund and Natural Sciences and Engineering Research Council Discovery Grant programs.

Author contributions

R.L.P. designed the research, collected and analysed the data; K.S., P.F. and D.C.F. assisted in developing the research design, discussion and writing; R.L.P., A.L.P., L.S. and V.C. performed the calibration experiment; V.C., R.P., C.P., A.K., J.L.B., G.A.B.G., L.D., I.H., R.L.M., O.S., A.M.M., and M.G.W. provided data for the northern hemisphere analysis and aided with writing.

Conflict of interest

The authors declare that they have no conflict of interest.

References

- Aguadé D, Poyatos R, Rosas T, Martínez-Vilalta J. 2015.** Comparative drought responses of *Quercus ilex* L. and *Pinus sylvestris* L. In a montane forest undergoing a vegetation shift. *Forests* **6**: 2505–2529.
- Anfodillo T, Petit G, Carraro V. 2013.** The effect of axial conduit widening on sap flow sensors readings. *Acta Horticulturae* **991**: 25–30.
- Anfodillo T, Rento S, Carraro V, Furlanetto L, Urbinati C, Carrer M. 1998.** Tree water relations and climatic variations at the alpine timberline: seasonal changes of sap flux and xylem water potential in *Larix decidua*, *Picea abies* and *Pinus cembra*. *Annals de Sciences Forestières* **55**: 159–172.
- Ansley RJ, Dugas WA, Heuer ML, Trevino BA. 1994.** Stem flow and porometer measurements of transpiration from honey mesquite (*Prosopis glandulosa*). *Journal of Experimental Botany* **45**: 847–856.
- Barbour MM, Whitehead D. 2003.** A demonstration of the theoretical prediction that sap velocity is related to wood density in the conifer *Dacrydium cupressinum*. *New Phytologist* **158**: 477–488.
- Bates D, Maechler M, Bolker B, Walker S. 2015.** Fitting Linear Mixed-Effects Models Using lme4. *Journal of Statistical Software* **67**: 1–48.
- Beauchamp K, Mencuccini M, Perks M, Gardiner B. 2013.** The regulation of sapwood area, water transport and heartwood formation in Sitka spruce. *Plant Ecology & Diversity* **6**: 45–56.
- Berdanier AB, Miniati CF, Clark JS. 2016.** Predictive models for radial sap flux variation in coniferous, diffuse-porous and ring-porous temperate trees. *Tree physiology* **36**: 932–41.
- Berkelhammer M, Hu J, Bailey A, Noone DC, Still CJ, Barnard H, Gochis D, Hsiao GS, Rahn T, Turnipseed A. 2013.** The nocturnal water cycle in an open-canopy forest. *Journal of Geophysical Research Atmospheres* **118**: 10225–10242.
- Brinkmann N, Eugster W, Zweifel R, Buchmann N, Kahmen A. 2016.** Temperate tree species show identical response in tree water deficit but different sensitivities in sap flow to summer soil drying. *Tree Physiology* **36**: 1508–1519.

- Brown-Mitic C, Shuttleworth WJ, Chawn Harlow R, Petti J, Burke E, Bales R. 2007.** Seasonal water dynamics of a sky island subalpine forest in semi-arid southwestern United States. *Journal of Arid Environments* **69**: 237–258.
- Burgess SOS, Adams MA, Turner NC, Beverly CKO, Khan AAH, Bleby TM. 2001.** An improved heat pulse method to measure low and reverse rates of sap flow in woody plants. *Tree Physiology* **21**: 589–598.
- Bush SE, Hultine KR, Sperry JS, Ehleringer JR, Phillips N. 2010.** Calibration of thermal dissipation sap flow probes for ring- and diffuse-porous trees. *Tree Physiology* **30**: 1545–1554.
- Caird MA, Richards JH, Donovan LA. 2007.** Nighttime stomatal conductance and transpiration in C-3 and C-4 plants. *Plant Physiology* **143**: 4–10.
- Carrer M, Castagneri D, Prendin AL, Petit G, von Arx G. 2017.** Retrospective analysis of wood anatomical traits reveals a recent extension in tree cambial activity in two high-elevation conifers. *Frontiers in Plant Science* **8**: 1–13.
- Čermák J, Cienciala E, Kucera J, Lindroth A, Bednářová E. 1995.** Individual variation of sap-flow rate in large pine and spruce trees and stand transpiration: a pilot study at the central NOPEX site. *Journal of Hydrology* **168**: 17–27.
- Čermák J, Kučera J, Nadezhdina N. 2004.** Sap flow measurements with some thermodynamic methods, flow integration within trees and scaling up from sample trees to entire forest stands. *Trees - Structure and Function* **18**: 529–546.
- Clearwater MJ, Meinzer FC, Andrade JL, Goldstein G, Holbrook NM. 1999.** Potential errors in measurement of nonuniform sap flow using heat dissipation probes. *Tree Physiology* **19**: 681–687.
- Cuny HE, Rathgeber CBK, Frank D, Fonti P, Fournier M. 2014.** Kinetics of tracheid development explain conifer tree-ring structure. *New Phytologist* **203**: 1231–1241.
- De Schepper V, Steppe K. 2010.** Development and verification of a water and sugar transport model using measured stem diameter variations. *Journal of Experimental Botany* **61**: 2083–2099.
- Do F, Rocheteau A. 2002.** Influence of natural temperature gradients on measurements of xylem sap flow with thermal dissipation probes. 2. Advantages and calibration of a noncontinuous heating system. *Tree physiology* **22**: 649–654.
- Damour G, Simonneau T, Cochard H, Urban L. 2010.** An overview of models of stomatal conductance at the leaf level. *Plant, Cell and Environment* **33**: 1419–1438.

- Fan J, Guyot A, Ostergaard KT, Lockington DA. 2018.** Effects of earlywood and latewood on sap flux density-based transpiration estimates in conifers. *Agricultural and Forest Meteorology* **249**: 264-274.
- Fatichi S, Leuzinger S, Körner C. 2014.** Moving beyond photosynthesis: from carbon source to sink-driven vegetation modeling. *New Phytologist* **201**: 1086–1095.
- Fatichi S, Pappas C. 2017.** Constrained variability of modeled $T:ET$ ratio across biomes. *Geophysical Research Letters* **44**: 6795–6803.
- Fatichi S, Pappas C, Ivanov VY. 2016.** Modeling plant-water interactions: an ecohydrological overview from the cell to the global scale. *WIREs Water* **3**: 327–368.
- Fiora A, Cescatti A. 2006.** Diurnal and seasonal variability in radial distribution of sap flux density: implications for estimating stand transpiration. *Tree Physiology* **26**: 1217–1225.
- Ford CR, Hubbard RM, Kloeppel BD, Vose JM. 2007.** A comparison of sap flux-based evapotranspiration estimates with catchment-scale water balance. *Agricultural and Forest Meteorology* **145**: 176–185.
- Ford CR, McGuire MA, Mitchell RJ, Teskey RO. 2004.** Assessing variation in the radial profile of sap flux density in Pinus species and its effect on daily water use. *Tree Physiology* **24**: 241–249.
- Fuchs S, Leuschner C, Link R, Coners H, Schuldt B. 2017.** Calibration and comparison of thermal dissipation, heat ratio and heat field deformation sap flow probes for diffuse-porous trees. *Agricultural and Forest Meteorology* **244-245**: 151–161.
- González-Altozano P, Pavel EW, Oncins JA, Doltra J, Cohen M, Paço T, Massai R, Castel JR. 2008.** Comparative assessment of five methods of determining sap flow in peach trees. *Agricultural Water Management* **95**: 503–515.
- Good SP, Noone D, Bowen G. 2015.** Water Fluxes. *Science* **349**: 175–177.
- Granier A. 1985.** Une nouvelle methode pour la mesure du flux de seve brute dans le tronc des arbres. *Annales des Sciences Forestieres* **42**: 193–200.
- Granier A. 1987.** Evaluation of transpiration in a Douglas-fir stand by means of sap flow measurements. *Tree Physiology* **3**: 309–320.
- Green S, Clothier B, Jardine B. 2003.** Theory and Practical Application of Heat Pulse to Measure Sap Flow. *Agronomy Journal* **95**: 1371–1379.
- Greenwood S, Ruiz-Benito P, Martínez-Vilalta J, Lloret F, Kitzberger T, Allen CD, Fensham R, Laughlin DC, Kattge J, Bönisch G, et al. 2017.** Tree mortality across

biomes is promoted by drought intensity, lower wood density and higher specific leaf area. *Ecology Letters* **20**: 539–553.

Hatton TJ, Wu HI. 1995. Scaling theory to extrapolate individual tree water use to stand water use. *Hydrological Processes* **9**, 527–540.

Holbrook NM, Zwieniecki MA. 2003. Plant biology: water gate. *Nature* **425**: 361.

Isarangkool Na Ayutthaya S, Do FC, Pannengpetch K, Junjittakarn J, Maeght JL, Rocheteau A, Cochard H. 2010. Transient thermal dissipation method of xylem sap flow measurement: Multi-species calibration and field evaluation. *Tree Physiology* **30**: 139–148.

Kallarackal J, Otieno DO, Reineking B, Jung EY, Schmidt MWT, Granier A, Tenhunen JD. 2013. Functional convergence in water use of trees from different geographical regions: A meta-analysis. *Trees - Structure and Function* **27**: 787–799.

Kavanagh KL, Pangle R, Schotzko AD. 2007. Nocturnal transpiration causing disequilibrium between soil and stem predawn water potential in mixed conifer forests of Idaho. *Tree Physiology* **4**: 621–629.

King G, Fonti P, Nievergelt D, Büntgen U, Frank D. 2013. Climatic drivers of hourly to yearly tree radius variations along a 6°C natural warming gradient. *Agricultural and Forest Meteorology* **168**: 36–46.

Köstner B, Granier A, Cermák J. 1998. Sapflow measurements in forest stands: methods and uncertainties. *Annals of Forest Science* **55**: 13–27.

Kunert N, Schwendenmann L, Ho D. 2010. Seasonal dynamics of tree sap flux and water use in nine species in Panamanian forest plantations. *Agricultural and Forest Meteorology* **150**: 411–419.

Langensiepen M, Kupisch M, Graf A, Schmidt M, Ewert F. 2014. Improving the stem heat balance method for determining sap-flow in wheat. *Agricultural and Forest Meteorology* **186**: 34–42.

Lawrence DM, Thornton PE, Oleson KW, Bonan GB. 2007. The partitioning of evapotranspiration into transpiration, soil evaporation, and canopy evaporation in a GCM: Impacts on land-atmosphere interaction. *Journal of Hydrometeorology* **8**: 862–880.

Longuetaud F, Mothe F, Leban J-M, Mäkelä A. 2006. *Picea abies* sapwood width: Variations within and between trees. *Scandinavian Journal of Forest Research* **21**: 41–53.

- Lu P, Müller WJ, Chacko EK. 2000.** Spatial variations in xylem sap flux density in the trunk of orchard-grown, mature mango trees under changing soil water conditions. *Tree Physiology* **20**: 683–692.
- Lu P, Urban L, Zhao P. 2004.** Granier's Thermal Dissipation Probe (TDP) Method for Measuring Sap Flow in Trees: Theory and Practice. *Acta Botanica Sinica* **46**: 631–646.
- Lubczynski MW, Chavarro-Rincon D, Roy J. 2012.** Novel, cyclic heat dissipation method for the correction of natural temperature gradients in sap flow measurements. Part 1. Theory and application. *Tree Physiology* **32**: 894–912.
- Lundblad M, Lagergren F, Lindroth A, Lundblad M, Lagergren F, Lindroth A. 2001.** Evaluation of heat balance and heat dissipation methods for sapflow measurements in pine and spruce. *Annals of Forest Science* **58**: 625–638.
- Ma C, Luo Y, Shao M, Li X, Sun L, Jia X. 2017.** Environmental controls on sap flow in black locust forest in Loess Plateau, China. *Scientific Reports* **7**: 13160.
- Marañón-Jiménez S, Van den Bulcke J, Piayda A, Van Acker J, Cuntz M, Rebmann C, Steppe K. 2017.** X-ray computed microtomography characterizes the wound effect that causes sap flow underestimations by thermal dissipation sensors. *Tree Physiology* **2**: 287-301.
- Matheny AM, Bohrer G, Vogel CS, Morin TH, He L, Prata de Moraes Frasson R, Mirfenderesgi G, Schäfer KVR, Gough CM, Ivanov VY, et al. 2014.** Species-specific transpiration responses to intermediate disturbance in a northern hardwood forest. *Journal of Geophysical Research: Biogeosciences* **119**: 2292–2311.
- Meinzer FC, Johnson DM, Lachenbruch B, McCulloh KA, Woodruff DR. 2009.** Xylem hydraulic safety margins in woody plants: Coordination of stomatal control of xylem tension with hydraulic capacitance. *Functional Ecology* **23**: 922–930.
- Moore GW, Bond BJ, Jones JA, Meinzer FC. 2010.** Thermal-dissipation sap flow sensors may not yield consistent sap-flux estimates over multiple years. *Trees - Structure and Function* **24**: 165–174.
- Nadezhkina N, Cermák J, Ceulemans R. 2002.** Radial patterns of sap flow in woody stems of dominant and understory species: scaling errors associated with positioning of sensors. *Tree physiology* **22**: 907–18.
- Nourtier M, Chanzy A, Granier A, Huc R. 2011.** Sap flow measurements by thermal dissipation method using cyclic heating: A processing method accounting for the non-stationary regime. *Annals of Forest Science* **68**: 1255–1264.

- Novick KA, Oren R, Stoy PC, Siqueira MBS, Katul GG. 2009.** Nocturnal evapotranspiration in eddy-covariance records from three co-located ecosystems in the Southeastern U.S.: Implications for annual fluxes. *Agricultural and Forest Meteorology* **149**: 1491–1504.
- Oishi AC, Hawthorne DA, Oren R. 2016.** Baseliner: An open-source, interactive tool for processing sap flux data from thermal dissipation probes. *SoftwareX* **5**: 139–143.
- Oishi AC, Oren R, Stoy PC. 2008.** Estimating components of forest evapotranspiration: A footprint approach for scaling sap flux measurements. *Agricultural and Forest Meteorology* **148**: 1719–1732.
- Oliveras I, Llorens P. 2001.** Medium-term sap flux monitoring in a Scots pine stand: analysis of the operability of the heat dissipation method for hydrological purposes. *Tree physiology* **21**: 473–480.
- Oren R, Phillips N, Ewers BE, Pataki DE, Megonigal JP. 1999.** Sap-flux-scaled transpiration responses to light, vapor pressure deficit, and leaf area reduction in a flooded *Taxodium distichum* forest. *Tree physiology* **19**: 337–347.
- Pappas C, Matheny AM, Baltzer JL, Barr A, Black TA, Bohrer G, Detto M, Maillet J, Roy A, Sonnentag O, Stephens J. in press.** Boreal tree hydrodynamics: asynchronous, diverging, yet complementary. *Tree Physiology*. doi:10.1093/treephys/tpy043
- Paudel I, Kanety T, Cohen S. 2013.** Inactive xylem can explain differences in calibration factors for thermal dissipation probe sap flow measurements. *Tree Physiology* **33**: 986–1001.
- Pepin S, Körner C. 2002.** Web-FACE: A new canopy free-air CO₂ enrichment system for tall trees in mature forests. *Oecologia* **133**: 1–9.
- Peters RL, Klesse S, Fonti P, Frank DC. 2017.** Contribution of climate vs. larch budmoth outbreaks in regulating biomass accumulation in high-elevation forests. *Forest Ecology and Management* **401**: 147–158.
- Phillips N, Oren R, Zimmermann R. 1996.** Radial patterns of xylem sap flow in non-, diffuse- and ring-porous tree species. *Plant Cell and Environment* **19**: 983–990.
- Pinheiro J, Bates D, DebRoy S, Sarkar D, R Core Team. 2017.** nlme: Linear and Nonlinear Mixed Effects Models. R package version 3.1-131, <https://CRAN.R-project.org/package=nlme>.

- Poyatos R, Aguadé D, Galiano L, Mencuccini M, Martínez-Vilalta J. 2013.** Drought-induced defoliation and long periods of near-zero gas exchange play a key role in accentuating metabolic decline of Scots pine. *New Phytologist* **200**: 388–401.
- Poyatos R, Granda V, Molowny-Horas R, Mencuccini M, Steppe K, Martínez-Vilalta J. 2016.** SAPFLUXNET: towards a global database of sap flow measurements. *Tree physiology* **36**: 1449–1455.
- Poyatos R, Llorens P, Gallart F. 2005.** Transpiration of montane *Pinus sylvestris* L. and *Quercus pubescens* Willd. forest stands measured with sap flow sensors in NE Spain. *Hydrology and Earth System Sciences Discussions* **2**: 1011–1046.
- Rabbel I, Diekkrüger B, Voigt H, Neuwirth B. 2016.** Comparing ΔT_{max} determination approaches for Granier-based sapflow estimations. *Sensors* **16**: 1–16.
- Regalado CM, Ritter A. 2007.** An alternative method to estimate zero flow temperature differences for Granier's thermal dissipation technique. *Tree Physiology* **27**: 1093–1102.
- Renninger HJ, Schäfer KVR. 2012.** Comparison of tissue heat balance- and thermal dissipation-derived sap flow measurements in ring-porous oaks and a pine. *Frontiers in plant science* **3**: 1–9.
- Reyes-Acosta JL, Lubczynski MW. 2013.** Mapping dry-season tree transpiration of an oak woodland at the catchment scale, using object-attributes derived from satellite imagery and sap flow measurements. *Agricultural and Forest Meteorology* **174–175**: 184–201.
- Roderick ML, Berry SL. 2001.** Linking wood density with tree growth and environment: a theoretical analysis based on the motion of water. *New Phytologist* **149**: 473–485.
- Sánchez-costa E, Poyatos R, Sabaté S. 2015.** Contrasting growth and water use strategies in four co-occurring Mediterranean tree species revealed by concurrent measurements of sap flow and stem diameter variations. *Agricultural and Forest Meteorology* **207**: 24–37.
- Saveyn A, Steppe K, Lemeur R. 2008.** Spatial variability of xylem sap flow in mature beech (*Fagus sylvatica*) and its diurnal dynamics in relation to microclimate. *Botany* **86**: 1440–1448.
- Schlesinger WH, Jasechko S. 2014.** Transpiration in the global water cycle. *Agricultural and Forest Meteorology* **189–190**: 115–117.

- Smith DM, Allen SJ. 1996.** Measurement of sap flow in plant stems. *Journal of Experimental Botany* **47**: 1833–1844.
- Song X, Barbour MM, Farquhar GD, Vann DR, Helliker BR. 2013.** Transpiration rate relates to within- and across-species variations in effective path length in a leaf water model of oxygen isotope enrichment. *Plant, Cell and Environment* **36**: 1338–1351.
- Steppe K, De Pauw DJW, Doody TM, Teskey RO. 2010.** A comparison of sap flux density using thermal dissipation, heat pulse velocity and heat field deformation methods. *Agricultural and Forest Meteorology* **150**: 1046–1056.
- Steppe K, Vandegehuchte MW, Tognetti R, Mencuccini M. 2015.** Sap flow as a key trait in the understanding of plant hydraulic functioning. *Tree Physiology* **35**: 341–345.
- Sun H, Aubrey DP, Teskey RO. 2012.** A simple calibration improved the accuracy of the thermal dissipation technique for sap flow measurements in juvenile trees of six species. *Trees - Structure and Function* **26**: 631–640.
- Sutanto SJ, Van Den Hurk B, Dirmeyer PA, Seneviratne SI, Röckmann T, Trenberth KE, Blyth EM, Wenninger J, Hoffmann G. 2014.** HESS Opinions ‘a perspective on isotope versus non-isotope approaches to determine the contribution of transpiration to total evaporation’. *Hydrology and Earth System Sciences* **18**: 2815–2827.
- Swanson RH. 1994.** Significant historical developments in thermal methods for measuring sap flow in trees. *Agricultural and Forest Meteorology* **72**: 113–132.
- Vandegehuchte MW, Steppe K. 2012.** Sapflow+: A four-needle heat-pulse sap flow sensor enabling nonempirical sap flux density and water content measurements. *New Phytologist* **196**: 306–317.
- Van de Wal BAE, Guyot A, Lovelock CE, Lockington DA, Steppe K. 2015.** Influence of temporospatial variation in sap flux density on estimates of whole-tree water use in *Avicennia marina*. *Trees - Structure and Function* **29**: 215–222.
- Vergeynst LL, Vandegehuchte MW, McGuire MA, Teskey RO, Steppe K. 2014.** Changes in stem water content influence sap flux density measurements with thermal dissipation probes. *Trees - Structure and Function* **28**: 949–955.
- Ward EJ, Domec J, King J, Sun G, McNulty S, Noormets A, Ward EJ. 2017.** TRACC : an open source software for processing sap flux data from thermal dissipation

probes. *Trees - Structure and Function* **31**: 1737–1742. doi: 10.1007/s00468-017-1556-0.

Wiedemann A, Marañón-jiménez S, Herbst M, Cuntz M. 2016. An empirical study of the wound effects on sap flow measured with thermal dissipation probes. *Acta Horticulturae* **991**: 107–114.

Wightman MG, Martin TA, Gonzalez-Benecke CA, Jokela EJ, Cropper WP, Ward EJ. 2016. Loblolly pine productivity and water relations in response to throughfall reduction and fertilizer application on a poorly drained site in northern Florida. *Forests* **7**: 214. doi: 10.3390/f7100214.

Wilson KB, Hanson PJ, Mulholland PJ, Baldocchi DD, Wullschleger SD. 2001. A comparison of methods for determining forest evapotranspiration and its components: Sap-flow, soil water budget, eddy covariance and catchment water balance. *Agricultural and Forest Meteorology* **106**: 153–168.

WMO (World Meteorological Organization). 2008. Guide to Meteorological Instruments and Methods of Observation, Appendix 4B, WMO-No. 8 (CIMO Guide), Geneva 2008. ISBN: 978-92-63-10008-5

Wullschleger SD, Childs KW, King AW, Hanson PJ. 2011. A model of heat transfer in sapwood and implications for sap flux density measurements using thermal dissipation probes. *Tree Physiology* **31**: 669–679.

Wullschleger SD, Meinzer FC, Vertessy RA. 1998. A Review of Whole-Plant Water Use Studies in Tree. *Tree Physiology* **18**: 499–512.

Zheng H, Wang Q, Zhu X, Li Y, Yu G. 2014. Hysteresis responses of evapotranspiration to meteorological factors at a diel timescale: Patterns and causes. *PLoS ONE* **9**: 1–10.

Zuur AF, Ieno EN, Elphick CS. 2010. A protocol for data exploration to avoid common statistical problems. *Methods in Ecology and Evolution* **1**: 3–14.

Zweifel R, Häsler R. 2001. Dynamics of water storage in mature subalpine *Picea abies*: temporal and spatial patterns of change in stem radius. *Tree Physiology* **21**: 561–569.

New Phytologist

Supporting information

Article title: Quantification of uncertainties in conifer sap flow measured with the thermal dissipation method

Authors: Richard L. Peters, Patrick Fonti, David C. Frank, Rafael Poyatos, Christoforos Pappas, Ansgar Kahmen, Vinicio Carraro, Angela Luisa Prendin, Loïc Schneider, Jennifer L. Baltzer, Greg A. Baron-Gafford, Lars Dietrich, Ingo Heinrich, Rebecca L. Minor, Oliver Sonnentag, Ashley M. Matheny, Maxwell G. Wightman, Kathy Steppe

Article acceptance data: 24 April 2018

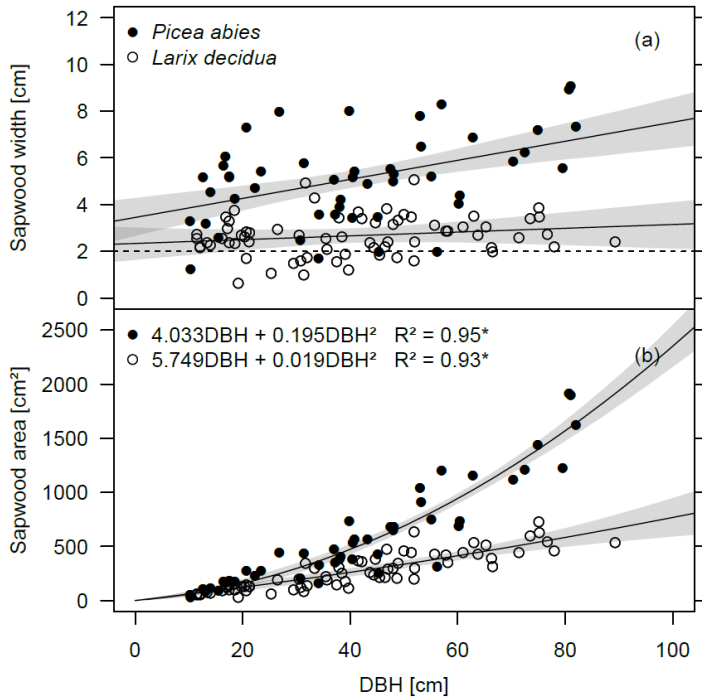


Figure S1. Allometric relationships between diameter at breast height for *Picea abies* and *Larix decidua* (DBH), (a) sapwood width and (b) sapwood area. No significant fit was found for DBH versus sapwood width. Grey areas presents the Bayesian credible interval of the fitted function (cf. Gelman & Hill, 2007).

Table S1. General statistics for generalized least squares models, correcting for first order auto-correlation (using corAR1 correlation), when explaining K (pre-dawn ΔT_{\max}) with vapour pressure deficit (D [hPa]), temperature (T [°C]), soil moisture (θ [%]) and seasonality (DOY in day of year). For every tree the intercept (Int.) and slopes (ε) of the model are provided, in addition to the residual standard error (RSE), degrees of freedom (df) and temporal auto-correlation coefficient (Φ).

Site	Species	Tree	Generalized Least Squares – Linear model									
			Int.	ε_1	ε_2	ε_3	ε_4	ε_5	ε_6	RSE	df	Φ
N13W	<i>P. abies</i>	1	-0.04	-0.0004*	-5.71	0.0019	-4.7E-06	-0.03*	0.020*	0.07	532	0.95
		2	0.27*	-0.0004*	-15.93*	0.0002	2.8E-09	-0.04*	0.023*	0.05	540	0.81
		3	0.09	-0.0002*	-6.08	0.0011	-2.6E-06	-0.02*	0.010*	0.05	530	0.95
	<i>L. decidua</i>	1	-1.70*	-0.0004*	-27.99*	0.0234*	-5.4E-05*	-0.02*	0.014*	0.08	402	0.94
		2	-2.58*	-0.0005*	0.02*	0.0175*	-4.1E-05*	-0.01*	0.021*	0.13	374	0.98
		3	-1.95*	-0.0006*	0.00*	0.0169*	-3.9E-05*	0.03*	0.024*	0.10	412	0.98
N13	<i>P. abies</i>	1	0.06	-0.0003*	-1.79*	0.0003	-7.7E-07	-0.04*	0.013*	0.03	374	0.90
		2	0.09	-0.0006*	-3.23*	0.0013	-3.4E-06	-0.06*	0.020*	0.06	414	0.91
		3	-0.06	-0.0006*	-4.12*	0.0035*	-8.1E-06*	-0.05*	0.022*	0.06	486	0.88
	<i>L. decidua</i>	1	-1.80*	-0.0008*	-5.97*	0.0220*	-5.1E-05*	-0.02*	0.028*	0.15	435	0.94
		2	-0.76*	-0.0001*	-2.70*	0.0100*	-2.3E-05*	-0.03*	0.006*	0.06	384	0.97
		3	-1.96*	-0.0012*	-8.78*	0.0237*	-5.2E-05*	-0.02*	0.041*	0.13	437	0.88
S16	<i>P. abies</i>	1	-0.02	-0.0004*	-1.96*	0.0014	-3.8E-06	-0.02*	0.017*	0.07	298	0.95
		2	0.04	-0.0005*	-3.35*	0.0019*	-4.5E-06*	-0.02*	0.017*	0.04	518	0.85
		3	-0.09	-0.0003*	0.20	0.0015	-3.8E-06	-0.01*	0.012*	0.07	410	0.97
	<i>L. decidua</i>	1	-1.08*	-0.0004*	0.08	0.0112*	-2.6E-05*	0.00	0.017*	0.07	281	0.96
		2	-0.75*	-0.0001*	1.40*	0.0077*	-1.8E-05*	0.00	0.006*	0.08	422	0.97
		3	-1.44	-0.0002*	0.57	0.0135*	-3.0E-05*	-0.01	0.010*	25.23	218	1.00
S19	<i>P. abies</i>	1	-0.20*	-0.0007*	-3.36*	0.0036*	-8.3E-06*	-0.02*	0.027*	0.04	328	0.81
		2	-0.36*	-0.0012*	-0.88	0.0044*	-1.1E-05*	-0.02*	0.047*	0.08	477	0.79
		3	0.03	-0.0003*	-1.42*	0.0012*	-2.8E-06*	-0.03*	0.011*	0.03	443	0.80
	<i>L. decidua</i>	1	-0.73	-0.0002	-1.37	0.0084*	-1.9E-05*	0.00	0.005	0.08	248	0.92
		2	-2.03*	-0.0003*	-0.32	0.0217*	-4.9E-05*	-0.01*	0.012*	0.06	381	0.77
		3	-1.27*	-0.0003*	0.06	0.0131*	-3.0E-05*	-0.01*	0.010*	0.08	268	0.96
S22	<i>L. decidua</i>	1	-1.47*	-0.0005*	-2.61*	0.0155*	-3.5E-05*	-0.03*	0.016*	0.04	310	0.82
		2	-1.23*	-0.0004*	-4.71*	0.0137*	-3.1E-05*	-0.01	0.011	0.09	320	0.89
		3	-2.14*	-0.0006*	-0.46*	0.0223	-5.1E-05*	-0.03*	0.018*	0.07	305	0.76

$$K = \text{Int.} + \varepsilon_1 D + \varepsilon_2 T + \varepsilon_3 \theta + \varepsilon_4 \text{DOY} + \varepsilon_5 \text{DOY}^2 + \varepsilon_6 \text{DOY}^3$$

Table S2. General statistics for non-linear models when explaining the dampening effect K (pre-dawn ΔT_{\max}) with time since installation (t [days]) and seasonality (DOY in day of year). For every tree values of the variable ($a-f$) are provided, in addition to the residual standard error (RSE) and degrees of freedom (df).

Site	Species	Tree	Non-linear model						RSE	df
			a	b	c	d	e	f		
N13W	<i>P. abies</i>	1	0.14*	0.000*	-0.001*	1.2E-06	2.1E-03	-5.46E-06*	0.038	527
		2	-0.33	0.001	1.137	4.2E-04	3.0E-03	-7.55E-06*	0.053	541
		3	0.14*	0.000	0.001	1.8E-06	1.1E-03*	-3.16E-06*	0.028	437
	<i>L. decidua</i>	1	-1.39*	-0.004	0.002	4.0E-08*	1.8E-02*	-4.13E-05*	0.043	403
		2	-0.59*	-0.001	0.001	7.6E-08	1.1E-02*	-2.44E-05*	0.046	375
		3	-0.70*	-0.002*	0.002*	6.0E-08	1.2E-02*	-2.72E-05*	0.042	413
N13	<i>P. abies</i>	1	0.28*	0.005*	0.039*	2.4E-06	2.6E-05	-7.39E-07*	0.023	375
		2	0.28*	0.002	0.011	-1.7E-06	3.9E-04	-2.07E-06*	0.058	415
		3	0.23*	0.003	0.020	1.8E-06	1.5E-03*	-4.76E-06*	0.061	480
	<i>L. decidua</i>	1	-0.19*	-0.005*	0.007*	1.1E-06*	9.7E-03*	-2.35E-05*	0.094	436
		2	-0.31*	-0.002	0.004	-3.6E-07	6.2E-03*	-1.57E-05*	0.051	337
		3	-0.58*	-0.005	0.006	8.9E-07	1.2E-02*	-2.67E-05*	0.133	438
S16	<i>P. abies</i>	1	0.17*	0.000*	0.000	-6.6E-07	1.1E-03*	-3.27E-06*	0.031	277
		2	0.21*	0.001	0.007	-7.8E-07	0.6E-03*	-2.29E-06*	0.040	519
		3	0.31*	0.000	0.006*	-3.6E-06	0.6E-03*	-2.30E-06*	0.024	324
	<i>L. decidua</i>	1	-0.64*	-0.002	0.002	2.2E-07	9.7E-03*	-2.24E-05*	0.036	282
		2	-0.11*	-0.003*	0.005*	8.2E-07	5.6E-03*	-1.30E-05*	0.023	407
		3	-1.01*	0.000*	0.000	0.0E-07	12.9E-03*	-2.92E-05*	0.034	171
S19	<i>P. abies</i>	1	0.28*	0.008	0.069*	-5.4E-06	6.7E-04	-1.85E-06*	0.041	329
		2	-0.03	0.000	0.002	2.6E-06	5.0E-03*	-1.23E-05*	0.062	478
		3	0.15*	0.000	0.011*	-2.2E-06*	7.8E-04*	-2.12E-06*	0.019	434
	<i>L. decidua</i>	1	0.02	-0.003*	0.010*	1.9E-06*	2.9E-03*	-6.84E-06*	0.017	249
		2	-1.78*	-0.003	0.001	5.2E-08*	2.1E-02*	-4.64E-05*	0.043	382
		3	-0.39*	-0.012*	0.018*	-5.5E-07*	7.5E-03*	-1.71E-05*	0.019	269
S22	<i>L. decidua</i>	1	-1.12*	-0.028	0.025	-1.2E-06	13.1E-03*	-2.98E-05*	0.030	311
		2	-0.26*	-0.002*	0.002*	8.3E-07*	6.0E-03*	-1.32E-05*	0.032	321
		3	-1.71*	-0.007*	0.003*	2.9E-07*	20.1E-03*	-4.60E-05*	0.037	306

$$K = (a + b \cdot t) / (1 + c \cdot t + d \cdot t^2) + e \cdot \text{DOY} + f \cdot \text{DOY}^2$$

Table S3. Raw data of the cut-segment calibration experiment. Mean F_d [$\text{cm}^3 \text{cm}^{-2} \text{h}^{-1}$] against K measured at a specific water column height (level in cm, increasing or decreasing) with thermal dissipation method (TDM) for four stems from *Larix decidua* and *Picea abies* trees.

Species	Tree	Level	K mean	Stdev.	SFD mean	Stdev.	Species	Tree	Level	K mean	Stdev.	SFD mean	Stdev.
<i>Larix decidua</i>	1	L2	0.217	0.009	7.430	0.219	<i>Picea abies</i>	1	L2	0.146	0.005	4.892	0.078
		L5	0.198	0.007	7.119	0.275			L5	0.137	0.001	5.173	0.063
		L10	0.189	0.005	6.998	0.329			L10	0.143	0.002	5.932	0.073
		L15	0.182	0.005	6.603	0.338			L15	0.164	0.004	6.642	0.067
		L25	0.187	0.003	6.984	0.240			L25	0.211	0.009	8.711	0.118
		L33	0.190	0.003	7.293	0.151			L33	0.271	0.007	12.771	0.279
		L-25	0.150	0.010	5.542	0.285			L-25	0.244	0.003	9.529	0.141
		L-15	0.106	0.008	3.765	0.132			L-15	0.218	0.006	6.702	0.128
		L-10	0.078	0.005	2.950	0.100			L-10	0.199	0.004	5.550	0.086
	L-5	0.060	0.004	2.304	0.081	L-5		0.176	0.005	4.682	0.067		
	L-2	0.048	0.003	1.928	0.077	L-2		0.159	0.003	4.211	0.056		
	2	L5	0.441	0.012	24.795	0.370		2	L10	0.372	0.003	17.085	0.118
		L10	0.474	0.006	27.047	0.409			L15	0.403	0.003	19.025	0.137
		L15	0.491	0.003	28.997	0.458			L25	0.446	0.004	22.818	0.294
		L25	0.538	0.003	33.718	0.450			L33	0.479	0.005	24.846	0.421
		L33	0.567	0.003	36.908	0.558			L-25	0.434	0.008	19.548	0.643
		L-25	0.510	0.009	29.828	0.716			L-15	0.355	0.005	13.995	0.417
		L-15	0.425	0.009	22.217	0.608			L-10	0.296	0.011	10.989	0.363
		L-10	0.367	0.010	17.911	0.440			L-5	0.235	0.011	8.575	0.259
		L-5	0.303	0.008	14.182	0.355			L-2	0.190	0.010	7.146	0.223
	L-2	0.267	0.006	11.878	0.285								
3	3	L5	0.496	0.003	26.549	0.455	L2	0.427	0.007	24.179	0.190		
		L10	0.531	0.005	28.417	0.518	L5	0.453	0.004	25.682	0.217		
		L15	0.567	0.003	30.460	0.463	L10	0.486	0.006	28.725	0.213		
		L25	0.646	0.007	36.186	0.296	L15	0.511	0.002	31.866	0.215		
		L33	0.707	0.006	41.185	0.312	L25	0.570	0.003	38.080	0.335		
		L-25	0.664	0.009	36.071	0.497	L33	0.626	0.009	42.873	0.285		

Species	Tree	Level	K mean	Stdev.	SFD mean	Stdev.	Species	Tree	Level	K mean	Stdev.	SFD mean	Stdev.
		L-15	0.603	0.010	29.521	0.542			L-25	0.580	0.010	36.444	0.484
		L-10	0.525	0.009	25.067	0.437			L-15	0.521	0.008	29.225	0.258
		L-5	0.457	0.005	21.055	0.354			L-10	0.484	0.003	25.309	0.306
		L-2	0.412	0.005	18.298	0.311			L-5	0.444	0.004	21.935	0.306
									L-2	0.399	0.005	19.433	0.321
	4	L2	0.492	0.015	24.818	0.334		4	L10	0.366	0.006	17.515	0.176
		L5	0.483	0.003	26.029	0.346			L15	0.390	0.005	19.294	0.171
		L10	0.521	0.002	28.201	0.353			L25	0.430	0.004	23.298	0.230
		L15	0.547	0.005	30.427	0.320			L33	0.455	0.003	26.330	0.244
		L25	0.606	0.005	35.682	0.341			L-25	0.406	0.002	22.496	0.209
		L33	0.654	0.004	39.537	0.454			L-15	0.340	0.005	17.781	0.210
		L-25	0.606	0.007	33.910	0.476			L-10	0.300	0.005	15.506	0.190
		L-15	0.523	0.009	27.026	0.326			L-5	0.260	0.006	13.138	0.131
		L-10	0.470	0.007	23.309	0.343			L-2	0.242	0.004	11.920	0.199
		L-5	0.417	0.007	19.722	0.293							
		L-2	0.376	0.010	17.396	0.244							

Table S4. General statistics of linear mixed-effect modelling for the thermal dissipation calibration curves (K [-] against F_d [$\text{cm}^3 \text{cm}^{-2} \text{h}^{-1}$]). Effects of species was tested on the calibration curve while using the individual stems as a random factor (model 1) or excluding the species effect (model 2). Additionally, the power-type function proposed by Granier *et al.*, (1985) is presented (model 3). The slope (Estimate), standard error of the slope (Std. error), frequentist statistics (t-value, p), goodness of fit [R^2] and the Akaike Information Criterion (AIC) is provided.

Model	Formula (in R)	Random effects	Coefficients	Estimate	Std. error	t-value	p	R^2	AIC
1	lmer(SFD ~ 0 + K * species + I(K^2) * species + (K tree))	Tree: Int. var. = 7.3 K var. = 75.7	K	25.82	10.59	6.08	0.050	0.96	267.8
			speciesLarix	0.47	2.53	3.89	0.862		
			speciesPicea	3.95	2.67	5.83	0.190		
			I(K^2)	52.34	11.85	7.60	0.003		
			kn:speciesPicea	-24.33	17.24	8.53	0.194		
			speciesPicea:I(K^2)	44.48	21.79	10.88	0.066		
2	lmer(SFD ~ 0 + K + I(K^2) + (K tree))	Tree: Int. var. = 1.3 K var. = 46.4	K	26.24	1.56	16.85	<0.001	0.96	283.9
			I(K^2)	56.50	4.51	12.53	<0.001		
3	nls(SFD ~ $\alpha * K^\beta$)	None	α	69.97	2.09196	33.45	<0.001	0.96	356.9
			β	1.364	0.04101	33.25	<0.001		

Table S5. Literature review on calibration curves. We distinguish: DB = Deciduous Broad-leaved, EB = Evergreen Broad-leaved, EC = Evergreen Coniferous, DC = Deciduous Coniferous. Wood anatomical properties include, DP = Diffuse-porous, RP = Ring-porous, SW = Softwood, DRP = Diffuse- to semi-ring-porous. For some of the measurements the standard error of the mean (SE) is provided. The symbol * indicates that the calibration curves is $\alpha K + \beta K^2$ instead of αK^β . All α values were recalculated to provide F_d in $\text{cm}^3 \text{cm}^{-2} \text{h}^{-1}$.

Site	Coordinates	Species	Leaf type	Wood type	n	Diameter (cm) [SE]	Sapwood area (cm ²) [SE]	Sapwood depth (mm) [SE]	K range	R ²	α	β	Source	
USA; Gibbs Farm	83°35'W 31°26'N	<i>Liriodendron tulipifera</i>	DB	DP							53.97	1.2	Bosch <i>et al.</i> , (2014)	
		<i>Pinus elliotii</i>	EC	SW							48.96	1.2		
		<i>Pinus palustris</i>	EC	SW							612	31		
USA; Salt Lake Valley	111°55'W 40°66'N	<i>Populus fremontii</i>	DB	DP	6	5.08 [0.15]	16.02 [1.01]	12.8 [1.46]	0-6		42.84	1.2	Bush <i>et al.</i> , (2010)	
		<i>Tilia cordata</i>	DB	DP	5	4.83 [0.15]	13.08 [0.75]	15.20 [0.80]	0-3		42.84	1.2		
		<i>Elaeagnus angustifolia</i>	DB	RP	7	4.36 [0.30]	1.70 [0.18]	1.63 [0.23]	0-0.7	0.	3348	1.6		
		<i>Gleditsia triacanthos</i>	DB	RP	6	5.06 [0.26]	0.73 [0.09]	0.98 [0.09]	0-0.8	0.	1105	1.4		
		<i>Quercus gambelii</i>	DB	RP	6	4.37 [0.08]	0.35 [0.06]	0.88 [0.04]	0-0.5	0.	2091	1.8		
		<i>Sophora japonica</i>	DB	RP	6	4.47 [0.22]	0.51 [0.12]	1.08 [0.14]	0-0.55	0.	4284	1.2		
											84	4		
											86	5		
France; Montfavet		<i>Malus pumila</i>	DB	DP	4				0-1	0.	49.24	1.2	Cabibel & Co (1991)	
										97	8	99		
		<i>Quercus palustris</i>	DB	RP	4				0-1	0.	49.24	1.2		
										97	8	99		
												71		
												4		

Site	Coordinates	Species	Leaf type	Wood type	n	Diameter (cm) [SE]	Sapwood area (cm ²) [SE]	Sapwood depth (mm) [SE]	K range	R ²	α	β	Source
		<i>Castanea sativa</i>	DB	RP	4				0-1	0.97	49.248	1.2714	
		<i>Quercus pedunculata</i>	DB	RP					0-0.8		42.84	1.231	Granier, (1985)
		<i>Pinus nigra</i>	EC	SW					0-1		42.84	1.231	
		<i>Pseudotsuga menziesii</i>	EC	SW					0-1.1		42.84	1.231	
UK; Swindon	1°42'W 51°36'N	<i>Acer campestre</i>	DB	DP	3	6-23			0-1.1	0.98	46.44	1.46	Herbst <i>et al.</i> , (2007)
		<i>Crataegus monogyna</i>	DB	DP	5	6-23			0-0.8	0.88	73.44	1.387	
UK; Wytham Woods	1°20'W 51°47'N	<i>Fraxinus excelsior</i>	DB	RP	5					0.96	728.28	0.428	Herbst <i>et al.</i> , (2008)*
Brasil; Piracicaba	46°38'W 23°33'S	<i>Eucalyptus grandis x urophylla</i>	DB	DP	4				0-0.8	0.95	304.46	1.606	Hubbard <i>et al.</i> , (2010)
USA; Utah's Entrada Field Station	-109°12'E 38°47' N	<i>Tamarisk ramosissima Ledeb. × chinensis</i>	DB	DP	11	4.15 [0.2]	4.45 [0.77]	5.8 [0.6]	0-1	0.98	86.4	1.16	Hultine <i>et al.</i> , (2010)
Australia; Darwin	130°52'E 12°25'S	<i>Mangifera indica</i>	EB	DP	1						42.84	1.231	Lu & Chacko, (1998)
Sweden; Norunda forest	17°29'E 60°5'N	<i>Picea abies</i>	EC	SW	2	22.1 [2.7]	290.5 [35.5]	78 [13]	0-0.20	0.95	248.832	1.816	Lundblad <i>et al.</i> , (2011)
		<i>Pinus sylvestris</i>	EC	SW	3	21.2 [2.4]	214 [61.4]	57 [1.3]	0-0.30	0.95	252.828	1.822	

Site	Coordinates	Species	Leaf type	Wood type	n	Diameter (cm) [SE]	Sapwood area (cm ²) [SE]	Sapwood depth (mm) [SE]	K range	R ²	α	β	Source
New Zealand; Huapai	174°30'E 36°48'S	<i>Agathis australis</i>	EC	SW	1	19				0.57	42.84	1.231	Macinnis-Ng, et al., (2016)
Panama; Santa Cruz	79°W 9°N	<i>Pseudobombax septenatum</i>	DB	DP	3	6.4 [0.12]	18.1 [0.69]				42.84	1.231	McCulloh et al., (2007)
		<i>Calophyllum longifolium</i>	EB	DP	3	6.0 [0.17]	21.3 [1.62]				42.84	1.231	
Germany; Grossfahner	10°49'E 51°30'N	<i>Populus nigra</i> × <i>P. maximowiczii</i>	DB	DRP	5	10.30 [0.48]			0-0.8	0.93	126.756	1.552	Schmidt-Walter et al., 2014
USA; Whitehall forest	83°21'W 33°54'N	<i>Fagus grandifolia</i>	DB	DP	2	18 [3]				0.70	82.8	0.9519	Steppe et al., (2010)
USA; Whitehall Forest	83°21'W 33°54'N	<i>Liquidambar styraciflua</i>	DB	DP	5	7.5 [0.4]	29.3 [3.1]	26 [1]	0-1.2	0.89	44.64	1.151	Sun et al., (2012)
		<i>Populus deltoides</i>	DB	DP	5	7.5 [0.4]	29.3 [3.1]	27 [1]	0-0.7	0.94	43.56	1.141	
		<i>Quercus alba</i>	DB	RP	5	7.5 [0.4]	29.3 [3.1]	28 [1]	0-0.4	0.87	46.08	1.47	
		<i>Ulmus americana</i>	DB	RP	5	7.5 [0.4]	29.3 [3.1]	29 [1]	0-0.8	0.95	97.92	2.572	
		<i>Pinus echinata</i>	EC	SW	5	7.5 [0.4]	29.3 [3.1]	30 [1]	0-0.9	0.91	36.36	1.303	
		<i>Pinus taeda</i>	EC	SW	5	7.5 [0.4]	29.3 [3.1]	31 [1]	0-1.2	0.88	34.92	1.336	

Site	Coordinates	Species	Leaf type	Wood type	n	Diameter (cm) [SE]	Sapwood area (cm ²) [SE]	Sapwood depth (mm) [SE]	K range	R ²	α	β	Source
USA; Red Butte Canyon	111°47'W 47°48'N	<i>Acer grandidentatum</i>	DB	DP	1	5-6					198	1.02	Taneda & Sperry (2008)
		<i>Quercus gambelii</i>	DB	RP	1	5-6					2084.4	1.38	
Italy; San Vito di Cadore		<i>Larix decidua</i>	EC	SW	4	16.5 [0.6]	71.9 [6.7]	18.4 [3.9]	0-0.72	0.	26.23	56.	This study*
		<i>Picea abies</i>	EC	SW	4	15.9 [1.5]	121.2 [15.5]	35.8 [4.9]	0-0.65	96	6	49	
												5	

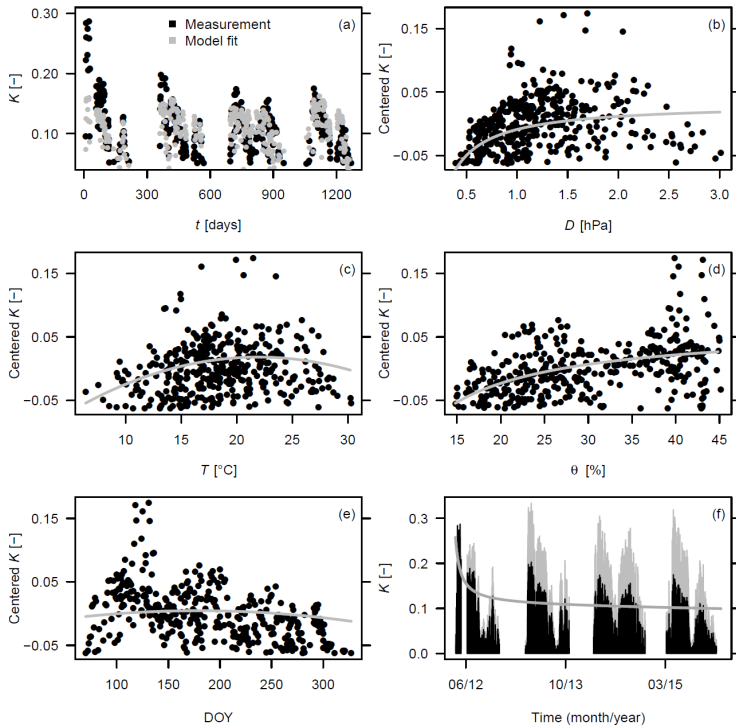


Figure S2. Example of the procedure to isolate the damping effect for K (pre-dawn ΔT_{max}) measured for a *Picea abies* tree at N13. (a) Residuals are calculated by subtracting the measurements from the model values constructed with environmental factors and seasonality. This model, explained in Table S2, uses daily maximum vapour pressure deficit (b), daily mean temperature (c), daily mean soil moisture (d) and a seasonality term (e) to explain the daily maximum K pattern. Then the residuals containing the damping are explained with a non-linear model (f), after which this model is used on the raw values (black lines) and transformed to corrected values (grey lines).

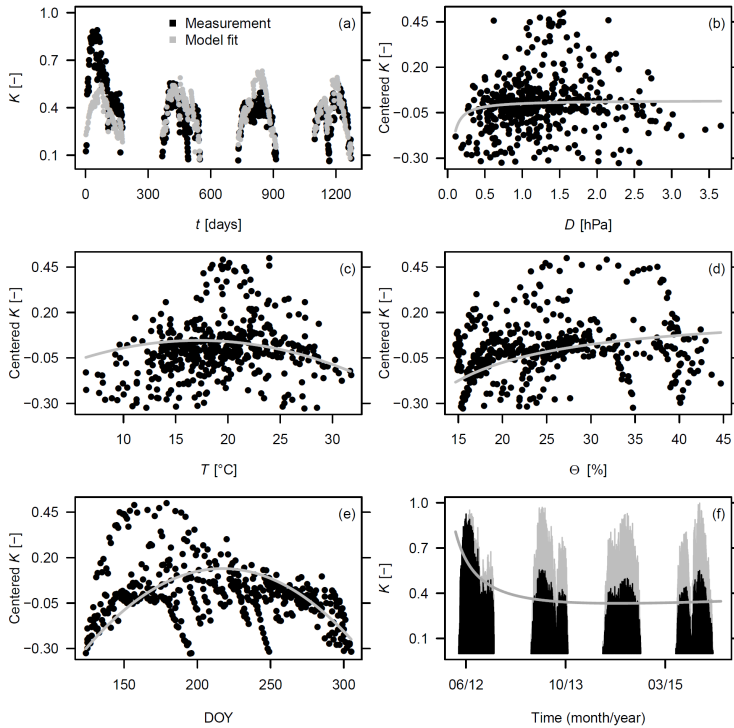


Figure S3. Example of the procedure to isolate the dampening effect for K (pre-dawn ΔT_{max}) measured for a *Larix decidua* tree at N13. (a) Residuals are calculated by subtracting the measurements from the model values constructed with environmental factors and seasonality. This model, explained in Table S2, uses daily maximum vapour pressure deficit (b), daily mean temperature (c), daily mean soil moisture (d) and a seasonality term (e) to explain the daily maximum K pattern. Then the residuals containing the dampening are explained with a non-linear model (f), after which this model is used on the raw values (black lines) and transformed to corrected values (grey lines).

References

- Bosch DD, Marshall LK, Teskey R. 2014.** Forest transpiration from sap flux density measurements in a Southeastern Coastal Plain riparian buffer system. *Agricultural and Forest Meteorology* **187**: 72–82.
- Cabibel BDF. 1991.** Mesures thermiques des flux de sève dans les troncs et les racines et fonctionnement hydriques des arbres. *Agronomie* **8**: 669–678.
- Gelman A., & Hill J. 2007.** Data analysis using regression and multilevel/hierarchical models (Vol. 1). New York, NY, USA: Cambridge University Press. ISBN: 978-0-521-86706-1.
- Herbst M, Roberts JM, Rosier PTW, Gowing DJ. 2007.** Seasonal and interannual variability of canopy transpiration of a hedgerow in southern England. *Tree physiology* **27**: 321–33.
- Herbst M, Rosier PTW, Morecroft MD, Gowing DJ. 2008.** Comparative measurements of transpiration and canopy conductance in two mixed deciduous woodlands differing in structure and species composition. *Tree physiology* **28**: 959–970.
- Hubbard RM, Stape J, Ryan MG, Almeida AC, Rojas J. 2010.** Effects of irrigation on water use and water use efficiency in two fast growing Eucalyptus plantations. *Forest Ecology and Management* **259**: 1714–1721.
- Hultine KR, Nagler PL, Morino K, Bush SE, Burtch KG, Dennison PE, Glenn EP, Ehleringer JR. 2010.** Sap flux-scaled transpiration by tamarisk (*Tamarix spp.*) before, during and after episodic defoliation by the saltcedar leaf beetle (*Diorhabda carinulata*). *Agricultural and Forest Meteorology* **150**: 1467–1475.
- Lu P, Chacko E. 1998.** Evaluation of Granier's sap flux sensor in young mango trees. *Agronomie* **18**: 461–471.
- Macinnis-Ng C, Webb T, Lin Y-S, Schwendenmann L, Medlyn B. 2016.** Leaf age-related and diurnal variation in gas exchange of kauri (*Agathis australis*). *New Zealand Journal of Botany* **8643**: 1–20.
- Mcculloh KA, Winter K, Meinzer FC, Aranda J, Lachenbruch B. 2007.** A comparison of daily water use estimates derived from constant-heat sap-flow probe values and gravimetric measurements in pot-grown saplings. *Tree Physiology* **27**: 1355–1360.

- Schmidt-Walter P, Richter F, Herbst M, Schuldt B, Lamersdorf NP. 2014.** Transpiration and water use strategies of a young and a full-grown short rotation coppice differing in canopy cover and leaf area. *Agricultural and Forest Meteorology* **195–196**: 165–178.
- Taneda H, Sperry JS. 2008.** A case-study of water transport in co-occurring ring-versus diffuse-porous trees: contrasts in water-status, conducting capacity, cavitation and vessel refilling. *Tree Physiology* **28**: 1641–1651.

Chapter 3

No role for xylem embolism or carbon decrease in temperate trees during a severe drought

Lars Dietrich^{†,1}, Sylvain Delzon², Günter Hoch¹, Ansgar Kahmen¹

¹Department of Environmental Sciences, University of Basel, Totengässlein 3, CH-4051 Basel, Switzerland

²UMR BIOGECO INRA-UB, University of Bordeaux, Avenue des Facultés, 33405 Talence, France

[†]To whom correspondence should be addressed.

E-mail: larsdietrich.plantphys@gmail.com

Phone: +41612073518

Submitted to Journal of Ecology.

Abstract

1. World-wide, temperate forests are predicted to face an increase in the frequency and intensity of climate change-induced summer droughts and heat waves in the near future. Yet, it remains unclear how these climate-change related increases in drought and heat will affect forests, especially concerning interrelated effects of water relations like xylem embolism, and the carbon economy.

2. Here, we tested the sensitivity of six temperate tree species to severe water limitation during three consecutive growing seasons including the exceptional 2015 central European summer drought and heat wave. Specifically, we assessed stem increment growth, sap flow, water potentials, hydraulic traits, and non-structural carbohydrate concentrations in leaves and branches to determine how mature temperate trees responded to this exceptional weather event and how the observed responses relate to variation in xylem embolism and carbon economy.

3. We found that the trees' pre-dawn water potentials reached their minimum values during the 2015 summer drought and decreased much more than during the other study years. Also, most species reduced their sap-flow by up to 80% during the 2015 summer drought and increment growth ceased with the onset of the drought. Midday water potentials decreased strongly during the drought, but levelled off at a species-specific low-point with decreasing soil water availability. Despite the strong responses in the trees' growth and water relations, all species exhibited minimum leaf water potentials well away from values associated with severe embolism (P_{50}). In addition, we detected no distinct decrease in non-structural carbohydrates in leaves, bark and stems during the drought event. Therefore, we conclude that although the six species responded sharply in their water relations, all trees exhibited water potentials that indicate for only a low amount of xylem embolism and showed no depletion of carbohydrate reserves in leaves and branches.

4. *Synthesis*: This study shows that mature individuals of six common central European forest tree species strongly reacted to a severe summer drought by reducing their water consumption and stopping growth. At the same time, however, we found no indications for high amounts of xylem embolism or strong carbohydrate depletion in the trees. This suggests, that xylem embolism formation and carbohydrate reserve depletion are not routine in temperate trees during seasonal strong drought.

Introduction

Current climate models predict an increased frequency and intensity of heat waves and drought events globally (Trenberth 2011) and for central Europe in particular (Fischer *et al.* 2014; Orth, Zscheischler & Seneviratne 2016). The consequences of the increased frequency and duration of heat waves and drought events for terrestrial forest ecosystems are predicted to be manifold (Reichstein *et al.* 2013). Among others, heat waves and drought events can disrupt the physiological and metabolic integrity of trees which in turn affects tree growth and can even cause large-scale tree mortality leading to forest dieback with severe consequences for the ecosystem goods and services (Allen *et al.* 2010; Carnicer, Coll & Ninyerola 2011; Williams, Allen & Macalady 2013).

The physiological susceptibility of trees in the temperate forest biome to heat and drought is surprisingly poorly understood. Those studies that have assessed the water relations of temperate trees during naturally occurring drought indicate that mature trees respond very sensitively to drought (Hölscher *et al.* 2005; Köcher *et al.* 2009; Hoffmann *et al.* 2011; Meinzer *et al.* 2013; Brinkmann *et al.* 2016). For example, Brinkmann *et al.* (2016) have shown that trees strongly reduced their sap flow for several weeks in response to low soil moisture. Also, during the 2003 centennial heatwave and drought in central Europe, various temperate tree species revealed a dramatic decline in sap flow for extended periods of time (Leuzinger *et al.* 2005). While these previous studies clearly showed the drought sensitivity of different temperate tree species, it remains unclear to what extent this drought response indicates a high vulnerability of these trees with respect to their physiological integrity.

Besides other factors, xylem embolism and carbohydrate depletion are thought to be among the main processes that can compromise the physiological and metabolic integrity of trees during drought (McDowell 2011; Martínez-Vilalta, Lloret & Breshears 2012; Zeppel, Anderegg & Adams 2012; Mencuccini *et al.* 2015). Xylem embolism is the result of a disruption of the water column due to very high tensions in the xylem conduits (Sperry 2000). High levels of embolism are assumed to impair the water supply to the foliage and ultimately lead to tissue desiccation. While some studies suggest that xylem embolism might play an important role during exceptional and devastating drought events (Anderegg *et al.* 2016), it is still discussed whether xylem embolism is a common phenomenon in mature trees under non-lethal drought events (Cochard & Delzon 2013; Klein *et al.* 2016). The depletion of non-structural

carbohydrate pools has been suggested to result from the extended closure of stomata during drought leading to reduced photosynthesis and eventually a shortage of carbohydrate metabolites in the different tree tissues (Hartmann 2015). However, tree carbohydrate reserve pools were often only measured towards the end of drought periods (Galiano, Martinez-Vilalta & Lloret 2011; Adams & Zeppel 2017) or observed in seedlings under additional shading treatment (Hartmann, Ziegler & Trumbore 2013a; Hartmann *et al.* 2013b; Hartmann, McDowell & Trumbore 2015; Maguire & Kobe 2015). Hence, most of the information on the vulnerability of temperate trees to xylem embolism and carbon depletion was obtained in experimental work or from very few scattered measurements throughout or at the end of a given period of time. Evidence is therefore needed, that document the physiological sensitivity of mature temperate trees during naturally occurring drought events, in particular with respect to xylem embolism and carbohydrate depletion.

In the months July, August and September 2015, most parts of central Europe were hit by an exceptional heat wave and dry spell. The 2015 summer received one of the lowest rainfall amounts since 1901 and soil moisture was even lower than during the centennial heat wave of 2003 (Orth *et al.* 2016). The 2015 summer drought thus exposed forests to weather conditions which are predicted to regularly occur during central European summers by the end of this century. The impacts of the 2015 heat wave and dry spell on agriculture and human health were dramatic with substantial losses in yield, and an estimated number of 800 human fatalities that were attributed to the heat wave in Switzerland alone (FOEN, 2016). We took advantage of this exceptional climatic event and tested (i) how mature individuals of six different temperate tree species responded in their water relations and growth to the severe water limitation during the 2015 summer drought, and (ii) determined the physiological integrity of these trees with respect to levels of xylem embolism and carbohydrate reserves or resources.

Material and methods

Study site and study species

We conducted our study from 2014 – 2016 in a diverse mixed forest 15 km south of Basel, Switzerland (47°28'N, 7°30'E), that was equipped with a canopy crane (Swiss Canopy Crane facility; Pepin & Körner, 2002). The forest is located at an elevation of 550 m a.s.l. and has a stony rendzina-type soil based upon calcareous bedrock at ~1 m depth. The forest contains a mix of coniferous and deciduous tree species, dominated by *Fagus sylvatica* L. and *Quercus petraea* (Matuschka) Liebl. Other frequent species are *Abies alba* Mill., *Larix decidua* Mill., *Picea abies* (L.) Karst, *Pinus sylvestris* L. and *Carpinus betulus* L. (Pepin & Körner 2002). The trees of the forest are about 130 years old and between 35 and 40 m tall. We performed measurements on four mature individuals of the species *C. betulus*, *F. sylvatica*, *L. decidua*, *P. abies*, *P. sylvestris* and *Q. petraea* during the growing seasons of 2014, 2015 and 2016 (Mai 1 to October 31) resulting in a total of 24 study trees. *L. decidua* was only investigated in 2015 and 2016.

The climate at the site is temperate-humid with mild winters and moderately warm summers (mean January and July temperatures of 2.1 and 19.2°C, respectively). Total mean annual precipitation of the region is 900 mm with two thirds of precipitation generally falling during the growing season (15 April – 31 October). We measured air temperature, relative humidity and precipitation during all three years with a weather station (Davis Vantage Pro 2, Scientific Sales Inc., Lawrenceville, NJ, USA) on ten minute intervals. We also recorded soil water potential (Ψ_{soil}) at 20 cm depth with dielectric sensors (MPS-2, Decagon Devices, Pullman, WA, USA) on ten-minutes intervals. We employed 20 Ψ_{soil} sensors in 2014 and 12 in 2015 and 2016.

To put our three-year sampling campaign into the long-term climatic context of the site, we analysed precipitation and temperature data from 1900 until present for the weather station Basel-Binningen, which is located at 8 km from the research site. The data were provided by the Federal Office of Meteorology and Climatology (Zurich, Switzerland).

Sap-flow measurements

To determine the transpiration response of the species investigated to drought, we measured the sap flow of four individuals of each of the six study species from April 2014 to October 2015. Sap-flow was measured with Granier-type heat dissipation

probes (SFS2-M, UP GmbH, Ibbenbüren, Germany) installed at the NE and SW sides of the tree stems. At the two insertion points of the sensor needles (at ca. 1.5 m stem height) the bark of the tree was carefully peeled off. Aluminium sleeves were inserted 20 mm deep into the sapwood with a 10-cm vertical distance from each other. Then the greased sensor needles were inserted into the sleeves and sealed with Teroson MS 930[®] sealing adhesive from the outside. Sensors were protected from weather influences and solar radiation by a radiation shield made of thick bubble wrap aluminium foil. During operation, the upper needle constantly heated the sapwood and measured temperature with a copper-constantan thermocouple, while the lower needle measured the ambient sapwood temperature. Sensor voltage values were recorded every ten minutes with a sensor node (Channel Node, Decentlab GmbH, Dübendorf, Switzerland), wirelessly transmitted to a data logger (Base Station, Decentlab GmbH) and then broadcasted to a server via cellular network.

Data evaluation was done in compliance with the method of Granier (1985; 1987) and the considerations of Peters *et al.* (Richard Peters *et al.*, unpublished data). We calculated the temperature difference between the two needles (ΔT) of each sap-flow device from voltage values. In order to precisely estimate no-flux-conditions during night-time and account for night-time transpiration, no-flux-conditions were defined as the maximum ΔT (ΔT_{\max}) during the night within a seven-day period. In case of a drift over time in ΔT_{\max} we applied a linear regression through ΔT_{\max} over 7 days and set ΔT_{\max} to the regression values if it was below the regression line. If the individual trees were found to exhibit a sapwood depth shorter than the length of the sensor needles, we performed a correction of ΔT to determine sapwood ΔT excluding the fraction of the probes that was inserted into non-conducting heartwood (Clearwater *et al.* 1999):

$$\Delta T_{SW} = \frac{\Delta T - b\Delta T_{\max}}{a}$$

where a and b are the fractions of the sensor needle in sapwood and inactive heartwood, respectively, and ΔT_{SW} is the temperature difference between the sapwood proportions of the needles.

Total sap-flow density u was calculated (Granier 1985; 1987) by

$$K = \frac{\Delta T_{\max} - \Delta T}{\Delta T}$$

where K is a dimensionless parameter, and subsequently

$$u = 119 * 10^{-6} * K^{1.231}$$

To make sap-flow values of both years comparable in our analysis, we corrected sap flow of each sensor per individual by the difference among the two years to account for year-to-year differences: We screened for days with similar environmental conditions (Ψ_{soil} , VPD, PAR) in both summers of the two growing seasons and divided the mean daily maximum sap-flow of 2014 on these days by the respective mean of the 2015 values. All maximum daily sap-flow values of 2015 were then multiplied with the resulting conversion factor.

In our study, we only considered relative daily maximum sap-flow values which were calculated for each sensor by dividing the daily maximum absolute sap-flow by the 95th percentile of maximum sap-flow values throughout the respective growing season. We calculated the mean of both sensors per tree and then averaged these values to obtain mean values for each species ($n = 4$ per species).

Water potential measurements

To evaluate the water status of the trees, we measured midday (Ψ_{midday}) and pre-dawn ($\Psi_{\text{pre-dawn}}$) leaf water potentials. Ψ_{midday} was assessed around noon at an irregular interval throughout the two growing seasons (10 and 17 measurement campaigns in 2014 and 2015, respectively). $\Psi_{\text{pre-dawn}}$ was assessed shortly before dawn on nine days during the 2015 growing season. Ψ_{midday} and $\Psi_{\text{pre-dawn}}$ were measured with a Scholander pressure bomb (Model 1000, PMS Instruments, Albany, OR, USA) on three ca. 15 cm long terminal shoots per tree with two to four leaves (broad-leaved) from the upper part of the sunlit crown. To obtain values for a species, we first averaged the three shoot measurements per tree and then averaged the means of the individual trees resulting in a total number of four replicates per species.

Stem diameter variations and modeling of Ψ

To determine the seasonal increment growth and the water deficit of the trees, we installed automated point dendrometers (ZN11-T-WP, Natkon, Oetwil am See, Switzerland) to assess diurnal and seasonal stem diameter variations (SDV). On each tree, one dendrometer was installed on the north-east facing side of the stem at ~ 2 m of height at the beginning of the study (April 2014). From diurnal SDV, we calculated tree water deficit (TWD) as described in Dietrich, Zweifel & Kahmen (2018). In brief, TWD is a measure for the water loss in the non-conducting tissue of the stem that is expressed

in the shrinking of the stem when transpiration of the tree exceeds water uptake of its roots. TWD equals zero when the tree is fully hydrated. TWD increases when the tree is exposed to progressive soil drying and cannot refill its non-conducting tissue during night-time.

TWD has been shown to correlate with Ψ (Drew *et al.* 2011; Dietrich, Zweifel & Kahmen 2018). We thus employed TWD to model the seasonal variability of Ψ_{midday} and $\Psi_{\text{pre-dawn}}$ at a daily resolution for the 2014 – 2016 growing seasons. To do so, we employed linear functions that we empirically obtained for each of the six species from 27 and 9 observations of Ψ_{midday} and $\Psi_{\text{pre-dawn}}$, respectively, and their corresponding TWD values (Dietrich, Zweifel & Kahmen 2018). We then used the derived functions for each species to model Ψ_{midday} and $\Psi_{\text{pre-dawn}}$ for each day of the study period on a species level.

SDV were also used to calculate the daily increment growth for four individuals of each of the six species. We considered growth to occur only during periods of effective diameter increases, and assumed no growth during periods of stem shrinkage. Hence, during times of radial shrinkage, stem diameter was set to the last maximum measured before shrinkage for the calculation of daily increment growth. All individuals of a species were pooled to obtain a single mean stepwise-increasing increment growth curve per species. The stem increment data from all three years were standardized on the total increment growth from 2014 to 2016 and expressed as % growth of three years.

PLC curves, P_{50}/P_{88} and hydraulic safety margin

A branch segment of about 35 cm length and 1 cm of diameter was collected from the sunlit crown of each of four individual trees per species before dusk in October 2015. The branch segments were directly wrapped into moist paper towels and stored in plastic bags at 4°C. Branch segments were sent to the Caviplace lab at INRA Bordeaux within a week, where they were stored at -4°C prior to measurements. Samples were then recut to 28 cm long segments under tap water. Centrifuge measurements were performed within three weeks using the Cavitron technique (Cochard 2002; Cochard *et al.* 2005). For *Q. petraea*, we collected branch segments of 1.2 m and performed maximum vessel lengths estimations on additional stems by injecting air at 2 bars and cutting the apical end of the water-immersed stem section until the air bubbles emerged. This procedure

allowed us to find that *Q. petraea* stems have a maximum vessel length of ~ 50 cm, which confirms that vulnerability curves in this species cannot be adequately constructed using the 27 cm diameter rotor, where a significant proportion of open-cut vessels surpass the center of the plant segment or even permeate through its whole length. Therefore all samples were re-cut under water at 1m and measured with a large rotor Cavitron. The stem segments were spun at different speeds thereby creating water potentials from moderate to very negative values within the segments. The hydraulic conductance of the stem segments at each generated water potential was measured and based on the initial conductance of the segment, the loss of conductance at the generated water potentials was calculated according to Wang *et al.* (2014).

We fitted a logistic function through each set of data points per individual and extracted the pressure values at 50% loss of conductivity (P_{50}) and 88% loss of conductivity (P_{88}) from the resulting percent loss of conductivity (PLC) curve. P_{50} and P_{88} were then averaged per species. We calculated hydraulic safety margins ($\Delta\Psi$) for the species examined by subtracting the P_{50} or P_{88} value from the minimum Ψ_{midday} measured and modelled during the three growing seasons (Ψ_{min}). In order to account for the proposed higher sensitivity of conifers over angiosperm trees to hydraulic failure (Choat 2013; Delzon & Cochard 2014), we calculated $\Delta\Psi$ with P_{50} values to account for the three coniferous species ($\Delta\Psi_{50}$), and with P_{88} to account for the three angiosperm species ($\Delta\Psi_{88}$).

Non-structural carbohydrates (NSC)

NSC (i.e., starch, sucrose, fructose and glucose) were quantified in leaves, bark and xylem of sun-exposed 3- to 4-year-old branches in each of the four individuals of the six species (one branch per individual). Samples were collected throughout the summer of 2015. For chemical analysis in the lab we used a modified protocol after Wong (Wong 1990). 8-12 mg of the dried (24 hours at 75°C) and finely ground plant tissue was extracted with 2 mL of distilled water in glass vials which were covered with marbles and boiled over steam at 100°C for 30 minutes. To degrade sucrose and convert fructose to glucose, an aliquot of 200 μL of the solution was treated with invertase, an isomerase from baker's yeast. Then the glucose in the solution was converted to gluconate-6-phosphate with glucose-hexokinase. The total amount of gluconate-6-phosphate (equal to glucose concentration) was determined with a 96-well multi-plate photometer

(Multiscan EX, Thermo Fisher Scientific, Waltham, MA, USA) at 340 nm. For the determination of starch concentrations, a fungal amyloglucosidase from *Aspergillus niger* was added to an aliquot of 500 μ L of the remaining extract. The solution was put in a water bath at 49°C for 12 hours to progressively digest starch to glucose. The total glucose concentration in the solution was then determined with a photometer as described above. Starch concentration was calculated as the difference between the glucose concentrations with and without degradation of starch. Enzymes were purchased from Sigma-Aldrich (St. Louis, MO, USA) and solutions of glucose, fructose and sucrose as well as pure starch and a homogenized plant powder (Orchard leaves, Leco, St. Joseph, MI, USA) were used as standards and control of reproducibility.

Statistical analyses

Statistical analyses and data visualization were done using *R*, version 3.4.1 (R Foundation for Statistical Computing, Vienna, Austria 2013), with its packages zoo (Zeileis & Grothendieck, 2005), xts (Ryan & Ulrich, 2014), data.table (Dowle *et al.*, 2015), caTools (Tuszynski, 2014), scales (Wickham, 2015), gridExtra (Auguie, 2015) and ggplot2 (Wickham, 2009). We assumed a $p < 0.05$ as the level of significance for all statistical tests. For the regression analyses between Ψ_{midday} and Ψ_{soil} we used the *nls()* command with the function

$$\psi_{\text{midday}} = a * \left(1 - e^{-\frac{\psi_{\text{soil}}}{b}}\right).$$

The parameters *a* and *b* thereby determine the saturation value and curvature of the function, respectively. For linear regressions between sensitivity of sap-flow to Ψ_{soil} we used the *lm()* function.

Results

Environmental conditions

For Central Europe, the 2015 summer had the lowest rainfall since 1901, and soil moisture was even lower than during the centennial heat wave of 2003 (Orth, Zscheischler & Seneviratne 2016). For our research site, the year 2015 was the second warmest year since climate recordings began in 1900 at a nearby climate station. These temperature extremes account for both, the mean annual temperature and the mean July/August temperature (Fig. 1 and 2). In addition, the summer (i.e. July to September) 2015 was among the 10% of summers that exhibited the lowest rainfall amounts of the past 100 years with approximately 45% less precipitation in the months July – September compared to the long-term mean (Fig. 1 and 2). The extreme air temperatures in July, August and the beginning of September 2015 also caused VPD during this time to be substantially higher than in the same period in 2014 or 2016 (Fig. 1). High summer VPD in combination with low seasonal precipitation inputs resulted in substantial soil drying, where Ψ_{soil} at -20 cm progressively decreased to -1.3 MPa in July, August and September 2015 and remained low throughout these months (Fig. 1). The extent of soil drying during the summer of 2015 becomes particularly apparent when compared to the same months in 2014 and 2016. While long-term soil moisture records do not exist for our research site, regional hydrological models suggest that soil moisture in NW Switzerland in the 2015 summer was within the lowest five percentiles compared to the summer mean since 1979 (Orth, Zscheischler & Seneviratne 2016).

The heat and drought of 2015, however, did not lead to any apparent signs of reduced health or mortality in the study trees.

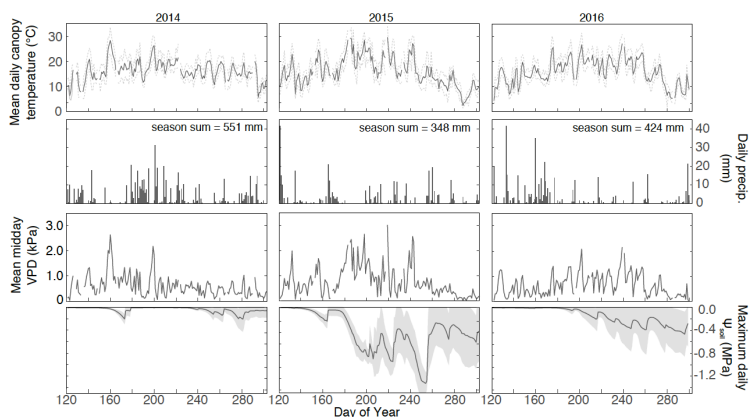


Figure 1 Environmental data for the growing seasons 2014 - 2016. Dashed lines around mean daily temperature are minimum and maximum temperatures of the respective day. All variables except Ψ_{soil} were measured with a weather station at the top of the canopy crane at 40 m above ground. Ψ_{soil} was calculated as the mean of the daily maxima of 20 (2014) and 12 (2015 and 2016) sensors at a depth of $-20 \text{ cm} \pm \text{SD}$.

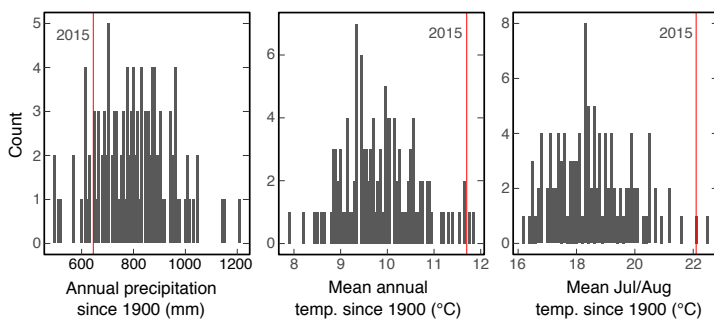


Figure 2 Frequency distribution of annual precipitation, mean annual temperature and mean July and August temperature since 1900 at Binningen (Canton Basel County) in the vicinity of the study site. Red lines indicate the value of the year 2015.

Seasonal patterns of $\Psi_{\text{pre-dawn}}$ and Ψ_{midday}

Modelled $\Psi_{\text{pre-dawn}}$ values of the six species were in good agreement with measured values ($R^2 = 0.76$; Supporting Fig. 1). Modelled seasonal variation in $\Psi_{\text{pre-dawn}}$ differed substantially among the six species and among years (Fig. 3). Importantly, however, all species reached the most negative $\Psi_{\text{pre-dawn}}$ of the three years during the 2015 summer drought (down to -2.1 MPa in *P. abies*) and exhibited the least negative minima in 2014. Also, $\Psi_{\text{pre-dawn}}$ remained low throughout July, August and September 2015, indicating that the 2015 summer drought severely impacted the water availability of the trees for an extended amount of time. We observed substantial differences in $\Psi_{\text{pre-dawn}}$ during the 2015 summer drought among the six species, where $\Psi_{\text{pre-dawn}}$ was particularly negative in *C. betulus*, *F. sylvatica* and *P. abies*, while *P. sylvestris*, *L. decidua* and *Q. petraea* showed less negative values. Variation in $\Psi_{\text{pre-dawn}}$ among years ranged between 0.5 and 1.5 MPa, and was higher in *P. abies*, *C. betulus* and *F. sylvatica* (above 1 MPa), while *Q. petraea*, *P. sylvestris* and *L. decidua* revealed comparably low amounts of variation (below 1 MPa).

Modelled midday values for Ψ were also in good agreement with measured values ($R^2 = 0.71$; Supporting Fig. 1). Similar to $\Psi_{\text{pre-dawn}}$, Ψ_{midday} differed substantially among the six species and years and the most negative values for each species were reached during the 2015 summer drought (Fig. 3). *C. betulus*, *F. sylvatica* and *P. abies* reached their most negative Ψ_{midday} towards the end of the 2015 summer drought, while *Q. petraea*, *L. decidua* and *P. sylvestris* exhibited Ψ_{midday} values that were consistently low throughout the 2015 summer drought. During 2015, *Q. petraea* reached the most negative Ψ_{midday} values of all species followed by *L. decidua*, *F. sylvatica*, *P. abies*, *C. betulus*, and *P. sylvestris*. In *P. sylvestris*, midday values turned out to vary only slightly throughout the 2015 summer drought, and unlike for the other species, no pronounced extreme values were observed (Fig. 3).

To test if the Ψ_{midday} values during the 2015 summer drought were saturating at minimum values, we plotted Ψ_{midday} over Ψ_{soil} for each species (Fig. 4). All of the species showed Ψ_{midday} to level off with decreasing Ψ_{soil} . This indicates that the species were still able to maintain a minimum Ψ_{midday} despite the continuous decrease of Ψ_{soil} during the investigated drought period.

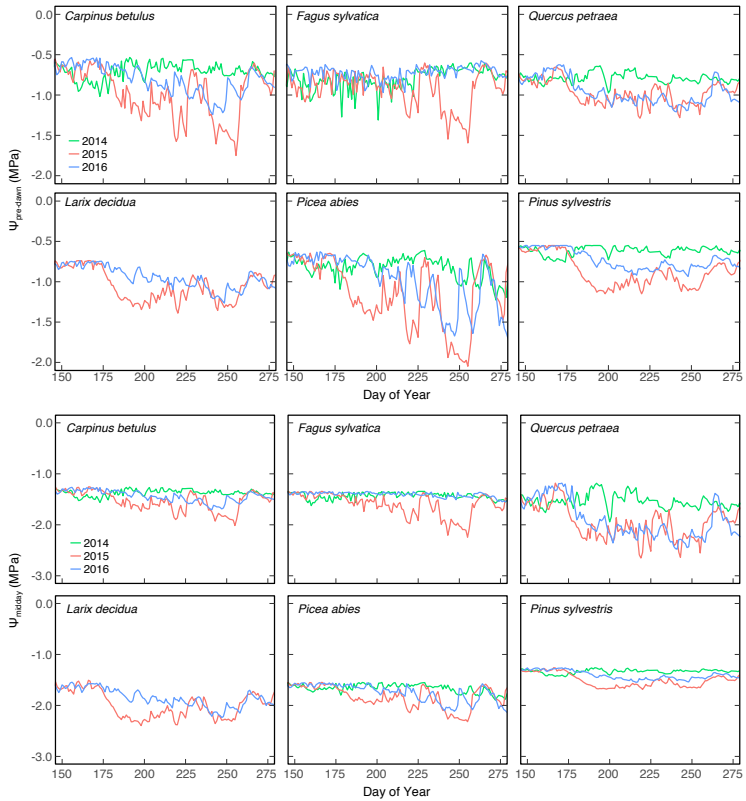


Figure 3 Modelled pre-dawn and midday Ψ_{leaf} of the six investigated species during the summers of 2014 - 2016. The values are derived from the relationship between pre-dawn and midday Ψ_{leaf} and tree water deficit measured at the base of the stem on 9 (pre-dawn) and 28 (midday) different days in the growing seasons of 2014 and 2015 (pre-dawn only in 2015).

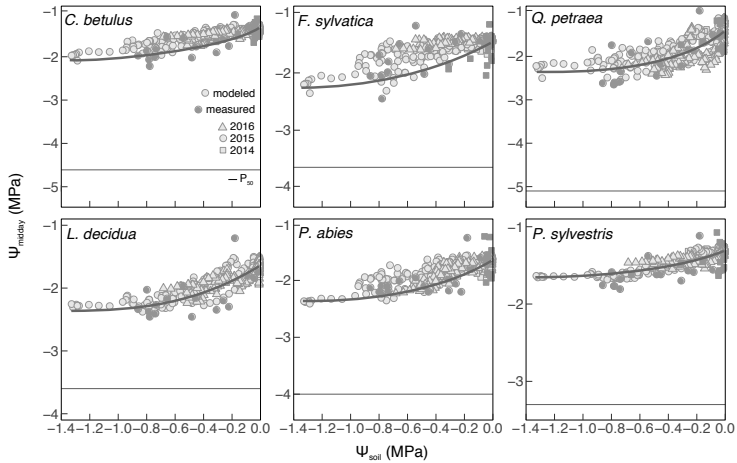


Figure 4 Relationship between modeled and measured midday Ψ_{leaf} and Ψ_{soil} in the considered species during the summer part of the growing seasons (June 1 to September 30) in 2014, 2015 and the P_{50} values. P_{50} values were obtained from PLC curves deriving from centrifuge measurements on one branch of each individual of the respective species (pooled logistic regression through all measurement points per species).

Hydraulic integrity

P_{50} and P_{88} values varied significantly among the six species (Tab 1, Supporting Fig. 2). *Q. petraea* was the most embolism-resistant species (most negative P_{50} and P_{88} values), while *P. sylvestris* showed the least negative values for P_{50} and P_{88} .

Ψ_{midday} of the different species was at least ~ 1 MPa higher than the measured P_{50} values throughout the whole study period (Fig. 4). Therefore, all species suffered from no or few embolism events (at most 10 % loss of conductance in branches), even during the 2015 summer drought (cf. Supporting Fig. 2). To determine the actual susceptibility of the study species to strong xylem embolism during the 2015 summer drought, we estimated the hydraulic safety margin (HSM, $\Delta\Psi$) for each species, which is the difference between the minimum Ψ_{midday} (Ψ_{min}) of a respective species that was reached during the 2015 summer drought and the P_{50} (conifers) or P_{88} (angiosperms) value. HSMs ranged between 1.2 MPa in *L. decidua* and 3.8 MPa in *Q. petraea* (Tab. 1). *C. betulus* showed a wide HSM similar to *Q. petraea* while *F. sylvatica* exhibited a

HSM which resembled more those of the coniferous species which generally exhibited safety margins slightly above 1 MPa (Tab. 1).

Table 1 P_{50} and P_{88} values measured on branches from the sun-exposed canopy of the investigated species with the cavitron technique and hydraulic safety margins ($\Delta\Psi$) calculated as the difference between the P_{50}/P_{88} value and the most negative measured/modeled Ψ of the respective species. $\Delta\Psi$ values in given in brackets are regarded as less meaningful for the respective species than those given without brackets cf. (Choat 2013). For the assessment of P_{50}/P_{88} values, one branch per tree (n=4) was harvested before dusk during October 2015, stored at 4°C and sent to the Cavitron lab in Bordeaux within one week. Pressures at 50 and 88% loss of conductance, respectively, were extracted from the resulting vulnerability curves.

Species	P_{50} (MPa)	P_{88} (MPa)	$\Delta\Psi_{50}$ (MPa)	$\Delta\Psi_{88}$ (MPa)
<i>C. betulus</i>	-4.71	-5.83	(2.6)	3.7
<i>F. sylvatica</i>	-3.79	-4.62	(1.5)	2.3
<i>Q. petraea</i>	-5.13	-6.45	(2.4)	3.8
<i>L. decidua</i>	-3.64	-4.7	1.2	(2.2)
<i>P. abies</i>	-4.01	-5.15	1.7	(2.8)
<i>P. sylvestris</i>	-3.31	-4.2	1.5	(2.4)

Sap-flow

For all species, daily maximum sap-flow remained consistently high throughout the 2014 growing season (Fig 5). Values decreased only towards the very end of that growing season, which can be attributed to leaf senescence. In contrast, daily maximum relative sap-flow decreased strongly in most species with the onset of the 2015 summer drought (around DOY 180) and stayed low until the end of the season (Fig. 5). In *C. betulus*, *F. sylvatica*, *P. abies* and *P. sylvestris*, almost 80% reduction of maximum daily sap-flow was observed during the 2015 drought. *L. decidua* showed a reduction of about 60%. The only exception was *Q. petraea*, which showed only a weak response to the 2015 summer drought.

All of the species revealed their highest sap-flow at a VPD of around 0.5 – 0.8 kPa (Supporting Fig. 3). The coniferous species generally showed a steeper decline of sap-flow with increasing VPD beyond 0.8 kPa than the angiosperm species of which *Q. petraea* showed the least intensive response (Supporting Fig. 3). *P. abies* and *P. sylvestris* reached sap-flow values close to zero at a VPD of ~3 kPa. All of the species

except *Q. petraea* showed a steep decline of sap-flow with decreasing Ψ_{soil} at -20 cm soil depth, with *P. sylvestris*, *P. abies*, and *F. sylvatica* revealing the highest sensitivity (Supporting Fig. 3).

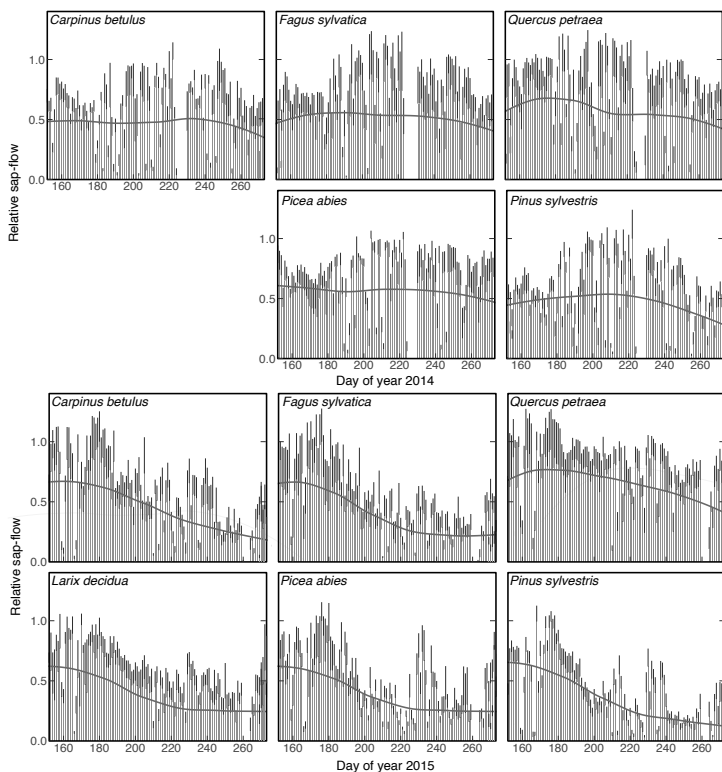


Figure 5 Relative sap-flow of the six investigated species from June 1 to September 30 in 2014 and 2015 ($n = 4$ individuals per species \pm SD) with a locally-fitted non-parametric regression (LOESS, green line). Sap-flow was measured with two thermal dissipation probes on each individual on both the north- and the south-facing site of the stem. *L. decidua* was only taken into account in 2015.

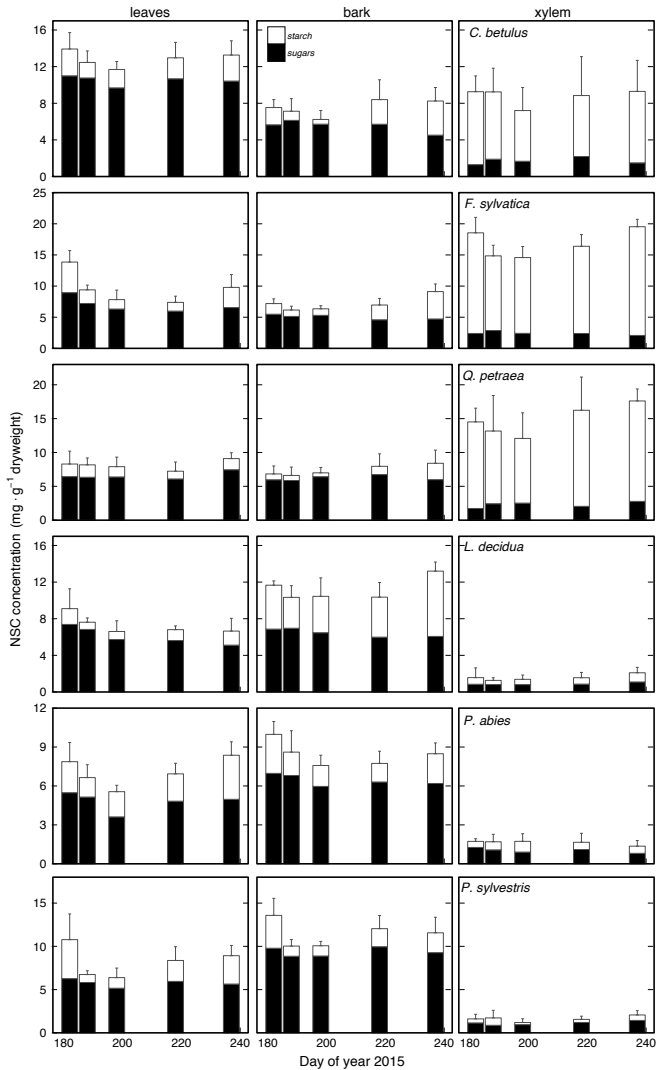


Figure 6 Non-structural carbohydrate concentrations (divided into starch and sugar) of leaf, bark and branch xylem in the six investigated species over the course of the 2015 summer drought (n = 4 individuals per species ± SD).

Non-structural carbohydrates

NSC concentrations in leaves, bark and xylem differed substantially among species and organs but showed no general trend of declining values during the 2015 summer drought. In leaves, NSC values ranged from 15 mg g⁻¹ dry weight in *C. betulus* to around 5 mg g⁻¹ in *P. sylvestris* (Fig. 6). In all species except *Q. petraea*, we observed slightly but non-significantly declining NSC values at the beginning of the 2015 summer drought, but either stable or increasing NSC concentrations throughout the two-month drought period. In bark tissues, NSC concentrations were in the same range as foliar NSC concentrations and showed similar temporal patterns as foliar NSC concentrations. As in leaves or bark tissues, we found that xylem NSC concentrations were either stable throughout the 2015 summer drought or declined slightly in the early summer but increased before the end of the drought (Fig. 6). Independent of the seasonal dynamics and drought, a clear difference in NSC concentrations was found in branch xylem between angiosperm and conifer species. While the angiosperms had high xylem NSC concentrations (with a high proportion of starch) of 8 to 20 mg g⁻¹, the conifers only had low concentrations of around 2 mg g⁻¹ (Fig. 6).

Stem increment growth

To determine if the 2015 summer drought impacted the stem growth, we investigated the progressive seasonal relative stem increment of the six species for the years 2014 – 2016. The relative stem increment differed substantially among species and years (Fig. 7). Interestingly, the 2015 summer drought had no consistent effect on total annual stem increment when comparing the increment of 2015 to 2014 or 2016. The onset of growth was similar among years in all species around DOY 120. Stem increment growth continued throughout the growing seasons 2014 and 2016 with the end of seasonal stem increment being variable among species and years. Importantly, however, stem growth in 2015 ceased sharply in all six species with the onset of the summer drought around DOY 180 and did not or only negligibly resume in the 2015 growing season (Fig. 7).

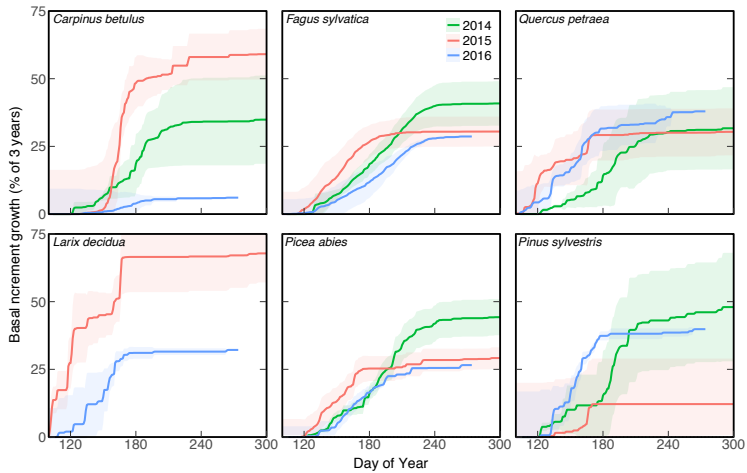


Figure 7 Basal increment growth of the six species during the study period ($n = 4$ trees per species \pm SD). To obtain growth curves, we connected the maxima of continuously measured stem diameter variations. Therefore, only increases in diameter above the last measured maximum were considered as growth.

Discussion

The goal of this study was to assess the physiological integrity of mature temperate trees, in particular with respect to xylem embolism and carbohydrate concentrations during a severe summer drought. For this purpose, we continuously determined the water and carbon relations of individuals of six common European temperate tree species. Our data indicate that the midday water potential of leaves (Ψ_{midday}) approached minimum values and that the trees responded by strongly reducing their sap flow (likely through stomatal closure) for several weeks during the drought event. Also, increment stem growth of all six species ceased sharply with the onset of the drought event and never resumed in that growing season. These findings indicate a high physiological sensitivity of all investigated temperate tree species to the 2015 summer drought. Importantly, however, minimum Ψ_{midday} of all species were far from values that would cause pronounced xylem embolism in the branches. Also, NSC reserves in leaves, bark or twigs remained rather stable and did not indicate NSC depletion in either species throughout the drought period. Hence, despite its stark negative effects on gas exchange and growth, the exceptional 12-week summer drought did not significantly deplete the trees' carbon

reserves. In summary, our data indicate a high sensitivity but a good physiological integrity of the hydraulic system and the carbon household of temperate tree species during the severe 2015 summer drought.

Ψ , sap-flow and growth during the 2015 drought

Low Ψ_{soil} and $\Psi_{\text{pre-dawn}}$ indicate that the high July, August and September 2015 temperatures and the low 2015 growing season precipitation substantially reduced the water availability in the soil and that the forest experienced indeed an exceptional drought in the months July, August and September of 2015. In fact, $\Psi_{\text{pre-dawn}}$ measured in the six species during the 2015 summer drought were in a similar low range as those observed in a previous study at the same site during the record-breaking 2003 centennial summer drought (Leuzinger *et al.* 2005).

Ψ_{midday} was also low and reached values of -1.9 MPa (*P. sylvestris*) to -2.8 MPa (*Q. petraea*). These values are similar to minimum Ψ_{midday} found in temperate tree species during natural and experimental soil drying (Lu *et al.* 1996; Maier-Maercker 1998; Backes & Leuschner 2000; Köcher *et al.* 2009). Importantly, plotting Ψ_{midday} against Ψ_{soil} throughout the 2015 summer drought, revealed that Ψ_{midday} levelled off at species specific minimum values (Fig. 3 and 4) and that transpiration was substantially down-regulated to avoid even more negative Ψ_{midday} (Jones & Sutherland 1991; Lemoine, Cochard & Granier 2002; Helfter *et al.* 2007). It remains, however, unclear to which degree the stabilization of Ψ_{midday} in the different species was caused by a regulation of stomatal conductance and cuticular transpiration or other changes in the conductivity of the hydraulic pathway such as changes in root conductivity, petiole embolism, or a decline of leaf hydraulic conductivity.

Our data indicate that the 2015 summer drought pushed the study tree species into a range of Ψ_{midday} values which were strongly regulated to avoid a further rapid decrease. However, far more negative Ψ_{midday} have already been shown in temperate trees, suggesting that under extreme conditions when $\Psi_{\text{pre-dawn}}$ decreases further, the physiological regulation of Ψ_{midday} cannot keep up with a progressively drying soil (Breshears *et al.* 2009; Hoffmann *et al.* 2011; Martínez-Vilalta *et al.* 2014; Blackman *et al.* 2016; Meinzer *et al.* 2016).

Interestingly, all species showing Ψ_{midday} to level off with declining Ψ_{soil} suggests that the physiological reaction to drought is rather uniform among the

temperate tree species investigated (Fig. 4, Supporting Fig. 3). Thus, a distinct classification of species into an iso- or anisohydric behaviour (Martínez-Vilalta *et al.* 2014) is not suitable in this case. Moreover, the isohydry/anisohydry concept has not proved useful when comparing drought susceptibility among species (Martínez-Vilalta & García-Fórner 2016).

Corroborating the stabilization of Ψ_{midday} at low Ψ_{soil} , we found that the species examined substantially reduced their sap-flow throughout the 2015 summer drought which is likely to be a measure to stabilize Ψ_{midday} . Except for *Q. petraea*, sap-flow was down-regulated in all other species by up to 80% for several weeks. Consequently, the gas exchange of the species was severely impacted for an extended period of time. Similar down-regulation of sap-flow in response to declining soil moisture (cf. Supporting Fig. 3) has previously been described for a variety of temperate forest tree species (Irvine *et al.* 1998; Pataki, Oren & Smith 2000; Hölscher *et al.* 2005; Leuzinger *et al.* 2005; Brinkmann *et al.* 2016). However, in most cases, the respective drought periods were shorter, lasting only for a few days to weeks. Only during the extreme heat drought of 2003, Leuzinger *et al.* (2005) showed that sap-flow and stomatal conductance were decreased up to 50 and 80%, respectively, for several weeks, a situation, similar to the 2015 summer drought investigated here.

Quite unexpectedly, we did not find an effect of the 2015 summer drought on total annual stem increment growth when comparing increment growth of 2015 to that of 2014 and 2016. The likely reason for the missing direct drought effect on annual growth is that spring growth in 2015 was substantial and exceeded that of the other two years (Fig. 7). However, the increment growth of 2015 ceased in all species with the onset of the drought while both 2014 and 2016 growth extended well beyond DOY 180 in most species.

It is an ongoing debate whether stem growth can occur during very negative Ψ and at times when there is a water deficit in the trunk (Zweifel *et al.* 2016). Our data suggest that there is no growth, which lines up with previous findings (Buell *et al.* 1961; Leuzinger *et al.* 2005; Pichler & Oberhuber 2007; Pflug *et al.* 2015). Our data also show that weather effects on annual tree growth depend not only on the intensity and duration of the event but also on the timing of the events and the environmental conditions that prevailed before (e.g. Zielis *et al.* 2014; D'Orangeville *et al.* 2018). It is, however, important to note here that we only investigated basal increment growth. Aboveground

leaf flushes and branch growth as well as belowground root growth remain unknown in this study.

Hydraulic integrity

All species were far away from water potential values that seriously challenged the hydraulic system of the branches even at the low end of measured Ψ_{soil} during the 2015 summer drought (cf. Fig. 4, Tab.1). At most, 10% of branch conductive capacity should have been affected by embolism during that period. The hydraulic safety margins that we found in the current study (Tab.1) are within the range of values that Hoffmann *et al.* (2011) reported for temperate tree species of North America under moderate and strong drought. Although we cannot predict how the species we investigated in our study will behave during an even stronger drought than that of 2015, the fact that the Ψ_{midday} of all species levelled off with declining soil moisture suggests that it would take a stronger decline in Ψ_{soil} to induce substantially more negative Ψ_{midday} values (combined with cuticular transpiration). By this means, the observed safety margins would only slightly be reduced for a range of further decreasing soil water availability until Ψ_{midday} gets solely dependent on Ψ_{soil} , and cuticular transpiration and stomatal leakiness. Our data, therefore, support the claims of Cochard & Delzon (2013) and Delzon & Cochard (2014) who stated that hydraulic failure is not routine in trees. Furthermore, our results are supported by a recent study on grapevine in which stomatal closure preceded embolism in leaves by days and leaves were shed before a significant amount of embolism did accumulate in the stem (Hochberg *et al.* 2017; cf. Charrier *et al.* 2018). However, we acknowledge that when Ψ_{soil} gets extremely negative, the trees will not be able to significantly uncouple their $\Psi_{\text{pre-dawn}}/\Psi_{\text{midday}}$ from the decrease in Ψ_{soil} as long as they do not take effective means to uncouple themselves from the soil matrix (cf. Cuneo *et al.* 2016). We conclude that the 2015 summer drought caused the tree species to significantly reduce their water loss but did not induce substantial amounts of xylem embolism in the branches of the trees. Therefore, xylem embolism is unlikely to disrupt the hydraulic integrity of the trees during the type of drought we investigated.

Non-structural carbohydrates

The NSC concentrations measured in leaves, bark and xylem of the six species throughout the 2015 summer drought are in the same range as NSC concentrations

measured in the same species (partly at the same location) in previous studies, when the trees were not exposed to drought (Körner 2003; Hoch, Richter & Körner 2003; Bazot *et al.* 2013). Given that NSC concentrations remained mostly constant throughout the 2015 summer drought and the fact that the concentrations that we measured are in the same ranges as concentrations of not drought-stressed trees measured in previous years, we conclude that the carbon balance was not significantly impacted by the 2015 summer drought in any of the six investigated species. It is important to note, however, that the cessation of basal increment growth (strong sink reduction) could have prevented decreasing NSC values in the leaves and branches (Anderegg 2012).

Overall, the response of NSC tissue concentrations to a 12-week-summer drought that we report here supports the increasing evidence from recent studies that NSC concentrations in trees are a very conservative and extremely resistant trait (cf. Weber *et al.* 2018) even under severe drought conditions. Previous studies investigating NSC concentrations in trees under drought revealed decreasing NSC concentrations only in potted seedlings or saplings (Mitchell *et al.* 2012; Adams, Germino & Breshears 2013; Hartmann *et al.* 2013a) or in trees that were heavily impacted or died due to extreme drought (Galiano *et al.* 2011; Adams *et al.* 2017). Other studies described only small or no differences in NSC concentrations between drought-treated and control trees (Gruber *et al.* 2011; Klein *et al.* 2014; Rowland *et al.* 2015), while Galvez, Landhäusser & Tyree (2011), and Anderegg (2012) even reported an increase of NSC concentrations in *Populus tremuloides* under drought. The data we present here are thus supported by previous findings suggesting that a depletion of NSC is rather unlikely to affect the physiological integrity of temperate tree species during drought events such as we observed (e.g. Körner 2003; Rosas *et al.* 2013).

Conclusion

This study reports the effects of a severe 12-week summer heat drought on the water and carbon relations of mature individuals of six different temperate forest tree species. We observed that the 2015 summer drought dramatically affected the water relations and growth of the trees. However, our data do not suggest supported xylem embolism in branches or the depletion of carbon reserves throughout the drought. Hence, our results indicate that xylem embolism and declining carbohydrate reserves do not compromise the physiological integrity of temperate trees during the type of severe

drought we observed. We would like to caution, however, that a sequence of reoccurring drought events in subsequent growing seasons or a different timing of the drought could possibly lead to stronger effects on the hydraulic system or the carbohydrate reserves of trees. Further, effects such as pest infestation or herbivory are likely to impact the vigour of temperate European tree species during intense droughts.

Acknowledgements

We acknowledge the help of crane operator Lucio Rizzelli and technical support by Decentlab GmbH and Georges Grun. Student assistant Florian Cueni helped with setting up the field site. Lab technician Sandra Schmid ran the NSC analyses. Lab technician Gaëlle Capdeville and student assistant Cédric Lemaire helped performing the centrifuge measurements in the lab of Sylvain Delzon, at INRA Bordeaux. We further thank Nadine Brinkmann, Werner Eugster and Richard Peters for fruitful discussions on sap-flow evaluation. Two anonymous reviewers provided helpful feedback on an earlier version of this manuscript. Funding for this work came from the department of Environmental Sciences at the University of Basel, Switzerland. The canopy crane was sponsored by the Swiss Federal Office of the Environment (FOEN).

Author contributions

LD and AK designed the study. LD conducted the fieldwork and analysed the data. Measurements of hydraulic vulnerability were done in the lab of SD. All authors jointly interpreted the data and wrote the manuscript.

Data archiving statement

The authors intend to upload the data used for this research to Dryad Data Repository once the article has been accepted for publication by the Journal.

References

Adams, H.D., Zeppel, M.J.B., Anderegg, W.R.L. *et al.* (59 more authors) (2017) A multi-species synthesis of physiological mechanisms in drought-induced tree mortality. *Nature Ecology and Evolution*, **1**, 1285-1292.

- Adams, H.D., Germino, M.J. & Breshears, D.D., Barron-Gafford, G.A., Guardiola-Claramonte, M., Zou, C.B. & Huxman, T.E. (2013) Nonstructural leaf carbohydrate dynamics of *Pinus edulis* during drought-induced tree mortality reveal role for carbon metabolism in mortality mechanism. *New Phytologist*, **197**, 1142–1151.
- Allen, C.D., Macalady, A.K., Chenchouni, H., Bachelet, D., McDowell, N., Vennetier, M., Kitzberger, T., Rigling, A., Breshears, D.D., Hogg, E.H.T., Gonzalez, P., Fensham, R., Zhang, Z., Castro, J., Demidova, N., Lim, J.-H., Allard, G., Running, S.W., Semerci, A. & Cobb, N. (2010) A global overview of drought and heat-induced tree mortality reveals emerging climate change risks for forests. *Forest Ecology and Management*, **259**, 660–684.
- Anderegg, W.R.L. (2012) Complex aspen forest carbon and root dynamics during drought. *Climatic Change*, **111**, 983–991.
- Anderegg, W.R.L., Klein, T., Bartlett, M., Sack, L., Pellegrini, A.F.A., Choat, B. & Jansen, S. (2016) Meta-analysis reveals that hydraulic traits explain cross-species patterns of drought-induced tree mortality across the globe. *Proceedings of the National Academy of Sciences USA*, **113**, 5024–5029.
- Auguie B. (2015) gridExtra: Miscellaneous Functions for “Grid” Graphics. R package version 2.0.0. <http://CRAN.R-project.org/package=gridExtra>.
- Backes, K. & Leuschner, C. (2000) Leaf water relations of competitive *Fagus sylvatica* and *Quercus petraea* trees during 4 years differing in soil drought. *Canadian Journal of Forest Research*, **30**, 335–346.
- Bazot, S., Barthes, L., Blanot, D. & Fresneau, C. (2013) Distribution of non-structural nitrogen and carbohydrate compounds in mature oak trees in a temperate forest at four key phenological stages. *Trees-Structure and Function*, **27**, 1023–1034.

- Blackman, C.J., Pfautsch, S., Choat, B., Delzon, S., Gleason, S.M. & Duursma, R.A. (2016) Toward an index of desiccation time to tree mortality under drought. *Plant Cell and Environment*, **39**, 2342–2345.
- Breshears, D.D., Myers, O.B., Meyer, C.W., Barnes, F.J., Zou, C.B., Allen, C.D., McDowell, N.G. & Pockman, W.T. (2009) Tree die-off in response to global change-type drought: mortality insights from a decade of plant water potential measurements. *Frontiers in Ecology and the Environment*, **7**, 185–189.
- Brinkmann, N., Eugster, W., Zweifel, R., Buchmann, N. & Kahmen, A. (2016) Temperate tree species show identical response in tree water deficit but different sensitivities in sap flow to summer soil drying. *Tree Physiology*, **36**, 1508–1519.
- Buell, M.F., Buell, H.F., Small, J.A. & Monk, C.D. (1961) Drought effect on radial growth of trees in the William L. Hutcheson Memorial Forest. *Bulletin of the Torrey Botanical Society*, **88**, 176–180.
- Carnicer, J., Coll, M. & Ninyerola, M. (2011) Widespread crown condition decline, food web disruption, and amplified tree mortality with increased climate change-type drought. *Proceeding of the National academy of Sciences* **108**, 1474–1478.
- Charrier, G., Delzon, S., Domec, J.-C., Zhang, L., Delmas, C.E.L., Merlin, I., Corso, D., King, A., Ojeda, H., Ollat, N., Prieto, J.A., Scholach, T., Skinner, P., van Leeuwen, C. & Gambetta, G.A. (2018) Drought will not leave your glass empty: Low risk of hydraulic failure revealed by long-term drought observations in world's top wine regions. *Science Advances*, **4**, eaao6969.
- Choat, B. (2013) Predicting thresholds of drought-induced mortality in woody plant species. *Tree Physiology*, **33**, 669–671.

- Clearwater, M.J., Meinzer, F.C., Andrade, J.L., Goldstein, G. & Holbrook, N.M. (1999) Potential errors in measurement of nonuniform sap flow using heat dissipation probes. *Tree Physiology*, **19**, 681–687.
- Cochard, H. (2002) A technique for measuring xylem hydraulic conductance under high negative pressures. *Plant Cell and Environment*, **25**, 815–819.
- Cochard, H. & Delzon, S. (2013) Hydraulic failure and repair are not routine in trees. *Annals of Forest Science*, **70**, 659–661.
- Cochard, H., Damour, G., Bodet, C., Tharwat, I., Poirier, M. & Améglio, T. (2005) Evaluation of a new centrifuge technique for rapid generation of xylem vulnerability curves. *Physiologia Plantarum*, **124**, 410–418.
- Cuneo, I.F., Knipfer, T., Brodersen, C.R. & McElrone, A.J. (2016) Mechanical Failure of Fine Root Cortical Cells Initiates Plant Hydraulic Decline during Drought. *Plant Physiology*, **172**, 1669–1678.
- D'Orangeville, L., Maxwell, J., Kneeshaw, D., Pederson, N., Duchesne, L., Logan, T., Houle, D., Arseneault, D., Beier, C.M., Bishop, D.A., Druckenbrod, D., Fraver, S., Girard, F., Halman, J., Hansen, C., Hart, J.L., Hartmann, H., Kaye, M., Leblanc, D., Manzoni, S., Ouimet, R., Rayback, S., Rollinson, C.R. & Phillips, R.P. (2018) Drought timing and local climate determine the sensitivity of eastern temperate forests to drought. *Global Change Biology*, 1–38.
- Delzon, S. & Cochard, H. (2014) Recent advances in tree hydraulics highlight the ecological significance of the hydraulic safety margin. *New Phytologist*, **203**, 355–358.
- Dietrich, L., Zweifel, R. & Kahmen, A. (2018) Daily stem diameter variations can predict the canopy water status of mature temperate trees. *Tree Physiology*, <https://doi.org/10.1093/treephys/tpy023>.

- Dowle M., Srinivasan A., Short T., Lianoglou S. (2015) data.table: Extension of Data.frame. R package version 1.9.6. <http://CRAN.R-project.org/package=data.table>.
- Drew, D.M., Richards, A.E., Downes, G.M., Cook, G.D. & Baker, P. (2011) The development of seasonal tree water deficit in *Callitris intratropica*. *Tree Physiology*, **31**, 953–964.
- Fischer, A.M., Keller, D.E., Liniger, M.A., Rajczak, J., Schär, C. & Appenzeller, C. (2014) Projected changes in precipitation intensity and frequency in Switzerland: a multi-model perspective. *International Journal of Climatology*, **35**, 3204–3219.
- Federal Office for the Environment (FOEN) (ed.) (2016) Hitze und Trockenheit im Sommer 2015. Auswirkungen auf Mensch und Umwelt. Bundesamt für Umwelt BAFU, Bern. Umwelt-Zustand Nr. 1629
- Galiano, L., Martinez-Vilalta, J. & Lloret, F. (2011) Carbon reserves and canopy defoliation determine the recovery of Scots pine 4 yr after a drought episode. *New Phytologist*, **190**, 750–759.
- Galvez, D.A., Landhausser, S.M. & Tyree, M.T. (2011) Root carbon reserve dynamics in aspen seedlings: does simulated drought induce reserve limitation? *Tree Physiology*, **31**, 250–257.
- Granier, A. (1985) Une nouvelle méthode pour la mesure du flux de sève brute dans le tronc des arbres. *Annales des Sciences Forestières*, **42**, 193–200.
- Granier, A. (1987) Evaluation of transpiration in a Douglas-fir stand by means of sap flow measurements. *Tree Physiology*, **3**, 309–320.
- Gruber, A., Pirkebner, D., Florian, C. & Oberhuber, W. (2011) No evidence for depletion of carbohydrate pools in Scots pine (*Pinus sylvestris* L.) under drought stress. *Plant Biology*, **14**, 142–148.

- Hartmann, H. (2015) Carbon starvation during drought-induced tree mortality – are we chasing a myth? *Journal of Plant Hydraulics*, **2**, 005.
- Hartmann, H., McDowell, N.G. & Trumbore, S. (2015) Allocation to carbon storage pools in Norway spruce saplings under drought and low CO₂. *Tree Physiology*, **35**, 243–252.
- Hartmann, H., Ziegler, W. & Trumbore, S. (2013a) Lethal drought leads to reduction in nonstructural carbohydrates in Norway spruce tree roots but not in the canopy. *Functional Ecology*, **27**, 413–427.
- Hartmann, H., Ziegler, W., Kolle, O. & Trumbore, S. (2013b) Thirst beats hunger - declining hydration during drought prevents carbon starvation in Norway spruce saplings. *New Phytologist*, **200**, 340–349.
- Helfter, C., Shephard, J.D., Martínez-Vilalta, J., Mencuccini, M. & Hand, D.P. (2007) A noninvasive optical system for the measurement of xylem and phloem sap flow in woody plants of small stem size. *Tree Physiology*, **27**, 169–179.
- Hoch, G., Richter, A. & Körner, C. (2003) Non-structural carbon compounds in temperate forest trees. *Plant Cell and Environment*, **26**, 1067–1081.
- Hochberg, U., Windt, C.W., Ponomarenko, A., Zhang, Y.-J., Gersony, J., Rockwell, F.E. & Holbrook, N.M. (2017) Stomatal Closure, Basal Leaf Embolism, and Shedding Protect the Hydraulic Integrity of Grape Stems. *Plant Physiology*, **174**, 764–775.
- Hoffmann, W.A., Marchin, R., Change, P.A.G. (2011) Hydraulic failure and tree dieback are associated with high wood density in a temperate forest under extreme drought. *Glob Chang Biol*, **17**, 2731–2742.
- Hölscher, D., Koch, O., Korn, S. & Leuschner, C. (2005) Sap flux of five co-occurring tree species in a temperate broad-leaved forest during seasonal soil drought. *Trees-Structure and Function*, **19**, 628–637.

- Irvine, J., Perks, M.P., Magnani, F. & Grace, J. (1998) The response of *Pinus sylvestris* to drought: stomatal control of transpiration and hydraulic conductance. *Tree Physiology*, **18**, 393–402.
- Jones, H.G. & Sutherland, R.A. (1991) Stomatal control of xylem embolism. *Plant Cell and Environment*, **14**, 607–612.
- Klein, T., Cohen, S., Paudel, I., Preisler, Y., Rotenberg, E. & Yakir, D. (2016) Diurnal dynamics of water transport, storage and hydraulic conductivity in pine trees under seasonal drought. *iForest - Biogeosciences and Forestry*, **9**, 710–719.
- Klein, T., Hoch, G., Yakir, D. & Korner, C. (2014) Drought stress, growth and nonstructural carbohydrate dynamics of pine trees in a semi-arid forest. *Tree Physiology*, **34**, 981–992.
- Köcher, P., Gebauer, T., Horna, V. & Leuschner, C. (2009) Leaf water status and stem xylem flux in relation to soil drought in five temperate broad-leaved tree species with contrasting water use strategies. *Annals of Forest Science*, **66**, 101–101.
- Körner, C. (2003) Carbon limitation in trees. *Journal of Ecology*, **91**, 4–17.
- Lemoine, D., Cochard, H. & Granier, A. (2002) Within crown variation in hydraulic architecture in beech (*Fagus sylvatica* L): evidence for a stomatal control of xylem embolism. *Annals of Forest Science*, **59**, 19–27.
- Leuzinger, S., Zotz, G., Asshoff, R. & Korner, C. (2005) Responses of deciduous forest trees to severe drought in Central Europe. *Tree Physiology*, **25**, 641–650.
- Lu, P., Biron, P., Granier, A. & Cochard, H. (1996) Water relations of adult Norway spruce (*Picea abies* (L) Karst) under soil drought in the Vosges mountains: whole-tree hydraulic conductance, xylem embolism and water loss regulation. *Annales des Sciences Forestières*, **53**, 113–121.

- Maguire, A.J. & Kobe, R.K. (2015) Drought and shade deplete nonstructural carbohydrate reserves in seedlings of five temperate tree species. *Ecology and Evolution*, **5**, 5711–5721.
- Maier-Maercker, U. (1998) Dynamics of change in stomatal response and water status of *Picea abies* during a persistent drought period: a contribution to the traditional view of plant water relations. *Tree Physiology*, **18**, 211–222.
- Martínez-Vilalta, J. & Garcia-Forner, N. (2016) Water potential regulation, stomatal behaviour and hydraulic transport under drought: deconstructing the iso/anisohydric concept. *Plant Cell and Environment*, **40**, 962–976.
- Martínez-Vilalta, J., Lloret, F. & Breshears, D.D. (2012) Drought-induced forest decline: causes, scope and implications., pp. 689–691. *Biology Letters*, **8**, 689–691..
- Martínez-Vilalta, J., Poyatos, R., Aguadé, D., Retana, J. & Mencuccini, M. (2014) A new look at water transport regulation in plants. *New Phytologist*, **204**, 105–115.
- McDowell, N.G. (2011) Mechanisms Linking Drought, Hydraulics, Carbon Metabolism, and Vegetation Mortality. *Plant Physiology*, **155**, 1051–1059.
- Meinzer, F.C., Woodruff, D.R., Eissenstat, D.M., Lin, H.S., Adams, T.S. & McCulloh, K.A. (2013) Above- and belowground controls on water use by trees of different wood types in an eastern US deciduous forest. *Tree Physiology*, **33**, 345–356.
- Meinzer, F.C., Woodruff, D.R., Marias, D.E., Smith, D.D., McCulloh, K.A., Howard, A.R. & Magedman, A.L. (2016) Mapping “hydroscares” along the iso- to anisohydric continuum of stomatal regulation of plant water status (ed J Penuelas). *Ecology Letters*, **19**, 1343–1352.

- Mencuccini, M., Minunno, F., Salmon, Y., Martínez-Vilalta, J. & Hölttä, T. (2015) Coordination of physiological traits involved in drought-induced mortality of woody plants. *New Phytologist*, **208**, 396–409.
- Mitchell, P.J., O'Grady, A.P., Tissue, D.T., White, D.A., Ottenschlaeger, M.L. & Pinkard, E.A. (2012) Drought response strategies define the relative contributions of hydraulic dysfunction and carbohydrate depletion during tree mortality. *New Phytologist*, **197**, 862–872.
- Orth, R., Zscheischler, J. & Seneviratne, S.I. (2016) Record dry summer in 2015 challenges precipitation projections in Central Europe. *Nature*, **6**, 1–8.
- Pataki, D.E., Oren, R. & Smith, W.K. (2000) Sap flux of co-occurring species in a western subalpine forest during seasonal soil drought. *Ecology*, **81**, 2557.
- Pepin, S. & Körner, C. (2002) Web-FACE: a new canopy free-air CO₂ enrichment system for tall trees in mature forests. *Oecologia*, **133**, 1–9.
- Pflug, E.E., Siegwolf, R., Buchmann, N., Dobbertin, M., Kuster, T.M., Günthardt-Goerg, M.S. & Arend, M. (2015) Growth cessation uncouples isotopic signals in leaves and tree rings of drought-exposed oak trees. *Tree Physiology*, **35**, 1095–1105.
- Pichler, P. & Oberhuber, W. (2007) Radial growth response of coniferous forest trees in an inner Alpine environment to heat-wave in 2003. *Forest Ecology and Management*, **242**, 688–699.
- R Core Team (2015) R: A language and environment for statistical computing. R Foundation for Statistical Computing, Vienna, Austria.
- Reichstein, M., Bahn, M., Ciais, P., Frank, D., Mahecha, M.D., Seneviratne, S.I., Zscheischler, J., Beer, C., Buchmann, N., Frank, D.C., Papale, D., Rammig, A., Smith, P., Thonicke, K., van der Velde, M., Vicca, S., Walz, A. & Wattenbach, M. (2013) Climate extremes and the carbon cycle. *Nature*, **500**, 287–295.

- Rosas, T., Galiano, L., Ogaya, R., Penuelas, J. & Martinez-Vilalta, J. (2013) Dynamics of non-structural carbohydrates in three Mediterranean woody species following long-term experimental drought. *Frontiers in Plant Sciences*, **4**, 1–16.
- Rowland, L., da Costa, A.C.L., Galbraith, D.R., Oliveira, R.S., Binks, O.J., Oliveira, A.A.R., Pullen, A.M., Doughty, C.E., Metcalfe, D.B., Vasconcelos, S.S., Ferreira, L.V., Malhi, Y., Grace, J., Mencuccini, M. & Meir, P. (2015) Death from drought in tropical forests is triggered by hydraulics not carbon starvation. *Nature*, **528**, 119–122.
- Ryan J.A., Ulrich J.M. (2014) xts: eXtensible Time Series. R package version 0.9-7. <http://CRAN.R-project.org/package=xts>.
- Sperry, J.S. (2000) Hydraulic constraints on plant gas exchange. *Agricultural and Forest Meteorology*, **104**, 13–23.
- Trenberth, K.E. (2011) Changes in precipitation with climate change. *Climate Research*, **47**, 123–138.
- Tuszynski J. (2014) caTools: moving window statistics, GIF, Base64, ROC, AUC, etc.. R package version 1.17.1. <http://CRAN.R-project.org/package=caTools>.
- Wang, Y., Burlett, R., Feng, F. & Tyree, M.T. (2014) Improved precision of hydraulic conductance measurements using a Cocharde rotor in two different centrifuges. *Journal of Plant Hydraulics*, **1**, 7–9.
- Weber, R., Schwendener, A., Schmid, S., Lambert, S., Wiley, E., Landhäusser, S.M., Hartmann, H. & Hoch, G. (2018) Living on next to nothing: tree seedlings can survive weeks with very low carbohydrate concentrations. *New Phytologist*, **218**, 107–118.
- Wickham H. (2009) ggplot2: elegant graphics for data analysis. Springer New York.

- Wickham H. (2015) scales: Scale Functions for Visualization. R package 0.3.0.
<http://CRAN.R-project.org/package=scales>.
- Williams, A.P., Allen, C.D. & Macalady, A.K. (2013) Temperature as a potent driver of regional forest drought stress and tree mortality. *Nature Climate Change*, **3**, 292–297.
- Wong, S.-C. (1990) Elevated atmospheric partial pressure of CO₂ and plant growth. *Photosynthesis Research*, **23**, 171–180.
- Zeileis A., Grothendieck G. (2005) zoo: S3 Infrastructure for Regular and Irregular Time Series. *Journal of Statistical Software* **14**, 1-27.
- Zeppel, M.J.B., Anderegg, W.R.L. & Adams, H.D. (2012) Forest mortality due to drought: latest insights, evidence and unresolved questions on physiological pathways and consequences of tree death. *New Phytologist*, **197**, 372–374.
- Zielis, S., Etzold, S., Zweifel, R., Eugster, W., Haeni, M. & Buchmann, N. (2014) NEP of a Swiss subalpine forest is significantly driven not only by current but also by previous year's weather. *Biogeosciences*, **11**, 1627–1635.
- Zweifel, R., Haeni, M., Buchmann, N. & Eugster, W. (2016) Are trees able to grow in periods of stem shrinkage? *New Phytologist*, **211**, 839–849.

Supporting Information

No role for xylem embolism or carbon decrease in temperate trees during a severe drought

Lars Dietrich^{†,1}, Sylvain Delzon², Günter Hoch¹, Ansgar Kahmen¹

¹Department of Environmental Sciences, University of Basel, Schoenbeinstrasse 6, CH-4056 Basel, Switzerland

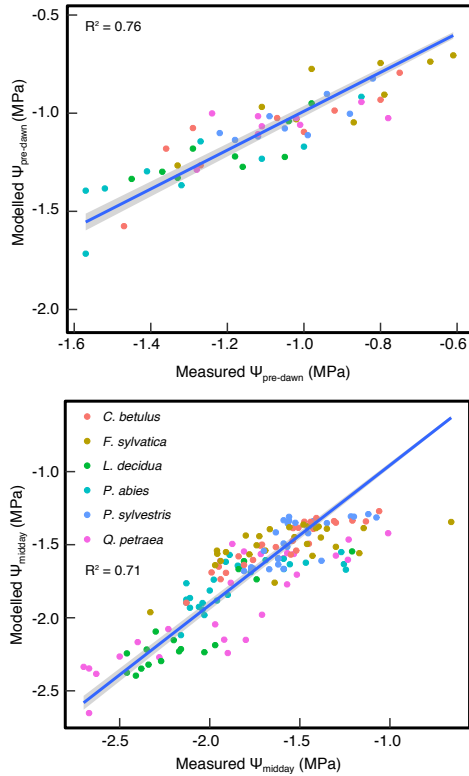
²UMR BIOGECO INRA-UB, Université de Bordeaux, Avenue des Facultés, 33405 Talence, France

[†]To whom correspondence should be addressed.

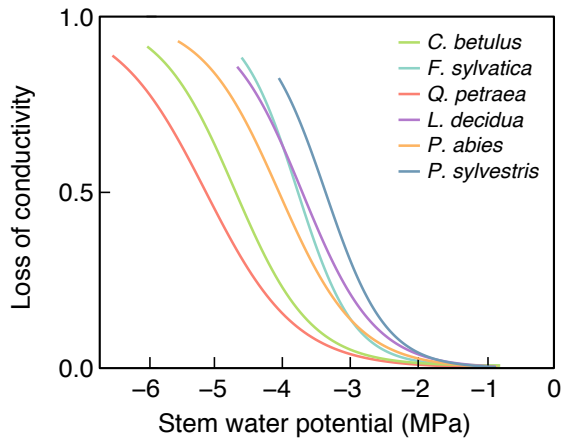
E-mail: larsdietrich.plantphys@gmail.com

Phone: [+41612073518](tel:+41612073518)

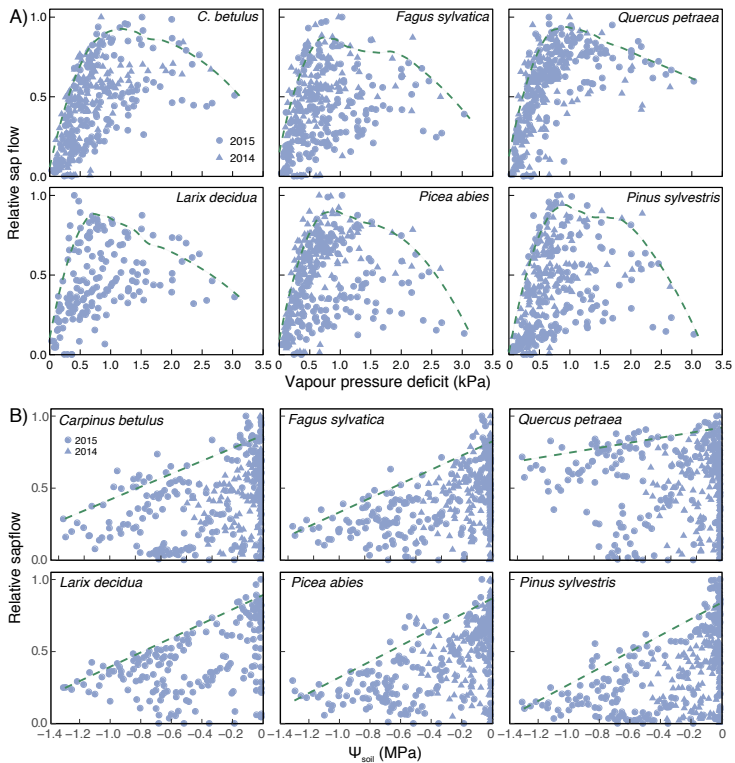
The following Supporting Information is available for this article:



Supporting Figure 1 Linear fits between modelled and measured $\Psi_{pre-dawn}$ and Ψ_{midday} . Modelled values are derived from an empirically derived function for the relationship between tree water deficit (TWD) and Ψ measured during the growing seasons of 2014 (11 independent midday data points per species) and 2015 (17 independent midday and 10 independent pre-dawn data points per species). A more detailed description of the relationship between TWD and Ψ_{leaf} can be found in Dietrich *et al.* (in rev.).



Supporting Figure 2 Mean PLC curves of the different temperate tree species examined in this study. PLC curves were measured on four branch segments per species in the Cavitron Lab in Bordeaux. Branches were harvested in October 2015, stored cool and were recut under tap water before the measurements.



Supporting Figure 3 Relative sap-flow of the considered species during the growing seasons (May 1 to October 31) of 2014 and 2015 as related to VPD (A) and Ψ_{soil} (B). The dashed green lines are boundary lines obtained from a LOESS (A) and a linear (B) regression through the 95th percentiles of sap-flow in categorical VPD and Ψ_{soil} groups of 0.5 kPa and 0.05 MPa, respectively.

Chapter 4

Letter

Losing half the conductive area hardly impacts the water status of mature trees

Lars Dietrich^{1*}, Günter Hoch¹, Ansgar Kahmen¹ and Christian Körner¹

¹Department of Environmental Sciences - Botany, University of Basel, Schönbeinstrasse 6,
CH-4056 Basel, Switzerland

*Corresponding author:

E-mail: larsdietrich.plantphys@gmail.com

Phone: +41612073518

Submitted to Nature Plants.

The water status of transpiring tree crowns depends on a hydraulic continuum from the soil matrix around roots to the sub-stomatal cavity of leaves, with a multitude of hydraulic resistors along this path. Although the stem xylem path may not be the most critical of these resistors, it had been suggested that a >50% interruption of that path by drought-stress induced embolization (air filling) of conduits is critical for tree survival¹. Here we show that cutting the sapwood of mature, 35 m tall trees in half hardly affects crown water status and transpiration. Counter expectation, this first adult tree sapwood interception experiment revealed that shoot water potential in the canopy (assessed by using a 45 m canopy crane) either remained unaffected (spruce) or became less negative (beech), associated with small reductions in leaf diffusive conductance for water vapour. We conclude that the stem xylem of these trees has a large overcapacity and the tree hydraulics debate requires a critical re-visitation.

The currently used concept of critical threshold values for the loss of conductivity in tree xylem rests on a number of assumptions and is based on data either obtained from twigs of severely stressed trees in the field, the hydraulic conductivity of which was assessed in the lab², or on experiments with pieces of twigs that were artificially embolized in a centrifuge³. From such works it was concluded, that a 50% loss of xylem conductivity (PCL₅₀) dramatically impairs the water supply of upstream plant organs, leading to tissue desiccation and eventually plant death, and is associated with a water potential (negative pressure) in the xylem of a cross-species average of -3.6 MPa in woody angiosperms and -5.6 MPa in gymnosperms⁴. These are exceptionally negative values indicating most severe stress. Currently, it is assumed that a 50% loss of conductivity corresponds to a 50% loss in conductive area which, recently, was often determined by micro CT imaging⁵. If a 50% loss of conduits by air filling critically affects tree water status⁶, the same hydraulic stress should also become evident when tree trunks lose half of their conducting cross sectional area by a cut with a chain saw.

To test the hypothesis that a 50 % loss of conducting stem area leads to significant hydraulic constraints in trees, we selected eight similarly sized tall trees, four from each of the two species *Fagus sylvatica* (European beech) and *Picea abies* (Norway spruce), which had a conducting sap wood width of 20-30 mm (ca. 10 annual rings; Supplementary Fig. 1). In two individuals per species, we cut stems 65 mm deep,

over half of their circumference 1.8 m above ground (at ca. 9 a.m. on a bright day in mid-August, DOY 226), with the other two individuals serving as controls (Fig. 1). For static reasons, we could not cut the entire half of the stems, but the applied cutting depth was sufficient to reach well beyond the sapwood, and thus completely interrupting water transport within half the stem (Supplementary Fig. 1). The trees' water status was monitored before, during and after the cutting by sap flow gauges in the trunk, and by pressure chamber and porometer readings in the canopy (shoot water potential Ψ , and leaf diffusive conductance g), working from the crane gondola. Sap-flow sensors were installed in July (DOY 198) 10 cm centrally above the cut, directly opposite the cut, and 3 m above ground, axially aligned with the two lower-position sensors (Fig. 1). Control trees were equipped with two sensors at 1.8 m above ground, placed opposite form each other. In the treatment trees, we added another set of sap-flow sensors horizontally aligned with the cut, 5 cm sideways from the edge of the cut, after the cut had been set in mid-September (DOY 263 – 268).

While sap-flow above the cut was reduced to zero in both species following the treatment (Supplementary Fig. 2), sap-flow opposite the cut slightly increased in *Fagus* (but only around midday) and remained unchanged in *Picea* (Fig. 2a). However, when we assessed sap-flow 5 cm to the side of the cut, we found higher flow rates as compared to sensors opposite the cut (Fig. 2b). Flow rates next to the cut were 200% (*Fagus*) and 40% (*Picea*) faster than opposite the cut. The sensors 1.3 m above the cut showed only about 10% of the pre-treatment flow (Supplementary Fig. 2). Hence, 1.3 m distance to the cut was too short to re-route sap flow back to the cut side of the stem.

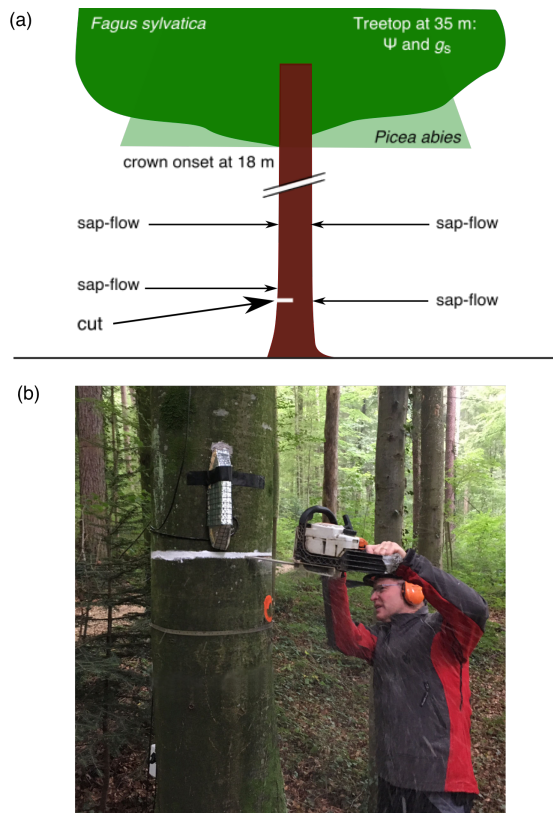


Figure 1 (a) Position of sap flow sensors that were installed before the treatment. (b) Interruption of half of all conductive sapwood on 14 August 2017 (DOY 226) with a chain saw.

Ψ in tree crowns on the day of the cut did not show any change in *Picea* and became less negative in *Fagus* around 2 p.m. (Fig. 2c). Initially, this counter-intuitive improvement of crown water status in *Fagus* could be explained by a relaxation of xylem tension due to the cut (the so-called 'Iwanoff effect', ^{7,8}). However, the persistent lack of a drop of water potential in response to the reduction in functional sap wood over the following weeks (even a persistent relaxation in *Fagus*; Fig. 2d) suggests that the trees had no problem meeting their water demand with half the conductive area even during warm summer weather.

Leaf conductance to water vapour was slightly but not significantly reduced on the day of the cut and on a sunny day in early September in the treated trees' upper crowns (Fig. 3, Supplementary Fig. 3). In *Fagus*, $\delta^{13}\text{C}$ analyses of leaf cellulose indicate that one of the treatment trees had consistently lower g even before the treatment (Supplementary Fig. 4). Yet, this stomatal response, had no significant effect on shoot net photosynthesis (A_n) in both, *Fagus* and *Picea* (Fig. 3). It is well known that small changes in g exert hardly any effect on photosynthesis when stomata are widely open, given that the maximum stomatal diffusion resistance represents only one fifth of the total resistance to CO_2 -uptake ⁹. Thus, we conclude that the stomatal responses to a 50% loss of conductive stem cross-sectional area did not significantly affect tree carbon capture (cf. Supplementary Fig. 5).

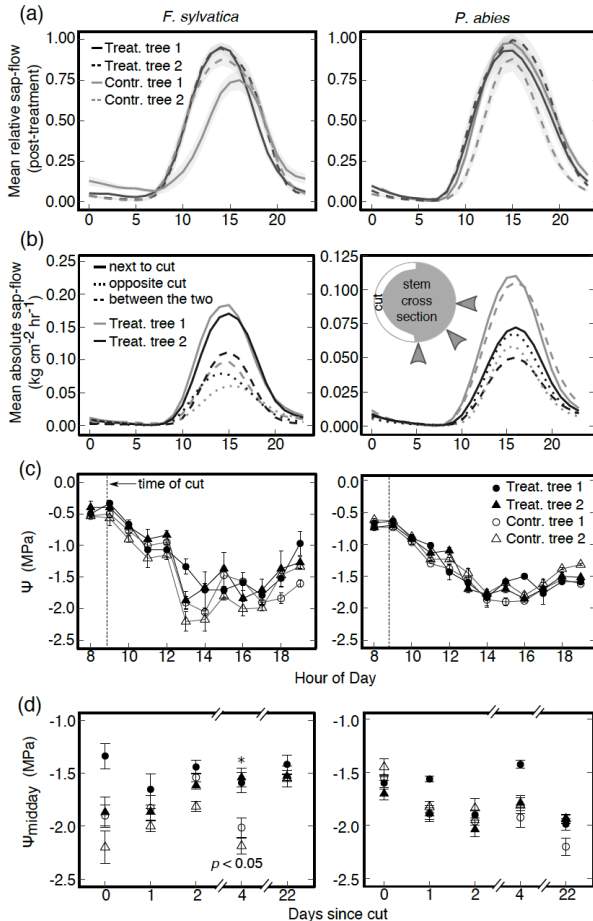


Figure 2 (a) Relative sap flow (half-hourly means) opposite the cut of treated and untreated trees during the first 18 days after cutting ($n = 18 \text{ days} \pm \text{SE}$). Sap flow was standardized by the mean of the maxima during the two-week pre-treatment period. (b) Mean absolute hourly sap flow of the subsequently installed sensors aligned sideways to the cut on 20 to 25 September 2017 (cut trees only). The inset image shows the position of the sensors at the stem. (c) Shoot water potential on the first day of the experiment (14 August 2017; mean \pm SE). Means for three sun-exposed current-year branches per tree per hour ($n = 3$). (d) Midday shoot water potential in the canopy after the cut was set (mean \pm SE for three sun-exposed branches per hour and tree). The cut was set on day 0 at 9:10 a.m.

Previous theoretical considerations predicted a severe reduction of Ψ with decreasing conductive area, leading to a so-called ‘runaway embolism’¹⁰ or the ‘embolism cycle’¹¹. The results of our treatment, however, show that the downregulation of sap flux at 50 % loss of sapwood area is very small and operates via stomata directly, with shoot water potential either unaffected or less rather than more negative. In contrast, *Fagus* was shown to reveal minimum canopy Ψ of -2.5 MPa at the same site during the summer drought of 2015¹² (Supplementary Fig. 6). So, leaves must receive and process signals associated with the cut other than a permanent decrease in shoot Ψ . We can only assume that this signal is either of a chemical (e.g. release of abscisic acid [ABA] along the flow path) or physical (hydraulic) nature¹³, or both. A brief reduction in leaf water status in a small fraction of the leaf tissue, like in the petiole or leaf veins, could trigger such a response (perhaps mediated by an ABA-release at leaf level¹³). Wounded tissue could exert a short-term signal but cannot explain a small though persistent effect as shown here¹⁴. Shaded leaves might have responded even less than the sun-exposed leaves we studied. Therefore, the overall crown transpiration might have undergone even less reduction as suggested by our stomatal conductance measurements from top canopy foliage only. Finally, our sensors placed close to the cut edge indicate that the sensor directly opposite the cut did not capture the full speed of the re-routed sap flow, which occurred right near the edge, similar to what would happen at a barrier inserted into a river.

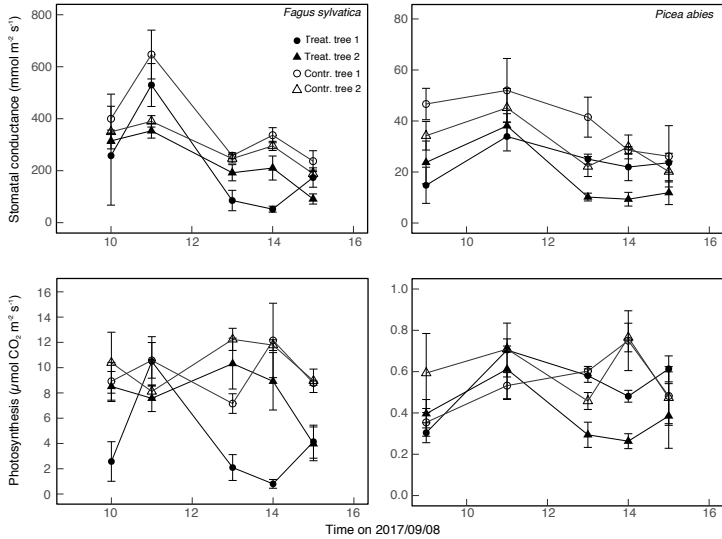


Figure 3 Stomatal conductance and net photosynthesis of the two treated and two control individuals of the two species 25 days after the cut was set (means \pm SE). We continuously measured three sun-exposed shoots per tree and hour throughout the day ($n = 3$) with a LI-COR4600 from a gondola on a canopy crane. We found no statistical differences among treatment and control trees.

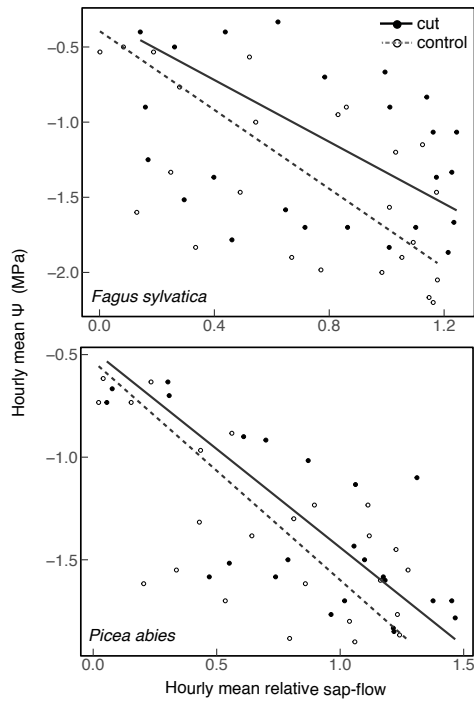


Figure 4 Mean shoot water potential in the canopy plotted against mean relative sap flow ($n = 2$ individuals per species). The slope of the regression represents the entire hydraulic resistance in the soil-shoot path. The water potential at zero flux represents pre-dawn conditions plus the hydrostatic compound at 35 m height (-0.35 MPa). Regressions are significant at $p < 0.001$.

The results of this experiment suggest a considerable over-capacity in the conduit system of mature tree trunk xylem. Accordingly, the classical sap-flow/ Ψ plot revealed no overall increase in hydraulic resistance (slope of the regression, Fig. 4) which calls PLC measurements from micro CT-derived active conduit area into question. Over-capacity in stem xylem is well known from practitioners in tree cultivation, who consider only a 90% or higher loss of bark and xylem as critical for tree survival¹⁵. Elazari-Volcani *et al.*¹⁶ found no effect on cell turgor by severe root pruning and stem incisions, and Scholander *et al.*¹⁷ assumed no significant impact on the water supply of a tropical liana when the stem was cut by half. This suggests that evolution of the conduit system selected for a high degree of insurance (redundancy), presumably not only accounting for mechanical damage, pathogen impact or damage by ground fires, but also for static demands. Yet, cutting sap wood in half does reduce the potential conductive capacity across all conduit diameter classes, and thus, may represent a greater effective reduction of conductivity than under a drought-induced halving of conductivity (when large vessels will quit first), because we also removed half of all smaller conduits that can be expected to remain intact under stress.

Perhaps, branch xylem rather than the trunk xylem represents a higher overall hydraulic constraint¹¹, although this would be in conflict with the conservation of xylem cross-sectional area during branching ('pipe model'¹⁸). A stem-cutting experiment in seedlings¹⁹ revealed no effects on g and Ψ of transpiring leaves when branches were cut by up to 90%. Only when two short-distance (2-8 cm) transverse cuts were made, the authors observed severe effects. Other studies employed even more drastic treatments (several overlapping cuts) causing leaf mortality^{20,21}. Similarly, introducing artificial embolism in stem xylem of *Pinus ponderosa* seedlings, continuously decreased stomatal conductance but only affected Ψ when 99% of the xylem was embolized, with Ψ dropping by only 0.6 MPa from -1.5 to -2.1 MPa¹³. This drop in Ψ was far less than expected for a 50% or even 88% reduction in hydraulic conductance due to embolism^{4,22}. Our study does not disprove the appropriateness of PLC₅₀ values for measuring xylem hydraulic vulnerability, but we question the direct causal linkage between PLC₅₀ or PLC₈₈ and tree death, as it is often assumed.

In summary, our results for tall trees match the results of earlier branch cutting experiments, underlining that there is a lot of extra conduit area in tree sapwood. Such

an over-dimension of xylem capacity is likely to play a role for tree mechanics, as a safety margin in the case of pathogen impact (e.g. wilt diseases²³), and perhaps, for cases of extreme drought stress, when sap flow becomes restricted to the small fraction of the narrowest conduits (tracheids). The main question in the ongoing debate about the causes for tree mortality during drought is the significance of a loss of conductive stem area in trees when soil moisture is severely reduced. Yet, in such situations the demand in conductive capacity approaches zero, as flux becomes reduced to rates of cuticular transpiration, or even less, when foliage is shed. So, paradoxically, the demand for xylem conducting capacity declines as drought stress increases. We argue that cuticular transpiration alone (commonly <1% of peak sap flow in taxa from potentially dry areas, represented by minimum leaf diffusive conductance²⁴) could not rupture all water capillaries in the stem xylem. So, the stem-system is unlikely representing the critical transfer resistance under severe drought. Unlike commonly assumed²⁵, the ultimate cause for a tree's death during drought would rather be the lack of radial moisture flow towards the root surface in the soil matrix, and as a consequence, shoot tissue desiccation. Rooting depth and species- and tissue-specific desiccation tolerance may be more likely to explain vulnerability during drought, with large diameter conduit cavitation a by-product or symptom rather than a cause.

Acknowledgements

The authors acknowledge the help of student assistants Tiffany Fioroni, Marie-Louise Schärer and Till Buser. Lucio Rizzelli operated the canopy crane. Funding came from the Department of Environmental Sciences of the University of Basel. The canopy crane was sponsored by the Swiss Federal Office for the Environment.

Author contributions

C.K. conceived the experiment with the help of L.D., G.H. and A.K. L.D. conducted fieldwork and analysed the data. All authors jointly interpreted the data and wrote the manuscript.

Competing financial interests

The authors declare that no financial interests are involved in the present study.

References

1. Choat, B. *et al.* Global convergence in the vulnerability of forests to drought. *Nature* **491**, 752–755 (2012).
2. Melcher, P. J. *et al.* Measurements of stem xylem hydraulic conductivity in the laboratory and field. *Methods in Ecology and Evolution* **3**, 685–694 (2012).
3. Cochard, H. *et al.* Methods for measuring plant vulnerability to cavitation: a critical review. *Journal of Experimental Botany* **64**, 4779–4791 (2013).
4. Lens, F. *et al.* Herbaceous Angiosperms Are Not More Vulnerable to Drought-Induced Embolism Than Angiosperm Trees. *Plant Physiology* **172**, 661–667 (2016).
5. Cochard, H., Delzon, S. & BADEL, E. X-ray microtomography (micro-CT): a reference technology for high-resolution quantification of xylem embolism in trees. *Plant, Cell & Environment* **38**, 201–206 (2014).
6. Brodribb, T. J. & Cochard, H. Hydraulic failure defines the recovery and point of death in water-stressed conifers. *Plant Physiology* **149**, 575–584 (2009).
7. Sheriff, D. W. & McGruddy, E. *Changes in leaf viscous flow resistance following excision, measured with a new porometer [broad beans (Vicia)].* *Journal of Experimental Botany* (1976).
8. Heber, U., Neimanis, S. & Lange, O. L. Stomatal aperture, photosynthesis and water fluxes in mesophyll cells as affected by the abscission of leaves. Simultaneous measurements of gas exchange, light scattering and chlorophyll fluorescence. *Planta* **167**, 554–562 (1986).
9. Korner, C., Scheel, J. A. & Bauer, H. Maximum leaf diffusive conductance in vascular plants. *Photosynthetica* (1979).
10. Tyree, M. T. & Sperry, J. S. Do Woody Plants Operate Near the Point of Catastrophic Xylem Dysfunction Caused by Dynamic Water Stress?: Answers from a Model. *Plant Physiology* **88**, 574–580 (1988).
11. Tyree, M. T. & Sperry, J. S. Vulnerability of xylem to cavitation and embolism. *Annual Review of Plant Physiology and Molecular Biology* **40**, 19–38 (1989).

12. Dietrich, L., Zweifel, R. & Kahmen, A. Daily stem diameter variations can predict the canopy water status of mature temperate trees. *Tree Physiology* **59**, 939–12 (2018).
13. Hubbard, R. M., Ryan, M. G., Stiller, V. & Sperry, J. S. Stomatal conductance and photosynthesis vary linearly with plant hydraulic conductance in ponderosa pine. *Plant, Cell & Environment* **24**, 113–121 (2001).
14. Teskey, R. O. & Hinckley, T. M. Effect of interruption of flow path on stomatal conductance of *Abies amabilis*. *Journal of Experimental Botany* (1983).
15. Moore, G. M. Ring-barking and girdling: how much vascular connection do you need between roots and crown? *14 th National Street Tree Symposium* (2013).
16. Elazari-Volcani, T. The influence of a partial interruption of the transpiration stream by root pruning and stem incisions on the turgor of citrus trees. *Palestine Journal of Botany and Horticultural Science* **1**, 94–96 (1936).
17. Scholander, P. F., Ruud, B. & Leivestad, H. The Rise of Sap in a Tropical Liana. *Plant Physiology* **32**, 1–6 (1957).
18. Petit, G. *et al.* Tree differences in primary and secondary growth drive convergent scaling in leaf area to sapwood area across Europe. *The New Phytologist* **34**, 87–10 (2018).
19. Mackay, J. & Weatherley, P. E. The effects of transverse cuts through the stems of transpiring woody plants on water transport and stress in the leaves. *Journal of experimental botany* **24**, 15–28 (1973).
20. Sperry, J. S. & Pockman, W. T. Limitation of transpiration by hydraulic conductance and xylem cavitation in *Betula occidentalis*. *Plant, Cell & Environment* **16**, 279–287 (1993).
21. Saliendra, N. Z., Sperry, J. S. & Comstock, J. P. Influence of leaf water status on stomatal response to humidity, hydraulic conductance, and soil drought in *Betula occidentalis*. *Planta* **196**, 357–366 (1995).
22. Urli, M. *et al.* Xylem embolism threshold for catastrophic hydraulic failure in angiosperm trees. *Tree Physiology* **33**, 672–683 (2013).
23. Korner, C. Stomatal behaviour and water potential in apricot with symptoms of wilt disease. *Angewandte Botanik* **55**, 469–476 (1981).

24. Körner, C. Leaf diffusive conductances in the major vegetation types of the globe. *Ecophysiology of Photosynthesis* 463–490 (Springer, Berlin, Heidelberg, 1995). doi:10.1007/978-3-642-79354-7_22
25. Adams, H. D. *et al.* A multi-species synthesis of physiological mechanisms in drought-induced tree mortality. *Nature Ecology and Evolution* **1**, 1285 (2017).

Methods

Study site and study species. The experiment was conducted in a diverse mixed forest in the vicinity of Basel, Switzerland (47°28'N, 7°30'E), at an elevation of 550 m a.s.l. using a canopy crane. The forest is a mix of needle- and broad-leaved tree species with individuals about 130 years old and stocking on a rendzina-type soil on calcareous bedrock²⁶. The climate is humid temperate with mean July temperatures of 19.2°C and two thirds of the 900 mm mean annual precipitation falling during the growing season. Yet, the site is prone to summer drought^{12,27,28}. This destructive experiment took place shortly before the study site was abandoned and the crane became dismantled. Weather data were available from the close weather service station in Binningen (c. 8 km distant; Supplementary Fig. 7). On-site soil moisture was measured with a TDR probe (ML2 ThetaProbe, Delta-T Devices, Cambridge, UK) at -10 and -20 cm at three different spots within freshly trenched soil profiles of -20 cm depth. Throughout the whole study period, soil water content did not drop below 25 % vol.

Study design. We selected four similar size trees each of the species *Fagus sylvatica* and *Picea abies* and determined two treatment and two control trees per species. On the North-East facing sites of the stem (downwind the main storm direction), we marked half of the circumference of the treatment trees with white paint to guide the chain saw cut at 1.8 m. Four weeks before the treatment, all trees were equipped with 20 mm long Granier-type sap-flow sensors (SFS2-M, UP GmbH, Ibbenbüren, Germany) 10 cm above the planned cut (white line, 1.8 m) and directly opposite the cut (Fig. 1). On the treatment trees, additional sap-flow sensors at 3 m height were installed axially aligned above the lower two sensors. Later in the season, we added sap-flow sensors 5 cm aside the cut and halfway between this sensor and the sensor opposite the cut in the treatment trees. The dead bark at the two insertion points for the sensor needles was carefully removed and aluminium sleeves were inserted into machine-drilled 20 mm deep holes

at a 10-cm vertical distance from each other. Sensor needles were greased with a heat conducting paste, inserted into the sleeves and sealed with Teroson MS-930[®] sealing adhesive from the outside. We protected the sensors from environmental influences with radiation shields made of bubble wrap aluminium foil. Data were recorded from July 24th until September 25th every ten minutes with a sensor node (Channel Node, Decentlab GmbH, Dübendorf, Switzerland), wirelessly transmitted to a data logger (Base Station, Decentlab GmbH) and then broadcasted to a server via cellular network.

Evaluation of sap-flow. Sap-flow data were analysed following Granier^{29,30}. In order to estimate zero flux during night and account for night time transpiration, night time maxima in temperature difference (ΔT_{\max}) were adjusted using the maximum during a seven-day period. We also performed a correction of the temperature difference in the sapwood (ΔT_{sw}) to account for the narrow sapwood in the investigated individuals³¹. For our analyses, we calculated relative sap-flow values which were normalized by the mean of daily sap-flow maxima during the pre-treatment period.

Shoot water potential. We measured shoot water potential (Ψ) with a Scholander pressure chamber (Model 1000, PMS Instruments, Albany, OR, USA) on three random terminal branches from the upper part of the sunlit crowns using the canopy crane. We cut ca. 15 cm long branchlets with two to four leaves (*Fagus*) or current-year shoots (*Picea*) with a razor blade immediately before measuring.

Stomatal conductance. In *Fagus*, stomatal conductance (g) was measured with a Decagon SC-1 Leaf Porometer (Decagon Devices, Pullman, WA, USA), and in both *Fagus* and *Picea* with the conifer chamber of the LI-6400XT gas exchange system (LI-COR, Lincoln, NE, USA), respectively on five (SC-1 Leaf Porometer) or three (LI-6400XT) sun-exposed branches per tree at each measuring time. Leaves (*Fagus*) and branches (*Picea*) were kept and analysed for leaf area in the lab. We calculated single (projected) leaf area from weight using a species-specific conversion factor for the weight/leaf area relationship in both species at the study site.

Sapwood depth. Sapwood depth was determined with an ink trial. One 10 cm deep core was taken with an increment corer on each tree and the hole was immediately filled with

a solution of black ink and sealed with Teroson MS-930[®] sealing adhesive. To guarantee a sufficient filling of the hole after sealing, more ink was injected through the sealing with a syringe and a needle until the ink started sprinkling out of the puncture. The puncture was sealed again straightaway. After half an hour, we took increment cores 1 cm above the filled holes and measured the length of the core that was infiltrated with the black ink solution. From earlier work, we know that conducting sapwood depth in comparably-sized trees of *Fagus sylvatica* and *Picea abies* is about 6 and 4.5 cm, respectively^{32,33}.

Cellulose extraction. Cellulose extraction was done on five current-year leaves from different parts of the canopy of each individual of the two species after the protocol by Brendel³⁴. Leaves were harvested on 9 September 2017, taken to the lab, dried for 24 hours at 75°C, and ground finely. The resulting powder was processed in filter bags (ANKOM Technology, Macedon, NY, USA), lipids and sugars were extracted by washing with toluene:ethanol (2:1) and DI water. Samples were bleached in an ultrasonic cleaner with an aqueous sodium chlorite/glacial acetic acid solution, rinsed with DI water afterwards, and dried at 50°C for two days.

$\delta^{13}\text{C}$ measurements. Dry powder obtained from extracted cellulose of 5 sunlit current-year leaves per individual from the upper part of the canopy was transferred into tin capsules and was analyzed in a Flash 2000 elemental analyzer coupled to a Delta V Plus continuous-flow isotope ratio mass spectrometer (IRMS) via a ConFlo IV interface (Thermo Fisher Scientific, Bremen, Germany). Samples went through flash combustion at ca. 1800 °C in the presence of oxygen, before the emerging CO₂ was fed into the IRMS. Stable isotope data were expressed in the delta notation ($\delta^{13}\text{C}$), relative to the ¹²C / ¹³C ratio of Vienna Pee Dee Belemnite standard ($R_{\text{VPDB}} = 0.0111797$).

Non-structural carbohydrates. NSC (i.e., starch, sucrose, fructose and glucose) were quantified in current-year leaves of sun-exposed branches in each individual of the two species (n = 4 leaves per individual). Samples were collected 9 September 2017, two weeks after the treatment took place. For chemical analysis in the lab, we used a modified protocol for enzymatic-photometric determination of low molecular weight sugars and starch^{35,36}.

Statistics. We used R statistical software (<http://cran.r-project.org>) to test the difference between control and treatment trees applying a two-sample t-test as well as a Tukey's range test in combination with an ANOVA (post-hoc) for each pair of data points. For diurnal sap-flow analysis, we divided the sap-flow measurements into three time periods (5-10h, 10-15h and 15-20h) and checked for significant differences between treatment and control with a two-sample t-test. Linear regression was used to investigate the relationship between hourly sap-flow and hourly Ψ and slopes of the regressions were compared by ANCOVA.

References

26. Pepin, S. & Körner, C. Web-FACE: a new canopy free-air CO₂ enrichment system for tall trees in mature forests. *Oecologia* **133**, 1–9 (2002).
27. Leuzinger, S., Zotz, G., Asshoff, R. & Körner, C. Responses of deciduous forest trees to severe drought in Central Europe. *Tree Physiology* **25**, 641–650 (2005).
28. Scherrer, D., Bader, M. & Körner, C. Drought-sensitivity ranking of deciduous tree species based on thermal imaging of forest canopies. *Agricultural and Forest Meteorology* **151**, 1632–1640 (2011).
29. Granier, A. Une nouvelle méthode pour la mesure du flux de sève brute dans le tronc des arbres. *Annales des Sciences Forestières* **42**, 193–200 (1985).
30. Granier, A. Evaluation of transpiration in a Douglas-fir stand by means of sap flow measurements. *Tree Physiology* (1987). doi:10.1093/treephys/3.4.309
31. Clearwater, M. J., Meinzer, F. C., Andrade, J. L., Goldstein, G. & Holbrook, N. M. Potential errors in measurement of nonuniform sap flow using heat dissipation probes. *Tree Physiology* **19**, 681–687 (1999).
32. Gall, R., Landolt, W., Schleppei, P., Michellod, V. & Bucher, J. B. Water content and bark thickness of Norway spruce (*Picea abies*) stems: phloem water capacitance and xylem sap flow. *Tree Physiology* **22**, 613–623 (2002).
33. Gebauer, T., Horna, V. & Leuschner, C. Variability in radial sap flux density patterns and sapwood area among seven co-occurring temperate broad-leaved tree species. *Tree Physiology* **28**, 1821–1830 (2008).
34. Brendel, O., Ianetta, P. & Stewart, D. A rapid and simple method to isolate pure alpha-cellulose. *Phytochemical Analyses* **11**, 7–10 (2000).

35. Wong, S.-C. Elevated atmospheric partial pressure of CO₂ and plant growth. *Photosynthesis Research* **23**, 171–180 (1990).
36. Weber, R. *et al.* Living on next to nothing: tree seedlings can survive weeks with very low carbohydrate concentrations. *The New Phytologist* **218**, 107–118 (2018).

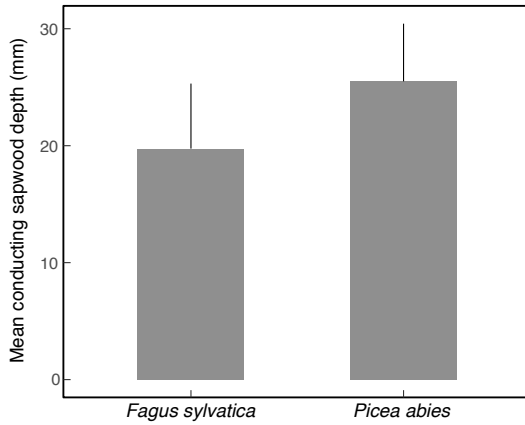
Supplementary Information

Losing half the conductive area hardly impacts the water status of mature trees

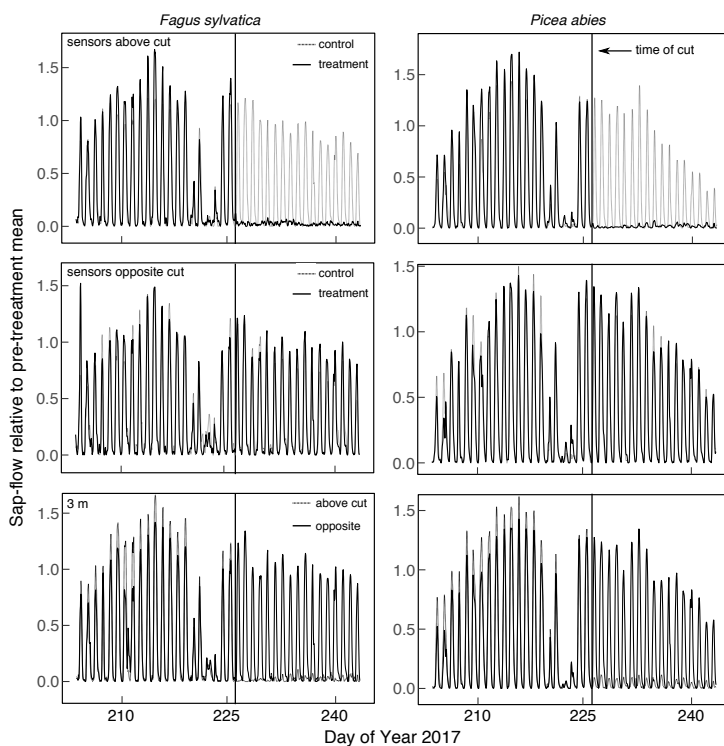
Lars Dietrich, Günter Hoch, Ansgar Kahmen, Christian Körner

Article acceptance date:

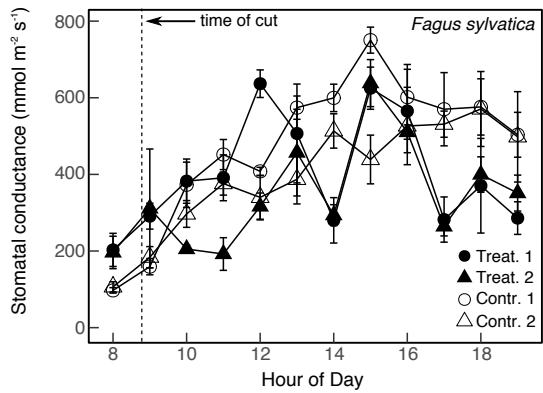
The following Supporting Information is available for this article



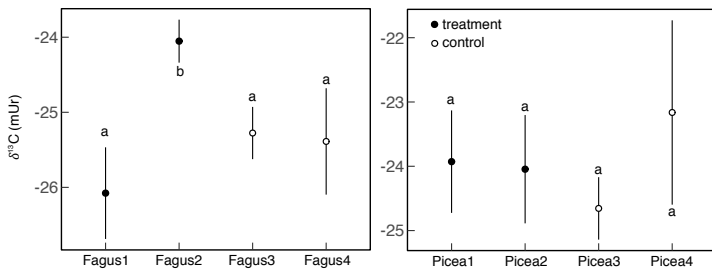
Supplementary Figure 1 Mean conducting sapwood depth in the four individuals of the respective study species ($n = 4 \pm \text{SD}$). Sapwood depth was determined with an ink injection trial where a 10-cm deep wood core was taken with an increment corer and the remaining hole immediately filled with black ink. After one hour, a second core was taken ca. 1 cm axially above the first hole and the dyed part of the core was measured.



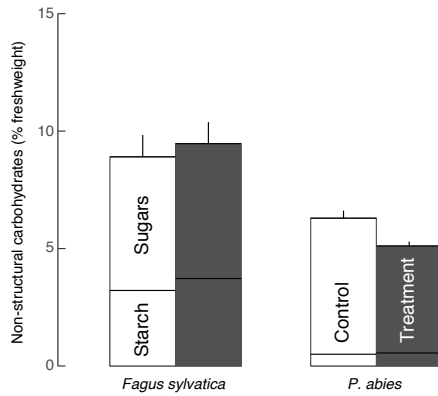
Supplementary Figure 2 Pre- and post-treatment sap-flow for the different sensors on the investigated trees (n=2 trees). The upper two panels compare sensors between treatment and control, the lower panel shows the two sensors at 3 m height on the treated individuals. Sap-flow was standardized on the mean of the maxima of the respective sensor on the respective tree during the two-week pre-treatment period. The horizontal dashed line marks the beginning of the treatment (cut).



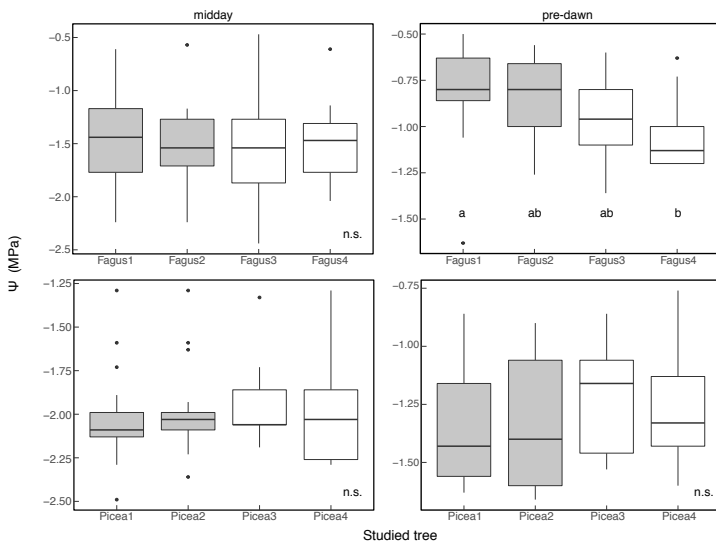
Supplementary Figure 3 Stomatal conductance of the two treated and the two non-treated individuals of *Fagus sylvatica* during the first day of the experiment ($n = 3$ leaves per tree \pm SE). We continuously measured five sun-exposed leaves per tree and hour from a gondola on a canopy crane throughout the day.



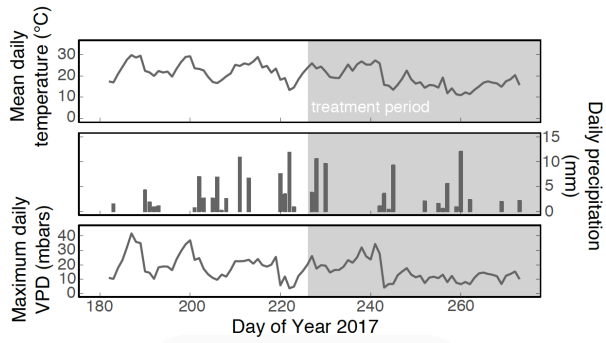
Supplementary Figure 4 $\delta^{13}C$ of the treatment and control trees' leaf cellulose ($n = 5$, means \pm SD). Cellulose $\delta^{13}C$ is independent from the treatment of the trees in this experiment since leaves were built long before the experiment took place. We only found a statistical different value of $\delta^{13}C$ in Fagus2. Significances were obtained from a posthoc Tukey's honest significance test.



Supplementary Figure 5 Mean non-structural carbohydrates (NSC) of the two treated and untreated trees per species (n = 2). NSC were measured in 4 current-year leaves from sunlit branches in the upper crown of each tree which were harvested on 9 September 2017 (14 days after cutting, DOY 240) and dried for 24 h at 75°C



Supplementary Figure 6 Boxplots of midday (n = 17) and pre-dawn (n = 9) leaf water potential of the study trees during the dry summer of 2015. Treatment trees are indicated by grey boxes. We only found a statistical difference between pre-dawn water potentials of Fagus1 and Fagus4 in a posthoc Tukey's honest significance test.



Supplementary Figure 7 Environmental conditions at the MeteoSwiss weather station in Basel Binningen in direct vicinity of the study site during the experimental period and the preceding weeks. The period after the cutting took place is highlighted by a grey box. Rainfalls at the beginning of the treatment period happened during the night.

Chapter 5

Water relations of drought-stressed temperate trees recover quickly after drought-intermittent short rainfall events

Lars Dietrich[†], Ansgar Kahmen

Department of Environmental Sciences - Botany, University of Basel, Schönbeinstrasse 6,
CH-4056 Basel, Switzerland

[†]Corresponding author:

Email: larsdietrich.plantphys@gmail.com

Phone: +41612073518

In preparation for Agricultural and Forest Meteorology.

Abstract

Decreasing amounts of precipitation and more frequent dry periods will challenge temperate Central European forest trees in the future. In this scenario, single drought-intermittent rainfall events might represent the only renewing water source for the trees during these episodes. We investigated the beneficial effects of low-amount drought-intermittent precipitation events during the exceptionally dry summer of 2015 on the water relations of mature individuals of six different tree species in a near-natural temperate forest. We found the trees to strongly profit from drought-intermittent rainfalls with maximum daily sap-flow recovering already at amounts of c. 1.5 mm by up to 20% and tree water deficit and Ψ_{midday} steadily profiting by up to 60% from rainfall amounts of 4.5 mm on. Duration of the rainfall-facilitated recovery was on average 3 days in the coniferous species and *Q. petraea* but distinctly longer in *C. betulus* and *F. sylvatica* the latter of which reached a duration of c. 9 days on average. Hydraulic conductivity was found to partly explain the differences in TWD release among species. We conclude that drought-intermittent rainfall events have a strong facilitative effect on temperate tree species and may be an important stress relief potentially helping the trees to endure longer periods of severely restricted water supply.

Key Words: mature trees, drought, recovery, tree water deficit, sap-flow, water potential

Introduction

The frequency and intensity of heat waves and drought events is predicted to increase in Central Europe in the near future (Kirtmann *et al.* 2013). Prolonged droughts have been shown to strongly affect the functioning of forest ecosystems globally and to cause even large die-offs in tree populations if drought stress persists for extended periods of time (Breshears *et al.* 2009, Allen *et al.* 2010). Since forests provide important ecosystem services, fatal effects of future drought events on tree populations are likely to affect these services, for example by altering the regional and global carbon and hydrological cycles (Bonan 2008, Reichstein *et al.* 2013).

The centennial heat waves and drought events in Central Europe during the summers of 2003 and 2015 are often referenced to as examples of weather scenarios that are predicted to occur more frequently in this region in the future (Orth 2016). Both events had strong impacts on the health of humans (FOEN, 2016) and on the functioning of ecosystems (Ciais *et al.* 2005, Leuzinger *et al.* 2005, Dietrich *et al.* in review). Several studies have investigated the impact of the 2003 and 2015 drought events on the water relations of temperate forests mainly focussing on effects on transpiration, tree water status and growth (Pataki *et al.* 2000, Hölscher *et al.* 2005, Leuzinger *et al.* 2005, Köcher *et al.* 2009, Dietrich *et al.* in review). The measures taken to investigate the trees' responses involved sap-flow and water potential measurements as well as calculating tree water deficit from stem diameter variations. All of these studies found strong physiological responses of the trees to drought emphasising the physiological sensitivity of temperate tree species to such drought events. However, these strong physiological reactions have been shown to occur without any sign declining tree health (Dietrich *et al.*, in review).

Extended drought periods in Central Europe such as the 2003 or 2015 summer droughts are typically interrupted by short and episodic rain events (Fischer *et al.* 2014). These rain events have no substantial impact on the water balance of the ecosystem, but could yet cause a short-term increase in tissue water supply and a relief in atmospheric water demand. The extent by which such short and episodic rain events can relieve the water status of mature trees is, however, unclear. Should temperate trees be able to use short and episodic rain events that occur during drought periods to relieve their water relations, this might be an important strategy to withstand as such longer periods of limited water supply and to avoid as such approaching thresholds of fatal

water stress. It is, however, unclear, if short and episodic rain events can indeed relax the water relations of drought stressed trees thereby leading to a mitigated risk of declining tree health under drought.

In this study, we took advantage of the exceptional 2015 summer drought in a near-natural 130-year-old forest in North-Western Switzerland. With a precipitation amount of only 96.6 mm during the months of July and August, the summer of 2015 was among the 10% driest summers of the past 100 years at our study site. Mean daily temperature averaged at 22°C throughout these two months and made the summer of 2015 the second hottest on record. High temperature and mostly low relative humidity resulted in a high summer VPD which, together with the mostly scattered and low-amount rainfall events that were not able to sufficiently re-wet the soil, caused Ψ_{soil} to progressively dry down to -1.3 MPa throughout the period from beginning of July to mid-September. This provided a good setting to quantify the effects of single drought-intermittent rainfall events on the water relations of temperate forest trees. To do so, we investigated (i) to what extent sap-flow, tree water deficit and leaf water potentials recovered from drought-intermittent low-amount precipitation events and (ii) from what rainfall amount on the trees start to benefit. We further tested (iii) how long the release of water stress lasted during the overall drought period.

Material and Methods

Study site and study trees

The study took place during the growing season of 2015 in a near-natural forest in the vicinity of Basel, Switzerland (47°28'N, 7°30'E). The site is located at an elevation of 550 m a.s.l. and experiences a temperate humid climate with a mean annual precipitation of ca. 900 mm two thirds of which fall during the growing season. Mean January and July temperatures are 2.1 and 19.2°C, respectively. Trees are stocking on a stony 1-m-deep soil of the rendzina type underslung by calcareous bedrock. In 1999, a canopy crane was installed at this site (Pepin and Körner 2002). The forest consists of mature individuals from different species, including *Fagus sylvatica* L. and *Quercus petraea* (Matuschka) Liebl., which are the dominant part of the canopy. Other species are *Carpinus betulus* L., *Larix decidua* Mill, *Picea abies* (L.) Karst, *Pinus sylvestris* L. and *Abies alba* Mill. The trees are about 130 years old and the canopy reaches a height of 35-40 m.

A weather station (Davis Vantage Pro 2, Scientific Sales Inc., Lawrenceville, NJ, USA) on top of the canopy crane recorded temperature, relative air humidity, radiation and precipitation on a ten-minute-interval throughout the growing season. We measured soil water potential (Ψ_{soil}) with matrix sensors (MPS-2, Decagon Devices, Pullman, WA, USA) at a depth of 20 cm, c. 1 m near the stems of 12 randomly chosen study trees distributed across the site. The site experienced a severe drought from July to mid-September during the growing season of 2015 in which our investigations took place. Strong VPD and low rainfall amounts led to soil water potentials decreasing down to -1.3 MPa (Fig. 1). From here on, we will refer to this drought event as the 2015 summer drought.

To test the influence of single short and episodic rainfall events on the water relations of the trees, we chose precipitation events that occurred during the 2015 summer drought from DOY 180 to DOY 260. We only considered those events for the analyses that were preceded by at least one day with less than 1 mm precipitation in order to allow the trees to have experienced some extent of water deficit before the rain event occurred. To be included in the analyses, precipitation events also had to have at least an amount of 1 mm d⁻¹ (as determined above the forest canopy). Precipitation amounts of less than 1 mm d⁻¹ were also taken into account if they occurred within a timeframe of at most two hours but not if they occurred throughout longer time periods. This was done to exclude rain events from our analyses which hardly reached the trees because of the very low rainfall intensity and amount.

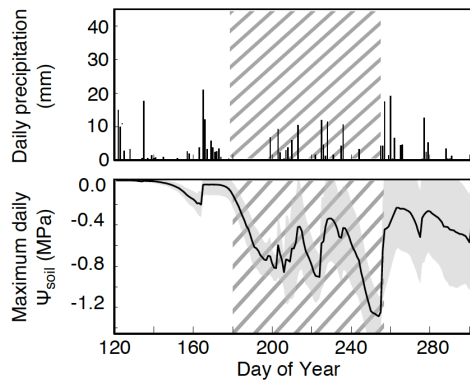


Figure 2 Daily precipitation and maximum daily soil water potential (\pm SD, $n = 12$ sensors at -20 cm) during the dry period in 2015 (grey-hatched). Precipitation was measured with a weather station on top of a canopy crane standing amidst the investigated trees. Soil water potential was measured with 12 sensors at 20 cm depth in between the trees.

Sap-flow measurements

We measured the sap-flow of all four individuals of the six species during the growing season of 2015 with Granier-type heat dissipation probes (SFS2-M, UP GmbH, Ibbenbüren, Germany) installed at the North-East and South-West sides of the stems. At the two insertion points of the sensor needles (ca. 1.5 m high) the bark of the tree was carefully peeled off. Aluminium sleeves were inserted 20 mm deep into the sapwood axially aligned at a 10-cm distance from each other. The sensor needles were slightly greased and then inserted into the sleeves. We sealed the insertion points with Teroson MS 930[®] sealing adhesive from the outside. Sensors were covered with radiation shields made of thick bubble wrap aluminium foil to protect them from weather and radiation influences. Data was recorded every ten minutes with a sensor node (Channel Node, Decentlab GmbH, Dübendorf, Switzerland), wirelessly transmitted to a data logger (Base Station, Decentlab GmbH) and then broadcasted to a server via cellular network.

Data evaluation was done after the method of Granier (Granier 1985, 1987). The temperature difference between the two needles (ΔT) of each sap-flow device was calculated from voltage values. In order to precisely estimate no flux conditions during nighttime and account for nighttime transpiration, no flux conditions were defined as

the maximum ΔT (ΔT_{\max}) during the night within a seven-day period. If a drift in ΔT_{\max} was observed, we applied a linear regression through ΔT_{\max} over the period of drift and set ΔT_{\max} to the regression values if it fell below the regression line. If the individual trees were found to exhibit a sapwood depth shorter than the length of the sensor needles (that was the case for *L. decidua* and *Q. petraea*), we performed a correction of ΔT to determine sapwood ΔT excluding the fraction of the probes that was inserted into non-conducting heartwood (Clearwater et al. 1999). Total sap-flow density u was then calculated using the following two equations (Granier 1987):

$$(1) \quad K = \frac{\Delta T_{\max} - \Delta T}{\Delta T}$$

and

$$(2) \quad u = 119 * 10^{-6} * K^{1.231}.$$

The values from both sensors on a tree were averaged. For our analyses, we only considered relative daily maximum sap-flow values which were calculated by dividing the daily maximum absolute sap-flow by the 95th percentile of maximum sap-flow values throughout the growing season. Relative sap-flow values were averaged for each species.

Tree water deficit and modelling of Ψ

To determine the water deficit of the investigated trees, we installed automated point dendrometers (ZN11-T-WP, Natkon, Oetwil am See, Switzerland) to assess diurnal and seasonal stem diameter variations (SDV). On each tree, we installed a dendrometer on the north-eastern site of the stem at around 2 m of height in April 2014. Data was collected on a ten-minutes interval throughout the growing season of 2015. From SDV, we calculated tree water deficit (TWD) as the difference between the last maximum in stem diameter and the pre-dawn maximum diameter on each day as described in Dietrich et al. (2018) and Zweifel et al. (2016). In brief, TWD is a measure for the water loss of the stem. It equals zero when the tree is fully hydrated. TWD increases when the tree is subjected to progressive soil drying and cannot refill its storage tissues during nighttime leading to a progressive decrease of internal storage water.

TWD has been shown to correlate with Ψ (Dietrich et al. 2018). Therefore, we employed TWD to model the variability of Ψ_{midday} at a daily resolution for the 2015 growing season. To do so, we used linear functions that we empirically obtained for each of the

six species from 27 single observations of Ψ_{midday} and the corresponding TWD values during the growing seasons of 2014 and 2015. We then used the derived function to model Ψ_{midday} for each day of the study period.

Calculation of recovery/releases and release duration

To calculate the recovery of sap-flow, Ψ_{midday} , and the release of TWD (x) in response to short and episodic rain events, we divided the absolute value of the difference between sap-flow, TWD, or Ψ_{midday} after the precipitation event (y_i) and the respective value before the event (y_{i-1}) by the maximum (sap-flow, TWD) or minimum (Ψ_{midday}) value of the season ($y_{\text{max/min}}$). The resulting values were multiplied with 100% to obtain percentage values:

$$x = \frac{\text{abs}(y_i - y_{i-1})}{y_{\text{max/min}}} * 100 \%$$

Rain events were defined by filtering the respective precipitation data of the summer 2015 for the days on which we detected short and episodic rainfall events as defined above. Since the TWD, sap-flow, and Ψ_{midday} values were obtained once a day, the exact timing of a precipitation event was important to assess whether the respective variable had been influenced by the event on a respective day or not. Therefore, we identified the start and end of the precipitation events and determined the sap-flow, Ψ_{midday} , and TWD values before and after the precipitation as follows: for pre-dawn TWD, which was measured at around 5 a.m. each day, the value after the precipitation event was considered the value of the day on which the last precipitation occurred before 5 a.m. This allowed to obtain two values of pre-dawn TWD one of which was unaffected by the precipitation event while the other one was affected. The amount of precipitation that fell in between was summed and considered as one event. In most cases, this was, in fact, only one event since precipitation often occurred during night-time (mostly due to thunderstorms). Since maximum daily sap-flow and Ψ_{midday} were measured/obtained at ca. 2 p.m. on each day, we considered the values of sap-flow and Ψ_{midday} on days with precipitation after 2 p.m. as the values before the precipitation event and the values on days with the last precipitation before 2 p.m. as the values after the precipitation event. To obtain sap-flow recovery values as clean as possible, we only chose pairs of subsequent days for the analysis on which the day after the rainfall exhibited a similar

maximum daily VPD than the day on which the precipitation event occurred (range of ± 5 mbars). This was the case in seven out of eleven events.

To estimate the duration of the TWD release after each precipitation event, we calculated the difference in days between the day after the precipitation event and the next following day on which 75% of the TWD the respective tree revealed on the day before the respective precipitation event was reached again. In some cases, there were precipitation events following each other on a relatively short time-scale, thereby progressively decreasing TWD with the result that TWD was affected by more than only one precipitation event before reaching 75% of its previous values again. This affected the release duration after every precipitation event. Since conditions were the same in every species, we do not think that this had a significant impact on inter-species differences. Also, we observed no differences when decreasing the amount of TWD to be reached after the precipitation events from 75 to 50 %.

Hydraulic conductivity

To determine the hydraulic conductivity of the xylem of the respective species, we harvested one branch segment of about 35 cm length and 1 cm of diameter from the sunlit crown of each of three individual trees per species before dusk in October 2015, directly wrapped it into moist paper towels and stored it in plastic bags at 4°C. Branch segments were sent to the Caviplace lab at INRA Bordeaux within a week, where they were stored at -4°C prior to measurements. Samples were then recut to 28 cm long segments under tap water. Centrifuge measurements were performed within three weeks using the Cavitron technique (Cochard 2002, Cochard et al. 2005). The stem segments got spun at different speeds thereby creating water potentials from moderate to very negative values within the segments. We took the hydraulic conductivity of the stem segments at full initial conductance (water potentials > -1 MPa). We did not take values for *Q. petraea* into the analysis since the method to measure stem segments of long-vesseled species was quite new and absolute values for hydraulic conductivity could not be trusted at the time of measurement.

Statistical analyses

Statistical analyses and data visualization were done using *R*, version 3.4.1 (R Foundation for Statistical Computing, Vienna, Austria 2013), with its packages zoo

(Zeileis and Grothendieck 2005), xts (Ryan and Ulrich 2014), data.table (Dowle et al. 2015), caTools (Tuszynski 2014), scales (Wickham 2015), gridExtra (Auguie, 2015) and ggplot2 (Wickham 2009). We assumed a $p < 0.05$ as the level of significance for all statistical tests. For the regression analyses between TWD release and Ψ_{midday} recovery and the amount of intra-drought rainfall we used the *lm()* command with a linear function forced through the origin. For the analysis on sap-flow recovery, we used the *nls()* function with the formula

$$\text{recovery} = a * (1 - e^{-\frac{\text{rainfall}}{b}}).$$

The parameters a and b thereby determine the saturation value and curvature of the function, respectively. To analyze the relationship between mean TWD release and hydraulic conductivity, we fitted the values using a second order polynomial function within a generalized linear model with the *glm()* command. Statistical comparison of the mean duration of TWD among the species was done with a posthoc Tukey's range test.

Results

Intermittent rain events during the summer drought of 2015

The summer drought of 2015 was intermitted by 16 rainfall events out of which 11 met our criteria. Rainfall events had an average amount of 6 mm. Maximum rainfall amount was 12 mm and minimum rainfall was less than 1 mm per day. The impact of different rainfall events on Ψ_{soil} differed and ranged from only minor influences to a partly re-wetting of the soil matrix (from -0.8 to -0.4 MPa, and from -1.2 to -0.5 MPa; Fig. 1). However, no rainfall event could completely saturate the soil matrix and Ψ_{soil} quickly decreased again after each drought-intermittent rainfall event (Fig. 1).

Sap-flow, TWD and Ψ_{midday} during the 2015 summer drought

Maximum daily sap-flow during the 2015 summer drought showed a clear decrease with drying soil in all species except *Q. petraea* (Fig.2). Towards the end of the drought (around DOY 260), most species except for *Q. petraea*, exhibited sap-flow reduced by up to 80% compared to the maximum values of the season. This underlines the impact of the 2015 summer drought on Central European tree species.

Pre-dawn relative TWD showed a strong variation throughout the 2015 summer drought reaching its highest values towards the end of the drought when the soil

was driest (around DOY 255). This was in all species except *P. sylvestris* which reached its highest TWD values already at the beginning of the drought around DOY 190 – 220 and stayed around these values throughout the drought (Fig. 2).

Modelled Ψ_{midday} showed a good correlation with measured values (Supporting Fig. 1) making it a reliable estimate of the trees' water status throughout the 2015 summer drought. In the broad-leaved species, Ψ_{midday} showed a wider range of values than in the coniferous species but the course over time was very similar in all species (Fig. 2). All species exhibited their lowest Ψ_{midday} between DOY 240 and 260 with *F. sylvatica* and *Q. petraea* reaching Ψ_{midday} as low as -2.5 and -2.8 MPa, respectively. *L. decidua* and especially *P. sylvestris* kept variation in Ψ_{midday} very small always oscillating around -2 and -1.8 MPa, respectively.

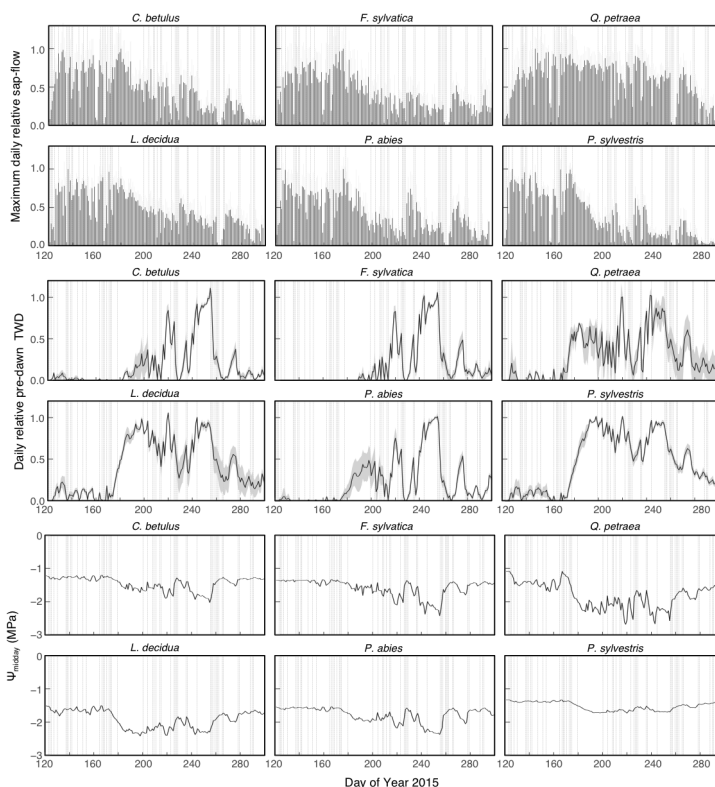


Figure 3 Daily maximum relative sap-flow (mean of 4 trees with 2 sensors each \pm SD), daily pre-dawn relative tree water deficit (mean of four individuals \pm SD) and modelled midday branch water potential of the studied tree species throughout the drought in 2015. Precipitation $>$ 1 mm is indicated by dashed vertical lines.

Drought release after rainfall

Both angiosperm and coniferous species were able to recover their sap-flow following short and episodic rain events to values up to 50% of the seasonal maximum (Fig. 2). Interestingly, even low intensity rain events with $<$ 2 mm triggered a moderate sap flow recovery of \sim 10%, indicating that the trees responded with an increase in stomatal conductance. The degree of recovery increased with the amount of drought-intermittent precipitation but did not exceed 30% following 4 mm of precipitation input (Fig 3).

Therefore, an asymptotic function was found to fit the relationship between sap-flow recovery and precipitation amount (Fig. 3). We found no difference in the increase with rain volume between angiosperm and coniferous species.

Short and episodic rain events during the drought period had a clear decreasing impact on TWD in all species. As for sap flow, even low-intensity rain events of less than 2 mm already triggered a TWD release, which was, however, small. Yet, at around 4.5 mm of precipitation, TWD was able to recover by on average 30%. TWD release steadily increased with the amount of precipitation up to a maximum of c. 50% at rainfalls of around 10 mm and we found a linear function to significantly fit the data (Fig. 3). However, from theoretical considerations, the relationship between TWD release and precipitation amount should saturate at a TWD release of 100 %. Interestingly, we further found that the severity of TWD before the rainfall was a significant determinant of TWD release following short and episodic rain events with a stronger recovery at low TWD (ANOVA, $p < 0.001$). We found no significant effect of species or phylogenetic groups (angiosperm/conifer) on TWD release following short and episodic rain events.

Ψ_{midday} recovered following short and episodic rain events during the drought by up to 1 MPa in *C. betulus*, *F. sylvatica*, *Q. petraea* and *P. abies* around DOY 225 and 265 (Fig. 2). The relationship between the recovery of Ψ_{midday} and rainfall amount was also found to be significant (Fig. 3). As for TWD, the relationship should in fact be saturating at a given recovery of Ψ_{midday} with increasing rainfall amounts. The values we found, however, seem to fall into the linear part of the overall relationship. The trees were able to progressively recover Ψ_{midday} with increasing amount of rainfall with on average 15% recovery already at amounts slightly less than 5 mm in the angiosperm species. However, as for TWD, precipitation events below 4 mm did only have a small effect on Ψ_{midday} . The highest recovery reached by a coniferous species was 18% at 8 mm precipitation. Angiosperm and coniferous species exhibited significantly different slopes of the linear regression lines with angiosperm species showing a greater recovery with increasing rainfall amounts than the conifers ($p < 0.01$, Fig. 3). We neither found an effect of Ψ_{midday} on the preceding day nor species-specific influences on the recovery of Ψ_{midday} after short an episodic rainfall events.

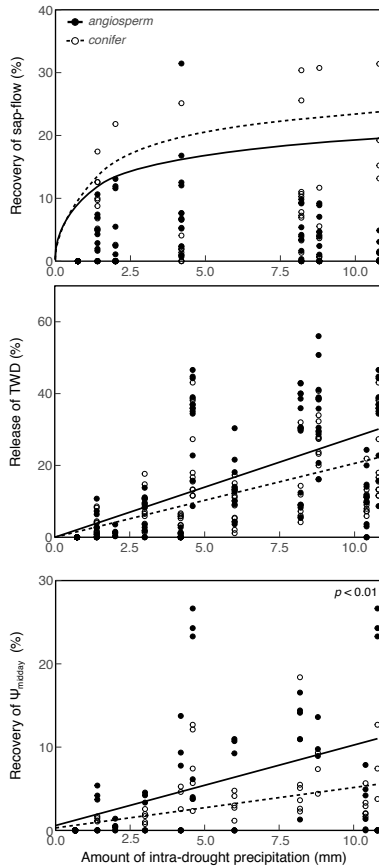


Figure 3 Regression analysis between the percentage recovery of sap-flow, release of pre-dawn tree water deficit (TWD) and recovery of midday branch water potential after precipitation events with impact on soil water potential and the respective amount of precipitation. Each data point represents one individual tree on one single day after a low amount precipitation event in sap-flow and TWD correlations. Branch water potential was modelled on a species level and is therefore lacking replication. The regression lines are encompassed by the 95th percentile confidence interval (grey area). All regressions we found were significant at $p < 0.01$ (sap-flow) and $p < 0.001$ (TWD and Ψ_{midday}). Significances for the difference between angiosperm and coniferous species are given in the upper right corner of each panel.

Duration of TWD release

We found that the TWD release following short and episodic rain events lasted between 2 and 9 days. Duration of TWD release was significantly correlated with the amount of precipitation across all species ($p < 0.001$, two-way ANOVA). We also observed significant differences in the mean duration of TWD release after drought-intermittent rainfalls among species (Fig. 4). With around a 9-day mean duration of TWD release, *F. sylvatica* exhibited by far the longest release of all investigated species. *C. betulus* revealed a bit more than half of that amount. *P. abies* and *Q. petraea* averaged at around four and three days, respectively, while *L. decidua* and *P. sylvestris* showed the shortest duration with two and a half and two days, respectively.

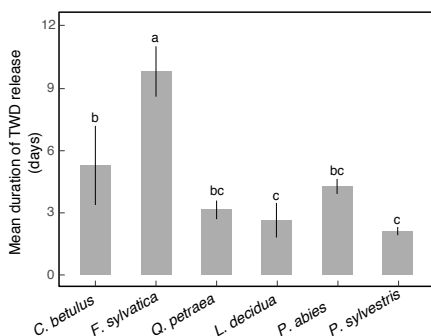


Figure 4 Mean duration for the alleviation of tree water deficit after intermittent rainfall events during drought for the different tree species. Duration is calculated as the time elapsed since a rain event until 75% of the preceding TWD is reached again. Values are means of individual means for the dry period of 2015 ($n = 4$ trees per species \pm SD). A posthoc Tukey's range test revealed significant differences among species (letter combinations above the columns).

Hydraulic conductivity and TWD release

A second order polynomial function was found to fit the significantly increasing relationship of mean TWD release during the 2015 summer drought with increasing hydraulic conductivity (Fig. 5). By this means, a tree with a higher hydraulic conductivity was able to recover more efficiently from water depletion than a tree with

a lower hydraulic conductivity. However, we find the relationship to saturate at high values for hydraulic conductivity indicating that the increase of TWD release with hydraulic conductivity is only significant at low conductivities. A one-way ANOVA revealed the relationship between hydraulic conductivity and TWD release to be significant at $p < 0.01$.

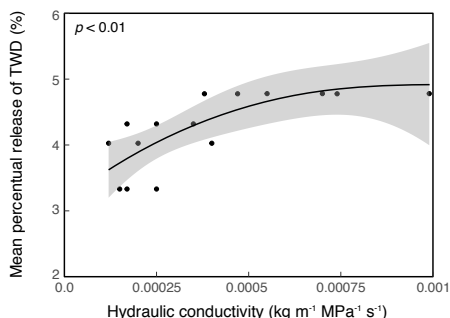


Figure 5 Second order polynomial regression analysis between the percentage release of tree water deficit (TWD) after chosen precipitation events and the hydraulic conductivity of branches of the respective species. Each data point represents the hydraulic conductivity of one branch of one individual tree and the species mean of TWD release. The regression line is encompassed by the 95th percentile confidence interval (grey area).

Discussion

Our study shows that the water relations of temperate tree species are able to recover from drought stress in response to short and episodic rain events that occur during exceptional summer droughts. Sap-flow recovered by a mean of 10% already at low amounts of drought-intermitting precipitation (< 2 mm). Also TWD and Ψ_{midday} recovered following drought-intermitting rainfall amounts by up to 30% (TWD) and 15% (Ψ_{midday}) on average. The recovery of water relations lasted for a mean of 5 days per drought-intermitting precipitation event. The duration of TWD release was significantly correlated with the amount of rainfall and was highly different among species. *F. sylvatica* exhibiting the longest while *P. sylvestris* revealed the shortest mean release duration. Hydraulic conductivity was found to explain differences in water stress recovery among species to a certain extent.

The 2015 summer drought and its physiological impact on temperate tree species

2015 was a very dry summer with a heat wave that was exceptional to Central Europe (Orth et al. 2016) and Switzerland in particular (FOEN 2016, Dietrich et al. in review). Low rainfall amounts caused progressively decreasing Ψ_{soil} down to -1.3 MPa, which show that the 2015 summer drought was a strong and long-lasting drought event that triggered severe water limitation in the soil. We saw sap-flow to decrease throughout the drought and TWD to increase at the same time. This emphasizes the water limitation of the trees during the 2015 summer drought. Decreasing sap-flow rates and increasing TWD have been shown in several studies before in temperate tree species throughout a drought or dry-spell (Hölscher et al. 2005, Köcher et al. 2009, Brinkmann et al. 2016) indicating that these are very common physiological reactions of the trees to soil drying. An up to 80% decrease in sap-flow, however, has only been observed during exceptional drought periods (Leuzinger et al. 2005). We therefore conclude that the trees we investigated in this study were indeed strongly water-limited during the summer drought of 2015. This is further corroborated by Ψ_{midday} falling into the range of the most negative measured values in temperate species both in literature and at the site (Lu et al. 1996, Maier-Maercker 1998, Backes and Leuschner 2000, Leuzinger et al. 2005, Köcher et al. 2009). Nevertheless, short and episodic rain events were scattered across the summer and occurred several times during the 2015 summer drought. They partly re-wetted the soil but never completely saturated the soil matrix. These scattered low-amount precipitation events during the 2015 summer drought provided an ideal setting to study their effects on the stress release of the water relations of temperate tree species.

Water uptake and drought release

Here, we only measured precipitation amounts on top of the canopy crane towering the forest canopy. Therefore, we were not able to distinguish between intercepted rain and throughfall. However, with an LAI of 5 m² m⁻² ground area at our site, 1 – 2 mm of precipitation during a rain event can be expected to be intercepted by the canopy (Crockford and Richardson 2000). Therefore, we were surprised by the fact that we saw an effect of small precipitation amounts of around 1 – 2 mm on both Ψ_{soil} and physiological variables in the trees. This could be due to the fact that the studied forest contains gaps in the canopy. By this means, and because the soil was very dry, even very

low-amounts of precipitation could affect the soil matrix, indicated by few sensors which led to a very slight increase in mean Ψ_{soil} .

Since uptake of precipitation water by plants can occur via roots or via direct absorption of the intercepted rain water by the leaves (Sherriff and Meidner 1975, Jackson et al. 2000), foliar water uptake could further have led to responses in the physiological variables already at low amounts of precipitation. Katz et al. (1989) and Breshears et al. (2008) have shown that trees can take up substantial amounts of water via their leaves during dry periods. Thus, in our study, the recovery effect is possibly a mix of rainfall taken up by leaves and roots, respectively. With increasing amounts of precipitation, however, water uptake through roots is likely to have gained a greater proportion because the intercepted amount of water by leaves cannot increase beyond these 1 – 2 mm, at least not during high rainfall rates and short rainfall duration since the surplus water would run off the leaves quickly and fall to the ground. Yates et al. (1995) observed the effect of leaf moistening on leaf water potential to be a function of time with the recovery process taking up to 10 hours or even 1.5 days (but see Katz et al. 1989). This underlines that water uptake through leaves is a slow process and short rainfall events during otherwise hot summer weather are, thus, not likely to have a great effect on leaf water status since the water intercepted by the leaves would quickly evaporate back into the atmosphere. However, this is likely to be dependent on the thickness of the respective leaf and its cuticula. Leaf water uptake being a long-lasting process indicates that measuring the benefits of drought-intermitting precipitation via leaf water uptake strongly depends on the timing of measurements with measurements taken directly after the precipitation event probably being least meaningful. We therefore conclude that our study preferentially captured the effects of root water uptake since this should lead to relieved water status way faster than the wetting of leaves. Moreover, the point of measurement in our study was the trunk base. Water is more likely to faster reach tissues at the trunk base if it is taken up by roots not by leaves simply because the distance to the point of measurement is way shorter. A replenishment of stem tissues at the base of the trunk by water taken up in the canopy would require reversed sap-flow. At such low amounts of intercepted water, a reversed sap-flow is unlikely to occur but is also very hard to measure (Burgess et al. 2001). The point of measurement at the base of the trunk is further more likely to capture the water status of the whole tree (Zweifel et al. 2001) rather than only the water status on a branch level

as investigated by previous studies (Katz et al. 1989, Breshears et al. 2008). Thus, we are confident that our results represent the whole tree recovery rather than only canopy recovery from water stress.

We see that that rainfall amounts around the interception volume (1 - 2 mm) have a strong impact on sap-flow indicating that water uptake by leaves might have an increasing effect on transpiration. This is puzzling, since we measured sap-flow at the base of the trunk. The only explanation we find is that a recovered water status on the branch level would trigger stomatal opening because of a higher water content in the leaves but we would expect this effect to diminish very fast. Sap-flow was generally least recovered of all three physiological variables that we assessed and recovery values saturated with increasing amounts of rainfall. This could be due to long-term ABA-regulated stomatal conductance during the drought (Comstock 2002). Therefore, we think that most of the trees were not able to strongly up-regulate sap-flow due to hormonal constraints (Edwards and Dixon 1995). By this means, the ABA-mediated decrease in stomatal conductance could be hindering the trees to greatly increase photosynthesis following intra-drought precipitation events but favour a longer retention of the up-taken water within the tissues. However, since CO₂ uptake is not linearly connected to stomatal conductance (Larcher 2003) assimilation was probably not strongly affected by the reported changes in sap-flow. This is supported by the stable non-structural carbohydrate concentration in the leaves of the study trees during the 2015 summer drought (Dietrich et al. in review).

TWD and Ψ_{midday} showed comparatively strong releases/recoveries only from 4.5 mm on which indicates for soil water uptake being more important for those two measures. In fact, a strong sap-flow recovery but only little TWD release or Ψ_{midday} recovery at very low amounts of precipitation could be interrelated as an increase in sap-flow which strongly depletes the water storage (Zweifel and Hasler 2001) thereby possibly leading to a mitigation of the release effect. However, TWD was measured in the early morning and should therefore be decoupled from sap-flow on the same day.

The duration of TWD release was longest by far in *F. sylvatica*. This could be due to a relatively high recharge of stored water after a precipitation event but sap-flow rates possibly kept low by intensive ABA signalling from the roots. A short duration of TWD release in the coniferous species could in this case be explained by a smaller total amount of water taken-up during the re-wetting events which would be lost

after shorter time periods because of stronger increased sap-flow after precipitation events. A weaker water uptake could be related to the hydraulic conductivity of the trees' xylem tissues. Indeed, we find the conifers to have a lower hydraulic conductivity possibly slowing their water uptake and disadvantaging them towards their angiosperm neighbours (Meidner and Sheriff 1976). As mentioned above, differences in soil-to-root transfer resistance could further make the difference among species (Larcher 2003). The short TWD release duration in *Q. petraea*, however, seems counter-intuitive given its efficient ring-porous hydraulic architecture and water transport physiology. However, the use of summer precipitation might further depend on rooting depth and differential soil water use (Flanagan et al. 1992, Williams and Ehleringer 2000). *Q. petraea* is discussed to take its water from deeper soil layers allowing this species to keep up transpiration during drought when others need to shut stomata (Leuschner et al. 2001, Zapater et al. 2011). Thus, the precipitation water will be taken up but also very quickly be transpired again because of the high overall transpiration rates in *Q. petraea*. Increasing TWD in a tree which has access to deep soil water might be due to a night-time redistribution of deep soil water to shallow soil layers by hydraulic lift instead of night-time refilling of storage tissues (Zapater et al. 2011). Thus, a tree can have a high water deficit, while still being connected to sufficient water sources.

In general, our study shows that the investigated tree species substantially profited from drought-intermittent rainfalls in 2015. All three investigated physiological response variables showed strong stress releases after precipitation events throughout the investigated period (Fig. 2). Indeed, it has been shown that trees quickly recover from water stress when receiving precipitation at the end of a drought event (Feres et al. 1979, Gallé et al. 2007). Previous investigations relate, however, to rainfalls or watering treatments that almost fully hydrated the soil matrix. We show that rainfall amounts from 4.5 mm on can substantially recover the water relations of mature trees and therefore assume that single drought-intermittent rainfall events that surpass this amount can be an important stress relief during extended periods of drought as assumed for future temperate climates. This, in turn, could add to the high resistance to drought-related mortality found for the studied species at the same site (Dietrich et al. in review).

Conclusions

This study investigated the beneficial effects of short and intermittent precipitation events that occurred during a severe drought event on the water relations of mature individuals of six different temperate tree species in a near-natural forest. During the exceptionally dry summer of 2015, we found the trees to strongly profit from short drought-intermittent rainfalls with maximum daily sap-flow recovering already at amounts of c. 1.5 mm by up to 20% and tree water deficit and Ψ_{midday} profiting even more from rainfall amounts of 4.5 mm on. Duration of the recovery by drought-intermittent precipitation events was on average 3 days in the coniferous species and *Q. petraea* but distinctly longer in *C. betulus* and *F. sylvatica* the latter of which reached a duration of c. 9 days on average. Hydraulic conductivity was found to partly explain the differences in TWD release among species. We conclude that drought-intermittent rainfall events have a strong facilitative effect on temperate forest tree species and may be an important stress relief potentially helping to endure longer periods of severely restricted water supply.

Author contributions

Both authors designed the study. LD performed field-work and analysed the data. Both authors jointly interpreted the data and wrote the manuscript.

Acknowledgements

We acknowledge the help of student assistant Florian Cueni and technical support from Georges Grun and Decentlab GmbH. Gaëlle Capdeville and Cédric Lemaire helped with measuring hydraulic conductivity at the Caviplace lab of Dr. Sylvain Delzon, Bordeaux. The canopy crane was sponsored by the Swiss Federal Office for the Environment.

References

- Allen CD, Macalady AK, Chenchouni H, Bachelet D, McDowell N, Vennetier M, Kitzberger T, Rigling A, Breshears DD, Hogg EHT, Gonzalez P, Fensham R, Zhang Z, Castro J, Demidova N, Lim J-H, Allard G, Running SW, Semerci A, Cobb N (2010) A global overview of drought and heat-induced tree mortality reveals emerging climate change risks for forests. *Forest Ecol Manag* 259:660–684.
- Auguie B (2015) gridExtra: Miscellaneous Functions for “Grid” Graphics. R package version 2.0.0. <http://CRAN.R-project.org/package=gridExtra>.
- Backes K, Leuschner C (2000) Leaf water relations of competitive *Fagus sylvatica* and *Quercus petraea* trees during 4 years differing in soil drought. *Can J Forest Res* 30:335–346.
- Federal office for the environment (ed.) (2016) Hitze und Trockenheit im Sommer 2015. Auswirkungen auf Mensch und Umwelt. Bundesamt für Umwelt BAFU, Bern. Umwelt-Zustand Nr. 1629
- Bonan GB (2008) Forests and climate change: forcings, feedbacks, and the climate benefits of forests. *Science* 320:1444–1449.
- Breshears DD, McDowell NG, Goddard KL, Dayem KE, Martens SN, Meyer CW, Brown KM (2008) Foliar absorption of intercepted rainfall improves woody plant water status most during drought. *Ecology* 89:41–47.
- Breshears DD, Myers OB, Meyer CW, Barnes FJ, Zou CB, Allen CD, McDowell NG, Pockman WT (2009) Tree die-off in response to global change-type drought: mortality insights from a decade of plant water potential measurements. *Front Ecol Environ* 7:185–189.

- Brinkmann N, Eugster W, Zweifel R, Buchmann N, Kahmen A (2016) Temperate tree species show identical response in tree water deficit but different sensitivities in sap flow to summer soil drying. *Tree Physiol* 36:1508–1519.
- Burgess SS, Adams MA, Turner NC, Beverly CR, Ong CK, Khan AA, Bleby TM (2001) An improved heat pulse method to measure low and reverse rates of sap flow in woody plants. *Tree Physiol* 21:589–598.
- Ciais P, Reichstein M, Viovy N, Granier A, Ogee J, Allard V, Aubinet M, Buchmann N, Bernhofer C, Carrara A, Chevallier F, De Noblet N, Friend AD, Friedlingstein P, Grunwald T, Heinesch B, Keronen P, Knohl A, Krinner G, Loustau D, Manca G, Matteucci G, Miglietta F, Ourcival JM, Papale D, Pilegaard K, Rambal S, Seufert G, Soussana JF, Sanz MJ, Schulze ED, Vesala T, Valentini R (2005) Europe-wide reduction in primary productivity caused by the heat and drought in 2003. *Nature* 437:529–533.
- Clearwater MJ, Meinzer FC, Andrade JL, Goldstein G, Holbrook NM (1999) Potential errors in measurement of nonuniform sap flow using heat dissipation probes. *Tree Physiol* 19:681–687.
- Cochard H (2002) A technique for measuring xylem hydraulic conductance under high negative pressures. *Plant Cell Environ* 25:815–819.
- Cochard H, Damour G, Bodet C, Tharwat I, Poirier M, Améglio T (2005) Evaluation of a new centrifuge technique for rapid generation of xylem vulnerability curves. *Physiologia Plantarum* 124:410–418.
- Comstock JP (2002) Hydraulic and chemical signalling in the control of stomatal conductance and transpiration. *Journal of experimental botany* 53:195–200.
- Crockford RH, Richardson DP (2000) Partitioning of rainfall into throughfall, stemflow and interception: effect of forest type, ground cover and climate. *Hydrological Processes* 14:2903–2920.

- Dietrich L, Delzon S, Hoch G, Kahmen A (in review) Strong physiological response yet no signs of hydraulic failure or carbon starvation in six temperate tree species during a severe summer drought.
- Dietrich L, Zweifel R, Kahmen A (2018) Daily stem diameter variations can predict the canopy water status of mature temperate trees. *Tree Physiology*
- Dowle M, Srinivasan A, Short T, Lianoglou S (2015) data.table: Extension of Data.frame. R package version 1.9.6. <http://CRAN.R-project.org/package=data.table>.
- Edwards DR, Dixon MA (1995) Mechanisms of drought response in *Thuja occidentalis* L. II. Post-conditioning water stress and stress relief. *Tree Physiol* 15:129–133.
- Federal Office for the Environment (FOEN) (ed.) (2016) Hitze und Trockenheit im Sommer 2015. Auswirkungen auf Mensch und Umwelt. Bundesamt für Umwelt BAFU, Bern. Umwelt-Zustand Nr. 1629
- Fereres E, Cruz-Romero G, Hoffman GJ (1979) Recovery of orange trees following severe water stress. *Journal of Applied ...* 16:833.
- Fischer AM, Keller DE, Liniger MA, Rajczak J, Schär C, Appenzeller C (2014) Projected changes in precipitation intensity and frequency in Switzerland: a multi-model perspective. *Int J Climatol* 35:3204–3219.
- Flanagan LB, Ehleringer JR, MARSHALL JD (1992) Differential uptake of summer precipitation among co-occurring trees and shrubs in a pinyon-juniper woodland. *Plant, cell & environment* 15:831–836.
- Gallé A, Haldimann P, Feller U (2007) Photosynthetic performance and water relations in young pubescent oak (*Quercus pubescens*) trees during drought stress and recovery. *New Phytologist* 174:799–810.

- Granier A (1985) Une nouvelle méthode pour la mesure du flux de sève brute dans le tronc des arbres. *Annales des Sciences Forestières* 42:193–200.
- Granier A (1987) Evaluation of transpiration in a Douglas-fir stand by means of sap flow measurements. *Tree Physiol*
- Hölscher D, Koch O, Korn S, Leuschner C (2005) Sap flux of five co-occurring tree species in a temperate broad-leaved forest during seasonal soil drought. *Trees-Struct Funct* 19:628–637.
- Jackson RB, Sperry JS, Dawson TE (2000) Root water uptake and transport: using physiological processes in global predictions. *Trends in plant science* 5:482–488.
- Katz C, Oren R, Schulze ED, Milburn JA (1989) Uptake of water and solutes through twigs of *Picea abies* (L.) Karst. *Trees-Struct Funct* 3:33–37.
- Kirtman B, Power SB, Adedoyin JA, Boer GJ, Bojariu R, Camilloni I, Doblas-Reyes FJ, Fiore AM, Kimoto M, Meehl GA, Prather M, Sarr A, Schär C, Sutton R, van Oldenborgh GJ, Vecchi G, Wang HJ (2013) Near-term Climate Change: Projections and Predictability. In: *Climate Change 2013: The Physical Science Basis. Contribution of Working Group I to the Fifth Assessment Report of the Intergovernmental Panel on Climate Change* [Stocker, T.F., D. Qin, G.-K. Plattner, M. Tignor, S.K. Allen, J. Boschung, A. Nauels, Y. Xia, V. Bex and P.M. Midgley (eds.)]. Cambridge University Press, Cambridge, United Kingdom and New York, NY, USA.
- Köcher P, Gebauer T, Horna V, Leuschner C (2009) Leaf water status and stem xylem flux in relation to soil drought in five temperate broad-leaved tree species with contrasting water use strategies. *Ann For Sci* 66:101–101.
- Larcher W (2003) *Physiological Plant Ecology*. Springer Berlin Heidelberg, Berlin, Heidelberg.

- Leuschner C, Hertel D, Coners H, Büttner V (2001) Root competition between beech and oak: a hypothesis. *Oecologia* 126:276–284.
- Leuzinger S, Zotz G, Asshoff R, Korner C (2005) Responses of deciduous forest trees to severe drought in Central Europe. *Tree Physiol* 25:641–650.
- Lu P, Biron P, Granier A, Cochard H (1996) Water relations of adult Norway spruce (*Picea abies* (L.) Karst) under soil drought in the Vosges mountains: whole-tree hydraulic conductance, xylem embolism and water loss regulation. *Annales des Sciences Forestières* 53:113–121.
- Maier-Maercker U (1998) Dynamics of change in stomatal response and water status of *Picea abies* during a persistent drought period: a contribution to the traditional view of plant water relations. *Tree Physiol* 18:211–222.
- Mayr S, Schmid P, Laur J, Rosner S, Charra-Vaskou K, Dämon B, Hacke UG (2014) Uptake of water via branches helps timberline conifers refill embolized xylem in late winter. *Plant physiology* 164:1731–1740.
- Meidner H, Sheriff DW (1976) Water and plants.
- Orth R, Zscheischler J, Seneviratne SI (2016) Record dry summer in 2015 challenges precipitation projections in Central Europe. *Nature Publishing Group* 6:1–8.
- Pataki DE, Oren R, Smith WK (2000) Sap flux of co-occurring species in a western subalpine forest during seasonal soil drought. *Ecology* 81:2557.
- Pepin S, Körner C (2002) Web-FACE: a new canopy free-air CO₂ enrichment system for tall trees in mature forests. *Oecologia* 133:1–9.
- R Core Team (2015) R: A language and environment for statistical computing. R Foundation for Statistical Computing, Vienna, Austria.

- Reichstein M, Bahn M, Ciais P, Frank D, Mahecha MD, Seneviratne SI, Zscheischler J, Beer C, Buchmann N, Frank DC, Papale D, Rammig A, Smith P, Thonicke K, van der Velde M, Vicca S, Walz A, Wattenbach M (2013) Climate extremes and the carbon cycle. *Nature* 500:287–295.
- Ryan JA, Ulrich JM (2014) xts: eXtensible Time Series. R package version 0.9-7. <http://CRAN.R-project.org/package=xts>.
- Sherriff DW, Meidner H (1975) Water movement into and through *Tradescantia virginiana* (L.) leaves. I. Uptake during conditions of dynamic equilibrium. *J. Exp. Bot.*
- Tuszynski J (2014) caTools: moving window statistics, GIF, Base64, ROC, AUC, etc.. R package version 1.17.1. <http://CRAN.R-project.org/package=caTools>.
- Wickham H (2009) ggplot2: elegant graphics for data analysis. Springer New York.
- Wickham H (2015) scales: Scale Functions for Visualization. R package 0.3.0. <http://CRAN.R-project.org/package=scales>.
- Williams DG, Ehleringer JR (2000) Intra- and Interspecific Variation for Summer Precipitation Use in Pinyon-Juniper Woodlands. *Ecological Monographs* 70:517–21.
- Yates DJ, Hutley LB (1995) Foliar Uptake of Water by Wet Leaves of *Sloanea woollsi*, an Australian Subtropical Rainforest Tree. *Aust J Bot* 43:157–12.
- Zapater M, Hossann C, Bréda N, Bréchet C, Bonal D, Granier A (2011) Evidence of hydraulic lift in a young beech and oak mixed forest using 18O soil water labelling. *Trees-Struct Funct* 25:885–894.
- Zeileis A, Grothendieck G (2005) zoo: S3 Infrastructure for Regular and Irregular Time Series. *Journal of Statistical Software* 14: 1-27.

Zweifel R, Hasler R (2001) Dynamics of water storage in mature subalpine *Picea abies*: temporal and spatial patterns of change in stem radius. *Tree Physiol* 21:561–569.

Zweifel R, Haeni M, Buchmann N, Eugster W (2016) Are trees able to grow in periods of stem shrinkage? *The New phytologist* 211:839–849.

Zweifel R, Häsler R, Item H (2001) Link between diurnal stem radius changes and tree water relations. *Tree Physiol* 21:869–877.

Supporting Information

Water relations of drought-stressed temperate trees recover quickly after drought-intermittent short rainfall events

Lars Dietrich[†], Ansgar Kahmen

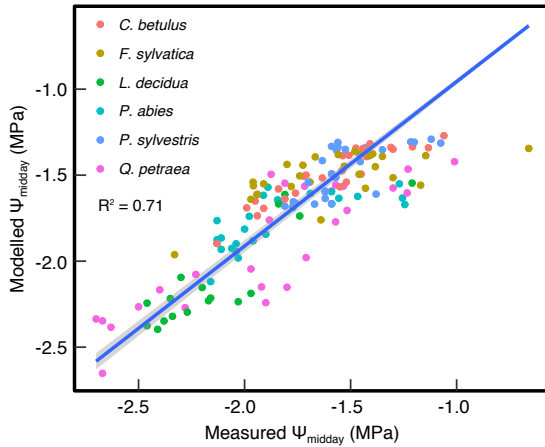
Department of Environmental Sciences - Botany, University of Basel, Schönbeinstrasse 6, CH-4056 Basel, Switzerland

[†]Corresponding author:

Email: larsdietrich.plantphys@gmail.com

Phone: +41612073518

The following supporting information is available for this article:



Supporting Figure 1 Linear fits between modelled and measured Ψ_{midday} . Modelled values are derived from an empirically derived function for the relationship between tree water deficit (TWD) and Ψ measured during the growing seasons of 2014 (11 independent midday data points per species) and 2015 (17 independent data points per species). A more detailed description of the relationship between TWD and Ψ_{leaf} can be found in Dietrich et al. (2018).

Concluding Discussion

This work aimed at assessing the physiological responses of six temperate Central European tree species to summer water limitation which is expected to occur more frequently in a future Central European climate (Fischer *et al.* 2014). Most of the work in this thesis was carried out in a near-natural 130-year-old forest that was equipped with a canopy crane thereby providing easy access to the crowns of the trees. My investigations took part during the growing seasons (1 May to 31 October) of four subsequent years from 2014 to 2017 one of which comprised an exceptional summer that was the second hottest and among the 10% driest summers on record. During this time, I assessed physiological parameters that are closely related to tree water relations and could therefore provide information on the trees' responses to low water availability. Specifically, I measured stem diameter variations with point dendrometers and sap-flow with Granier-type heat dissipation probes at the base of the tree trunks and quantified leaf water potentials in the canopy. During the dry summer of 2015, I additionally measured non-structural carbohydrate concentrations in leaves and the bark and xylem of branches. During the last growing season of my investigations, I tested the impacts of a 50% loss of conductive area in the stem on the water status of the two major tree species *Fagus sylvatica* and *Picea abies*, which is assumed to be an important determinant of drought-related mortality in trees.

As a result of this work, my co-authors and I were able to show that there is a close relationship between stem diameter variations, i.e. tree water deficit, measured at the base of the trunk and branch water potentials in the crown of the trees (Chapter 1). This is an exciting result as it facilitates the extensive assessment of the crown water status of tall trees by measurements at the base of the trunk. Costly and labour-intensive assessments of crown water status like tree climbing, branch shooting or canopy crane sampling therefore can be dispensable in the future. However, to model water potentials in the crown, calibration measurements would be needed which inevitably require the measurement of branch water potentials over at least one season to determine the species-specific parameters of the relationship between tree water deficit and branch water potentials. Yet, since we showed the relationship to be very close and linear throughout most of the range in branch water potentials, the variation in tree water deficit itself could be used as a measure for the water status of the trees and no calibration

would be needed. Caution should be used, however, at very low and very high tree water deficit values as the relationship with branch water potential was shown to change in these ranges and a very mild increase in TWD would imply a strong change in branch water potentials and, thus, canopy water status.

Another important physiological variable that reflects a plant's response to water availability is transpiration, most often estimated by sap-flow measurements. The sap-flow data measured in the coniferous species on my study site contributed to a project that assessed potential errors in sap-flow values obtained by the most frequently-used Granier-type heat dissipation method (Chapter 2). We were able to show that ignoring species-specific characteristics of water conduction and wounding effects after sensor insertion could lead to a substantial error in sap-flow estimations by up to 90 mm yr⁻¹. This supports previous studies that presumed errors in sap-flow measurements (Clearwater *et al.* 1999; Wullschleger *et al.* 2011) and highlights the importance of the assessment of species- and site-specific calibration curves to obtain reliable absolute values for absolute sap-flow. If calculations account for wounding effects, however, the assessment of normalized, species-specific relative sap-flow allows for comparative assessments among different species without bearing a big error potential.

The methods investigated in the first two chapters of this thesis especially allowed for assessing the physiological responses of the six investigated temperate tree species to severe water limitation during the 2015 summer drought (Chapter 3). All species could be shown to reveal a strong physiological response to soil drying with sap-flow being down-regulated by up to 80%. The only species that showed a minor response in sap-flow was *Quercus petraea*. However, all species revealed strongly negative leaf water potentials similar to minimum values that have been shown for the respective species before (Maier-Maercker 1998; Backes & Leuschner 2000; Leuzinger *et al.* 2005; Köcher *et al.* 2009) and asymptotically approached those minimum values with decreasing soil water potential indicating for a physiological response (i.e., stomatal closure) to prevent water potentials from a further decrease. By this means, all species were able to retain a broad hydraulic safety margin and operated far from fatal xylem embolism in the stem. Moreover, the species did not show substantial decreases in non-structural carbohydrates in leaves, bark and xylem tissues. This underlines that the carbon balance of the trees was not impacted by the drought and that the trees were far from carbon starvation. The trees being far from both hydraulic failure and carbon

starvation suggests that the observed physiological responses are not related to the two discussed mechanisms of drought-related tree mortality and that the trees respond to drought way before getting severely threatened (Sala 2009; Hochberg *et al.* 2017). Severe summer drought events like those in 2003 and 2015 are, thus, not likely to seriously harm Central European forests in the future. However, this study could not account for potential interactions with insect damage and drought recurrency rate (McDowell *et al.* 2011; Anderegg *et al.* 2015; Schwalm *et al.* 2017). While insect damage still remains an opaque factor in tree mortality scenarios, drought recurrence can be assumed to impact the trees if its frequency exceeds the recovery time of the trees after a respective drought event (Schwalm *et al.* 2017).

The hydraulic failure hypothesis for drought-related tree mortality is a controversial theoretical framework implying that once losing 50% or 88% of their hydraulic conductance during a drought, respectively, trees are not able to recover and eventually die (Choat 2013; Urli *et al.* 2013). However, this could never be directly shown in a study. We only see tree mortality to correlate with water potentials evoking the respective amount of loss in conductance (Adams *et al.* 2017). Our investigation of the impact of a 50% loss of conductive area on the water status of trees showed that the trees' water status does not suffer from such an amount of loss in conductance (Chapter 4). Water potentials in the crown stayed unchanged or even got less negative indicating for a relaxation of the trees' water status. However, the trees slightly closed stomata which indicates for a mechanism beyond steady changes in leaf water potential that regulates stomatal conductance (Hubbard *et al.* 2001). Our results are consistent with previous studies showing that the stem xylem of trees is a highly redundant system as lots of conductive area can be lost before the tree sees a severe water stress (Mackay & Weatherley 1973; Sperry *et al.* 1993; Saliendra *et al.* 1995; Hubbard *et al.* 2001). A loss of 50% or 88% hydraulic conductance is therefore unlikely to lead to the death of a tree during drought, especially because water demands are much lower during drought than under high water availability (Larcher 2003).

Since exceptional summer droughts like those in 2003 and 2015 have always been intermitted by short low-amount rainfall events, these events could potentially generate a short-term relief from water stress in trees. Therefore, we examined the drought stress recovery by short drought-intermitting rainfall events of the investigated trees during the 2015 summer drought (Chapter 5). The trees were found to greatly

benefit from these intermittent rainfall events with strong recovery responses from rainfall amounts of c. 4.5 mm on. The time of water stress release was highly different among species of which *Fagus sylvatica* showed the longest duration of stress release. It is therefore likely that drought-intermittent rainfall events help the trees to stay out of the range of life-threatening impacts on water status and carbon balance.

Altogether, the results of this work indicate that temperate Central European tree species hold a strong resistance to severe summer drought events such as the events in the years 2003 and 2015. An increase in the frequency of such summer drought events would therefore not lead to severe damage as long as not accompanied by pronounced insect attacks (Anderegg *et al.* 2015). However, as soon as the interim period of two subsequent drought events would become shorter than the recovery time that the trees need after a drought event (in Central Europe c. 6 - 12 months; Schwalm *et al.* 2017), the trees might get severely threatened.

References

- Adams H.D. et al. (2017) A multi-species synthesis of physiological mechanisms in drought-induced tree mortality. *Nature Ecology and Evolution* **1**, 1285–1291.
- Allen C.D., Macalady A.K., Chenchouni H., Bachelet D., McDowell N., Venetier M., et al. (2010) A global overview of drought and heat-induced tree mortality reveals emerging climate change risks for forests. *Forest Ecology and Management* **259**, 660–684.
- Anderegg W.R.L., Hicke J.A., Fisher R.A., Allen C.D., Aukema J., Bentz B., et al. (2015) Tree mortality from drought, insects, and their interactions in a changing climate. *New Phytol* **208**, 674–683.
- Anderegg W.R.L., Klein T., Bartlett M., Sack L., Pellegrini A.F.A., Choat B. & Jansen S. (2016) Meta-analysis reveals that hydraulic traits explain cross-species patterns of drought-induced tree mortality across the globe. *Proc Natl Acad Sci USA* **113**, 5024–5029.
- Backes K. & Leuschner C. (2000) Leaf water relations of competitive *Fagus sylvatica* and *Quercus petraea* trees during 4 years differing in soil drought. *Canadian Journal of Forest Research-Revue Canadienne De Recherche Forestiere* **30**, 335–346.
- Barigah T.S., Charrier O., Douris M., Bonhomme M., Herbette S., Améglio T., et al. (2013) Water stress-induced xylem hydraulic failure is a causal factor of tree mortality in beech and poplar. *Ann Bot* **112**, 1431–1437.
- Blizzard W.E. & J B. (1980) Comparative resistance of the soil and the plant to water transport. *Plant Physiol* **66**, 809–814.
- Bonan G.B. (2008) Forests and climate change: forcings, feedbacks, and the climate benefits of forests. *Science* **320**, 1444–1449.
- Bouche P.S., Larter M., Domec J.C., Burlett R., Gasson P., Jansen S. & Delzon S. (2014) A broad survey of hydraulic and mechanical safety in the xylem of conifers. *J Exp Bot* **65**, 4419–4431.
- Bréda N., Huc R., Granier A. & Dreyer E. (2006) Temperate forest trees and stands under severe drought: a review of ecophysiological responses, adaptation processes and long-term consequences. *Annals of Forest Science* **63**, 625–644.
- Brinkmann N., Eugster W., Zweifel R., Buchmann N. & Kahmen A. (2016) Temperate

- tree species show identical response in tree water deficit but different sensitivities in sap flow to summer soil drying. *Tree Physiology* **36**, 1508–1519.
- Brodrribb T.J. & Cochard H. (2009) Hydraulic failure defines the recovery and point of death in water-stressed conifers. *Plant Physiol* **149**, 575–584.
- Carnicer J., Coll M. & Ninyerola M. (2011) Widespread crown condition decline, food web disruption, and amplified tree mortality with increased climate change-type drought. *Proceedings of the National Academy of Sciences*, 108, 1474–1478.
- Choat B. (2013) Predicting thresholds of drought-induced mortality in woody plant species. *Tree Physiology* **33**, 669–671.
- Choat B., Jansen S., Brodrribb T.J., Cochard H., Delzon S., Bhaskar R., et al. (2012) Global convergence in the vulnerability of forests to drought. *Nature* **491**, 752–755.
- Ciais P., Reichstein M., Viovy N., Granier A., Ogee J., Allard V., et al. (2005) Europe-wide reduction in primary productivity caused by the heat and drought in 2003. *Nature* **437**, 529–533.
- Clearwater M.J., Meinzer F.C., Andrade J.L., Goldstein G. & Holbrook N.M. (1999) Potential errors in measurement of nonuniform sap flow using heat dissipation probes. *Tree Physiology* **19**, 681–687.
- De Schepper V., van Dusschoten D., Copini P., Jahnke S. & Steppe K. (2012) MRI links stem water content to stem diameter variations in transpiring trees. *J Exp Bot* **63**, 2645–2653.
- De Swaef T., De Schepper V., Vandegehuchte M.W. & Steppe K. (2015) Stem diameter variations as a versatile research tool in ecophysiology. *Tree Physiology* **35**, 1047–1061.
- Delzon S. & Cochard H. (2014) Recent advances in tree hydraulics highlight the ecological significance of the hydraulic safety margin. *New Phytol* **203**, 355–358.
- Drew D.M., Richards A.E., Downes G.M., Cook G.D. & Baker P. (2011) The development of seasonal tree water deficit in *Callitris intratropica*. *Tree Physiology* **31**, 953–964.
- Ehrenberger W., Rürger S., Fitzke R., Vollenweider P., Günthardt-Georg M., Kuster T., et al. (2012) Concomitant dendrometer and leaf patch pressure probe measurements reveal the effect of microclimate and soil moisture on diurnal stem water and leaf turgor variations in young oak trees. *Funct. Plant Biol.*, 39, 297–

- Ewers B.E. & Oren R. (2000) Analyses of assumptions and errors in the calculation of stomatal conductance from sap flux measurements. *Tree Physiology* **20**, 579–589.
- Fischer A.M., Keller D.E., Liniger M.A., Rajczak J., Schär C. & Appenzeller C. (2014) Projected changes in precipitation intensity and frequency in Switzerland: a multi-model perspective. *International Journal of Climatology* **35**, 3204–3219.
- Gebauer T., Horna V. & Leuschner C. (2008) Variability in radial sap flux density patterns and sapwood area among seven co-occurring temperate broad-leaved tree species. *Tree Physiology* **28**, 1821–1830.
- Granier A. (1985) Une nouvelle méthode pour la mesure du flux de sève brute dans le tronc des arbres. *Annales des Sciences Forestières* **42**, 193–200.
- Granier A. (1987) Evaluation of transpiration in a Douglas-fir stand by means of sap flow measurements. *Tree Physiology* **3**, 309–320.
- Hartmann H. (2015) Carbon starvation during drought-induced tree mortality – are we chasing a myth? *Journal of Plant Hydraulics* **2**, 1–5.
- Hartmann H., Adams H.D., Anderegg W.R.L., Jansen S. & Zeppel M.J.B. (2015) Research frontiers in drought-induced tree mortality: crossing scales and disciplines. *New Phytologist*, **205**, 965–969.
- Hartmann H., Ziegler W., Kolle O. & Trumbore S. (2013) Thirst beats hunger - declining hydration during drought prevents carbon starvation in Norway spruce saplings. *New Phytol* **200**, 340–349.
- Hochberg U., Windt C.W., Ponomarenko A., Zhang Y.-J., Gersony J., Rockwell F.E. & Holbrook N.M. (2017) Stomatal Closure, Basal Leaf Embolism, and Shedding Protect the Hydraulic Integrity of Grape Stems. *Plant Physiol* **174**, 764–775.
- Hölscher D., Koch O., Korn S. & Leuschner C. (2005) Sap flux of five co-occurring tree species in a temperate broad-leaved forest during seasonal soil drought. *Trees-Structure and Function* **19**, 628–637.
- Hubbard R.M., Ryan M.G., Stiller V. & Sperry J.S. (2001) Stomatal conductance and photosynthesis vary linearly with plant hydraulic conductance in ponderosa pine. *Plant Cell Environ* **24**, 113–121.
- Köcher P., Gebauer T., Horna V. & Leuschner C. (2009) Leaf water status and stem xylem flux in relation to soil drought in five temperate broad-leaved tree species with contrasting water use strategies. *Annals of Forest Science* **66**, 101–101.

- Körner C. (1995) Leaf Diffusive Conductances in the Major Vegetation Types of the Globe. In *Ecophysiology of Photosynthesis*. pp. 463–490. Springer, Berlin, Heidelberg, Berlin, Heidelberg.
- Larcher W. (2003) *Physiological Plant Ecology*. Springer Berlin Heidelberg, Berlin, Heidelberg.
- Leuzinger S., Zotz G., Asshoff R. & Korner C. (2005) Responses of deciduous forest trees to severe drought in Central Europe. *Tree Physiology* **25**, 641–650.
- Lu P., Urban L. & Zhao P. (2004) Granier's thermal dissipation probe (TDP) method for measuring sap flow in trees: theory and practice. *Acta Botanica Sinica*, **46**, 631–646.
- Mackay J. & Weatherley P.E. (1973) The effects of transverse cuts through the stems of transpiring woody plants on water transport and stress in the leaves. *J Exp Bot.*, **24**, 15–28
- Maier-Maercker U. (1998) Dynamics of change in stomatal response and water status of *Picea abies* during a persistent drought period: a contribution to the traditional view of plant water relations. *Tree Physiology* **18**, 211–222.
- McDowell N., Beerling D.J., Breashers D.D. & Fisher R.A. (2011) *Interrelated mechanisms of drought-induced tree mortality*. *Trends Ecol Evol.*, **26**, 523–532.
- McDowell N., Pockman W.T., Allen C.D., Breshears D.D., Cobb N., Kolb T., et al. (2008) Mechanisms of plant survival and mortality during drought: why do some plants survive while others succumb to drought? *New Phytol* **178**, 719–739.
- McDowell N.G. (2011) Mechanisms Linking Drought, Hydraulics, Carbon Metabolism, and Vegetation Mortality. *Plant Physiol* **155**, 1051–1059.
- McDowell N.G. & Sevanto S. (2010) The mechanisms of carbon starvation: how, when, or does it even occur at all? *New Phytologist* **186**, 264–266.
- Milburn J.A. (1973) Cavitation studies on whole *Ricinus* plants by acoustic detection. *Planta* **112**, 333–342.
- Myers N. (1997) The world's forests and their ecosystem services. In: Daily GC (ed.) *Nature's Services: societal dependence on natural ecosystems*. Island Press: Washington D.C.
- Oren R., Phillips N., Ewers B.E., Pataki D.E. & Megonigal J.P. (1999) Sap-flux-scaled transpiration responses to light, vapor pressure deficit, and leaf area reduction in a flooded *Taxodium distichum* forest. *Tree Physiology* **19**, 337–347.

- Pataki D.E., Oren R. & Smith W.K. (2000) Sap flux of co-occurring species in a western subalpine forest during seasonal soil drought. *Ecology* **81**, 2557.
- Reichstein M., Bahn M., Ciais P., Frank D., Mahecha M.D., Seneviratne S.I., et al. (2013) Climate extremes and the carbon cycle. *Nature* **500**, 287–295.
- Sala A. (2009) Lack of direct evidence for the carbon-starvation hypothesis to explain drought-induced mortality in trees. *Proc Natl Acad Sci U S A* **106**, E68–author reply e69.
- Sala A., Piper F. & Hoch G. (2010) Physiological mechanisms of drought-induced tree mortality are far from being resolved. *New Phytologist* **186**, 274–271.
- Saliendra N.Z., Sperry J.S. & Comstock J.P. (1995) Influence of leaf water status on stomatal response to humidity, hydraulic conductance, and soil drought in *Betula occidentalis*. *Planta* **196**, 357–366.
- Schwalm C.R., Anderegg W.R.L., Michalak A.M., Fisher J.B., Biondi F., Koch G., et al. (2017) Global patterns of drought recovery. *Nature* **548**, 202–205.
- Sevanto S., McDowell N.G., Dickman L.T., Pangle R. & Pockman W.T. (2014) How do trees die? A test of the hydraulic failure and carbon starvation hypotheses. *Plant Cell Environ* **37**, 153–161.
- Sperry J.S. (2000) Hydraulic constraints on plant gas exchange. *Agricultural and Forest Meteorology* **104**, 13–23.
- Sperry J.S., Alder N.N. & Eastlack S.E. (1993) The effect of reduced hydraulic conductance on stomatal conductance and xylem cavitation. *J Exp Bot* **44**, 1075–1082.
- Tyree M.T. & Dixon M.A. (1983) Cavitation Events in *Thuja occidentalis* L.? : Ultrasonic Acoustic Emissions from the Sapwood Can Be Measured. *Plant Physiol* **72**, 1094–1099.
- Tyree M.T. & Sperry J.S. (1989) Vulnerability of xylem to cavitation and embolism. *Annual Review of Plant Phys. Mol. Biol.*, **40**, 19-38.
- Urli M., Porte A.J., Cochard H., Guengant Y., Burrett R. & Delzon S. (2013) Xylem embolism threshold for catastrophic hydraulic failure in angiosperm trees. *Tree Physiology* **33**, 672–683.
- Wullschlegel S.D., Childs K.W., King A.W. & Hanson P.J. (2011) A model of heat transfer in sapwood and implications for sap flux density measurements using thermal dissipation probes. *Tree Physiology* **31**, 669–679.

- Zweifel R. & Hasler R. (2001) Dynamics of water storage in mature subalpine *Picea abies*: temporal and spatial patterns of change in stem radius. *Tree Physiology* **21**, 561–569.
- Zweifel R., Haeni M., Buchmann N. & Eugster W. (2016) Are trees able to grow in periods of stem shrinkage? *New Phytol* **211**, 839–849.
- Zweifel R., Häsler R. & Item H. (2001) Link between diurnal stem radius changes and tree water relations. *Tree Physiology* **21**, 869–877.
- Zweifel R., Zimmermann L. & Newbery D.M. (2005) Modeling tree water deficit from microclimate: an approach to quantifying drought stress. *Tree Physiology* **25**, 147–156.

Acknowledgements

I am very grateful to Prof. Dr. Ansgar Kahmen for competent mentoring and supervision throughout the past 3.5 years and for giving me the chance to work on a project that neither was restricted to a tight financial nor to a narrow conceptual frame. I further want to give thanks for the generosity of enabling me to participate in 7 international conferences throughout my doctorate studies which certainly promoted my scientific interconnectedness and presentation skills.

My further thanks go to Dr. Günter Hoch, Dr. Sylvain Delzon, Prof. em. Dr. Dr. h.c. Christian Körner and Dr. Roman Zweifel for being constructive and positive co-authors of my manuscripts and for intensive academic and non-academic discussions. I sincerely thank Prof. em. Dr. Dr. h.c. Christian Körner and Prof. em. Dr. Jürg Stöcklin for academic support and inspiration and Prof. em. Dr. Jürg Stöcklin in particular for giving me the trust to independently teach parts of the plant microscopic anatomy course. I thank Prof. Dr. Christiane Werner for agreeing on being the co-examinor of this thesis despite her tight schedule.

I greatly acknowledge the generous and vigorous support of so many people inside and outside the Physiological Plant Ecology Group at the University of Basel: Georges Grun for intensive and instructive technical help and amusing talks about anything and everything. Marua Ellenberger for her never-tiring administrative support. Dr. Oliver Rach and Dr. Victor Evrard for their capable lab support and advice. Dr. Urs Weber for strong help in the field and profound discussions about life. Dr. Nadine Brinkmann and Richard Peters for discussions and help on methodological issues. Dr. Erika Hiltbrunner for academic discussions and her always constructive and never too harsh criticism and for always being ready to help. Svenja Förster and Sandra Schmid for NSC analyses and their unbreakable lab support. Dr. Matthias Arend for theoretical help with a field sampling campaign and scientific discussions. Dr. Daniel B Nelson and Dr. Sarah L Newberry for discussion, shared football games and beer. Bruno Erny and the team of the botanic garden for giving me the freedom and trust to organize and arrange guided tours on my own and to take part in the everyday life of the garden. Dr. Georg

Armbruster is gratefully acknowledged for his repertoire of simple but funny jokes and his success in teaching me the 'Jass' card game.

I give many thanks to my fellow PhD candidates Claudia Hahn, Raphael Weber, Devesh Singh, Michael Thieme, Maria Vorkauf, Florian Cuéni, Lukas Schütz, Camilo Chiang and Wenna Wang for supporting me, cheering me up and distracting me from too much work. I am very thankful to the two Master students I supervised, Till Buser and Marie-Louise Schärer, for giving me such an easy time and intensive experiences in my life and for becoming good friends of mine.

Special and sincere thanks for strong human support go to Edith Zemp who never doubts any of my decisions and actions and who suscitated my deep interest in fine arts.

Many thanks to Dr. Roman Asshoff and Dr. Harald Kullmann for having been switchmen in my life and for being faithful friends afar.

I greatly acknowledge my friends in and around Lörrach as well as around the globe who make my life so much more worth living.

Finally, my most cordial and devoted thanks go to my loving and kindhearted parents Kordula and Robert Dietrich, my sister Lisa Wullenweber and my whole supportive family who never loses faith in me.



Lars Dietrich

Address:

Feldbergstrasse 36
79539 Lörrach
Germany

Tel.: +49 151 28 228 783

Email: larsdietrich.plantphys@gmail.com

Date of Birth: 16.02.1988

Nationality: German

Doctorate Studies in Botany, University of Basel, May 2014 – October 2017

Title: Physiological responses of six temperate tree species to water limitation.

Rated as: *summa cum laude*

Supervised by Prof. Dr. Ansgar Kahmen

Distance University of Hagen, Certificate in Business Administration and Business Management, June 2016 – August 2017

MSc Ecology, University of Basel, February 2013 – April 2014

Master's thesis about the functional growth response of mature spruce trees to elevated CO₂ using stable ¹³C isotopes as eco-physiological tracers (Swiss Canopy Crane Project).

Supervised by Prof. Dr. Christian Körner

BSc Biology/Chemistry, University of Münster, October 2009 – July 2012

Bachelor's thesis about eco-physiological responses of the water flea, *Daphnia magna*, to hypoxia and iron availability.

Supervised bei Dr. Bettina Zeis and Prof. Dr. Rüdiger Paul

University of Düsseldorf, Studies in Medicine, October 2008 – September 2009

St. Benedict's Grammar School, Meschede, 1998 - 2007

German Maturity Certificate, Major Subjects: Biology, French, Mathematics, Theory of Education